ELECTROPHYSIOLOGY OF THE OLIVO-CEREBELLAR LOOP

Cover painted by Sara Khosrovani, untitled (2006), acrylic on canvas, 70 x 50

ELECTROPHYSIOLOGY OF THE OLIVO-CEREBELLAR LOOP

Electrofysiologie van het olivocerebellaire circuit

Proefschrift
ter verkrijging van de graad van doctor aan de
Erasmus Universiteit Rotterdam
op gezag van de rector magnificus
Prof.dr. S.W.J. Lamberts
en volgens besluit van het College voor Promoties

De openbare verdediging zal plaatsvinden op
woensdag 23 april 2008 om 11:45 uur

door

Sara Khosrovani
Geboren te Teheran, Iran

Promotiecommissie

Promotor:	Prof.dr. C.I. de Zeeuw
Overige leden:	Prof.dr. J.G.G. Borst Dr. C.R.W. Hansel Dr. D.N. Meijer
Copromotor:	Dr. M.T.G. de Jeu

This work was supported by the Dutch Organization for Medical Sciences (ZON-MW), Life Sciences (NWO-ALW), Senter (Neuro-Bsik), Prinses Beatrix Fonds and the European Community (EEC;SENSOPAC).

I send my Soul through the Invisible,
Some letter of that After-life to spell:
And by and by my Soul return'd to me,
And answer'd "I Myself am Heav'n and Hell:"

Rubaiyat of Omar Khayyam
translated to English by
Edward Fitgerald

For my parents

Table Of Contents

Chapter 1

Introduction

General

In animals, motor function and muscle control are critical for an organisms ability to interact with and react to its environment. This behavior can have many different functions, from finding food to defending themselves against enemies. In general, we can subdivide movements into two categories: 1) involuntary movements, like reflexes, and 2) voluntary movements. From an evolutionary point of view, the more efficient these movements are, the higher the chance of survival. In vertebrates, the cerebellum controls movement and monitors its efficiency by collecting sensory information, such as limb position, balance information and vision. All this information is evaluated to control and correct our intended movements[1]. The cerebellum is located just above the brainstem at the lower back of the brain. In humans, it is the size of a fist and has a very high nerve cell (neuron) density. The outer layer of the cerebellum, also known as the cerebellar cortex, consists of grey matter and the inner layer consists of white matter. The neurons in the cerebellum are arranged in remarkably homogeneous and repetitive structural patterns with little variation in organization across species.

Structurally, the cerebellum can be divided into different anatomical as well as functional modules. Each module seems to be uniquely connected with different regions of the brain, both through its inputs and outputs. However, despite the origin of the information, the basic processing of incoming information within each module seems to be rather similar [5]. In general, each cerebellar module consists of three main regions: 1) the inferior olive (IO), 2) the cerebellar cortex and 3) the cerebellar nucleus (CN) (Figure 1). These three regions form a circuit known as the olivo-cerebellar loop that forms the computational backbone for the processing of the signals for cerebellum function. In short, when sensory input comes into the IO, olivary cells integrate the information and send the processed signal to the Purkinje cells (PC) of the cerebellar cortex and also, via en-passant collaterals, to the cerebellar nuclear cells [6]. This climbing fiber input is purely excitatory and causes a strong depolarisation. Sensory information also reaches the PCs via the parallel fibers and a second integration step takes place at the level of the PCs. The PC axons, in turn, exert a powerful synaptic inhibition onto cerebellar nuclear neurons, where the final step of cerebellar processing takes place. These nuclei not only project back to the cerebellar cortex, via the thalamus, and many other motor nuclei in the brain stem, but also to the inferior olive, thus creating a closed olivo-cerebellar loop [7-9]. The topography of the projections in the olivo-cerebellar loop are organized such that those parts of the inferior olive that project to a certain cortical zone receive feed-

1 The history of cerebellum involvement in motor behaviour is already known for a long time. In the 18th century Arne-Charles Lorry showed that damage to the cerebellum effects motor coordination. Later in the 19th century, neurophysiologists such as Luigi Rolando, Marie-Jean-Pierre Flourens, and John Call Dalton, Jr. ablated portions of the cerebellum and demonstrated that these animals exhibited strange movements, awkward gaits, and muscular weaknesses (1. Fine, E.J., C.C. Ionita, and L. Lohr, The history of the development of the cerebellar examination. Semin Neurol, 2002. 22(4): p. 375-84.). Later lesion studies showed that particular locations of the lesions exhibited rather specific defects (2. Ito, M., Cerebellar control of the vestibulo-ocular reflex--around the flocculus hypothesis. Annu Rev Neurosci, 1982. 5: p. 275-96, 3. Thompson, R.F., Neural mechanisms of classical conditioning in mammals. Philos Trans R Soc Lond B Biol Sci, 1990. 329(1253): p. 161-70, 4. Thach, W.T., H.P. Goodkin, and J.G. Keating, The cerebellum and the adaptive coordination of movement. Annu Rev Neurosci, 1992. 15: p. 403-42.) suggesting a variety of functional parts in cerebellum. Nevertheless, recent research focuses more on the role of cerebellum in motor learning, motor timing and fine adjustment of the movements.

back inhibition from cerebellar nuclei controlled by the same zone [10]. Although the role of modules in cerebellar function is still a controversial issue, it seems that this remarkably repetitive circuitry performs the same basic computation that can be involved in motor as well as non-motor cognitive processes [11, 12].

From a motor behaviour perspective, there are two main hypotheses proposed for the function of the olivo-cerebellar loop which are not necessarily mutually exclusive. The first hypothesis emphasizes the importance of the olivo-cerebellar loop in motor learning, whereas the second hypothesis emphasizes its importance for the timing of motor actions. Elucidating the role of the olivo-cerebellar circuit is the main goal of the research described in this thesis. We investigated this by studying the information flow through the olivo-cerebellar loop by determining the signal processing features of each individual unit.

Inferior Olive

The inferior olive (IO) is a bilateral, symmetrical nucleus located in the ventral part of the caudal bulbar region of the brain stem. In the mammalian brain, it consists of the principal olive (PO), the dorsal and medial accessory olive (DAO and MAO), and several smaller subnuclei such as the ventrolateral outgrowth (VLO), dorsal cap of Kooy (DCK), dorsomedial cell column (DMCC) and Beta-nucleus (β) [13] (see Figure 2A).

Besides the small number of GABAergic interneurons (<0.1%) [14], the population of inferior olive neurons have two distinct morphologies. The majority of olivary cells have curly dendrites where the main dendritic shafts extends back toward the cell body (Figure 2B, right panel), whereas a minority have straight, sparsely bifurcating dendritic shafts (Figure 2B, left panel) [15]. A recent study by Llinas and colleagues showed that the morphology of olivary neurons may be related to their location within the IO; they showed that the DCK/VLO region only contains cells with a "straight cell" morphology, as shown in figure 2B (left panel) [16].

Olivary neurons have several interesting electrophysiological characteristics. These cells possess membrane potential oscillations that are characteristically distinct from those of any other cell type [17, 18]. These 4-10 Hz oscillations are generated by an interaction between three specific voltage dependent ion channels that are unevenly distributed over the cell: a dendritic high–threshold Ca^{2+} channel, a somatic low-threshold Ca^{2+} channel, and a dendritic Ca^{2+}-activated K^+ channel [18-21]. Furthermore, like thalamic [22] and other brain stem cells [23], olivary neurons have the mixed Na^+/K^+ hyperpolarization-activated current (I_H) channel that contributes to the resting membrane potential [24] and actively influences the shape of the after-hyperpolarizations, therefore, this current might be important for the modulation of these membrane potential oscillations [24].

In vitro studies revealed a very interesting phenomenon. Although these membrane potential oscillations have an intrinsic origin, neighbouring neurons can oscillate in synchrony, suggesting the capacity of these oscillations to expand to the network level. This may be due to the electrical interconnections between olivary cells, which are formed by dendro-dendritic gap junctions [25] made from connexin 36 proteins [26, 27]. These gap junctions are mainly located in structures known as glomeruli. Considering that there are hardly any interneurons in the inferior olive

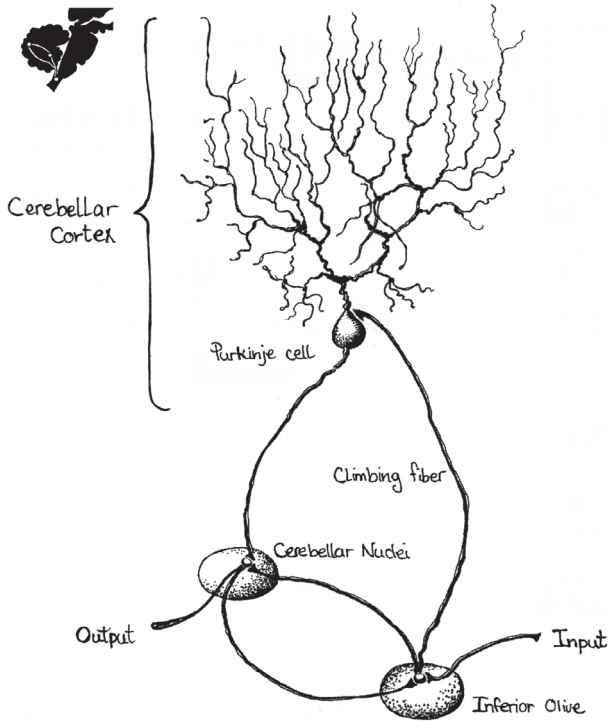

Figure 1. Simplified representation of the olivo-cerebellar module. The olivo-cerebellar circuit contain cells from the inferior olive (located at the brainstem), cerebellar cortex and cerebellar nuclei. Signals from inferior olive neurons are transmitted through the climbing fibres to Purkinje cells as well as through en-passant collaterals to the cerebellar nuclei. The complex and simple spike activities of Purkinje cells is relayed to the cerebellar nuclei and the signal of the cerebellar nuclei neurons in turn drives motor neurons or provides feedback to the inferior olive.

and that the density of gap junctions is extremely high, gap junctions are most likely the main path of intranuclear communication within the inferior olive. The dynamic intercellular passage of signalling molecules (from ions to small peptides) occurs through these junctions, which then generates a network of electronically coupled cells. Although electrical interconnection is not specific for the inferior olive, as other regions of the brain such as olfactory bulb, hippocampus, cerebral cortex and (hypo)thalamus also express gap junctions, the degree of coupling among olivary neurons is the most pronounced in the brain [28]. This emphasizes the importance of electrotonic coupling in the inferior olive and implies a possible role for it in synchronizing the oscillations. Synchronization of subthreshold oscillations in olivary cells leads to action potentials being generated in the same time window at the peaks of these quasisinusoidal subthreshold oscillations, causing a synchronized/time locked output of these coupled cells. In other words, the synchrony among olivary neurons might be responsible for the synchronized activity patterns of Purkinje cells observed in cerebellar microzones [29-31].

The extension (and thereby the functional capacity) of these electrotonically coupled networks is still unknown. Reports indicate sizes from 6-8, by Lucifer yellow in-

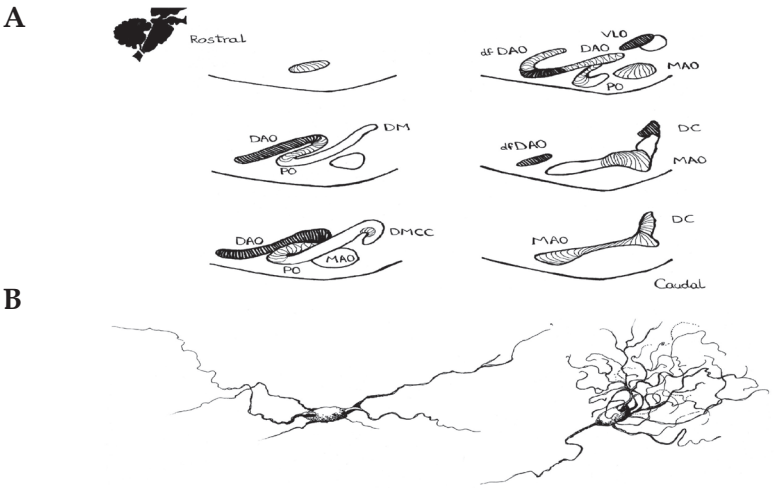

Figure 2. A. The gross anatomy of the inferior olive. The zonal arrangement of the inferior olive is illustrated by transversal slices of the brainstem. Abbreviations: DAO, dorsal accessory olive; dfDAO dorsal fold of DAO; PO, principal olive; DM, dorsomedial group of PO; MAO, medial accessory olive; VLO, ventrolateral outgrowth; DMCC, dorsomedialcell column; DC, dorsal cap of Kooy; β, beta nucleus. B. Two different morphologies of olivary neurons. Olivary cells can have straight sparsely bifurcating dendritic shafts or curly dendrites in which the main dendritic shafts extended back toward the cell body.

jection in guinea pig slices [32], to hundreds, by synchronous firing after Harmaline injection, of coupled neurons [33]. The degree of coupling among olivary neurons is most likely modulated by GABA-ergic inhibitory feedback from the cerebellar nuclei [34, 35] and glutamatergic excitatory input from the mesodiencephalic junction (MDJ) [36, 37]. It has been shown that these excitatory and inhibitory terminals are located around the gap junctions [38, 39] and it is likely that they affect the electrotonic coupling between IO neurons. This anatomic architecture allows for varying, evolving multi-cluster activity, hence time-changing pools of synchronously oscillating neurons [17, 30, 40].

Neurons in IO receive sensory input [41, 42]. Studies in awake [43] as well as anaesthetized and decerebrated [44] cats showed that the majority of IO cells respond to sensory stimulation. Stimuli such as brushing of hair or light tapping on the skin [45] as well as an airpuff to the cornea causes one or more olivary action potentials. These action potentials travel via the climbing fibres to the cerebellar cortex as well as via collaterals to the cerebellar nuclei. This is organized in such a way that each olivary subnucleus projects to one or more longitudinal zones of PCs, which then project to the cerebellar nuclei zone that also receives input from the same climbing fibre collateral [46, 47]. Despite our extensive knowledge of the anatomy of the inferior olive, the precise function of the inferior olive in the cerebellar system is still heavily discussed. It is known that the inferior olive processes somatosensory, visual, or cerebral cortical information, yet its role in transmitting information is limited given the relatively low intrinsic firing rate of the these cells (close to 1 Hz).

In this thesis, we examined a large variety of properties of olivary neurons *in vivo* in order to monitor their behaviour in an intact circuitry. To elucidate the mechanism of how the inferior olive integrates sensory information *in vivo*, we investigated the

impact of peripheral stimulations on olivary properties, like oscillations and spiking patterns (Chapter 2.1). To understand the role of the above mentioned electrotonic coupling in the inferior olive, we studied mutant mice (Cx36 -/-) that do not possess electrotonic coupling among olivary neurons (Chapter 2.2).

Cerebellar Cortex

The cerebellar cortex is the outer mantle of gray matter of the cerebellum and consists of three layers - from outermost to innermost, the molecular, Purkinje and granular layers. The molecular layer consists of inhibitory stellate and basket interneurons, dendritic trees of Purkinje cells, parallel fibres and the end branches of climbing fibres. The Purkinje layer contains only one layer of large cell bodies of Purkinje cells, and the granular layer consists of a vast number of granular cells and a few larger Golgi interneurons, Lugaro cells and brush cells (Figure 3). The ultimate destination of all the information that comes to the cerebellar cortex is the Purkinje cells, which is also the sole output of cerebellar cortex. Purkinje cells are responsible for the final state of information that is relayed to the cerebellar and vestibular nuclei (Figure 3).

Purkinje cells receive two major excitatory inputs; parallel fibres (pf) and climbing fibres (cf). Parallel fibres originate from granule cells and carry a broad range of sensory and motor associated signals. Each Purkinje cell receives input from approximately 200,000 parallel fibres that synapse onto dendritic spines of secondary and tertiary branches. The information coming to Purkinje cells through parallel fibres modulates the simple spike rate. Excitatory input from climbing fibres originates in the inferior olive. Each climbing fibre projects to approximately 10 Purkinje cells in the same sagittal microzone, but each Purkinje cell receives input from only one climbing fibre that wraps around its soma and proximal dendrite. This climbing fibre's input initiates a prolonged unique depolarization known as a "complex spike" [48], that can be easily distinguished from simple spikes. The Purkinje cell also receives inhibitory inputs coming from local interneurons that can manipulate the activity of Purkinje cells. The inhibitory synapses are located on both the dendritic shafts as well as the cell body. The most powerful inhibitory complexes of synapses are located around the PC bodies and originate from basket cells. The inhibitory synapses located around Purkinje cell dendrites originate from stellate cells. All the inhibitory and excitatory inputs mentioned above can modulate the activity and regularity of Purkinje cell firing.

Purkinje cells have a set of membrane conductances that allow them to fire spontaneous action potentials (40-50 Hz) in the absence of synaptic input [49]. When parallel fibre inputs arrive, they evoke excitatory post synaptic potentials (EPSPs) in Purkinje cells and increase their simple spike firing rate. Inhibitory inputs from interneurons are known to delay Purkinje cell firing by causing short pauses. The inputs from climbing fibres generate complex spikes in Purkinje cells. This strong excitation can, in and of itself, affect the simple spike firing pattern. It is known that complex spikes are normally followed by a pause in simple spike activity known as the "climbing fibre pause". The effect of complex spikes on simple spike activity is especially interesting because in several cases, it has been found that the topography of these two inputs is matching (i.e. sensory information from more or less the same

location can evoke signals in parallel fibre and climbing fibre pathways that unite upon the same Purkinje cell) [50-53].

The intriguing anatomical organization of the cerebellar cortex has put forward some interesting theories on its function. There are several hypotheses on the role of Purkinje cells in processing motor information. 1) Purkinje cells are important for guiding and learning specific motor tasks [54, 55]. This is based on the observation that low frequency input coming from climbing fibres can alter the response of the parallel fibre - PC synapse. IO lesion studies revealed an increase in simple spike activity [56], suggesting that climbing fibre activation can reduce the strength of the parallel fibre input. Later, Ito and Kano (1982) showed that by pairing the activity of parallel fibres and climbing fibres, it is possible to induce a long lasting reduction in synaptic strength, known as parallel fibre long term depression (PF-LTD) [52]. More recently, it has been shown that the degree of the synaptic transmission between parallel fibres and PCs can also be enhanced (parallel fibre long term potentiation: PF-LTP) and that the plasticity of the synaptic gain change depends on the amplitude of dendritic calcium transients [57]. Climbing fibre activation provides an additional calcium influx and thus favours the induction of PF-LTD. PF-LTD and -LTP can potentially be the memory storage mechanism necessary for motor learning. During real-life movements, on-going information about the movement is collected by the parallel fibres, while climbing fibres relay motor error events [58]. When an error in movement occurs, the efficacy of the ongoing parallel fibre input is altered by the influence of the climbing fibre error signal; the system is adjusted, i.e. the system learns. This idea is supported by the fact that cerebellar damage is associated with impairment in motor learning. 2) The Purkinje cells are a selective gate for the transfer of information. This hypothesis is based on the observation that Purkinje cells can show bistability in their electrical activity. *In vitro* studies demonstrated that Purkinje cells can exhibit both spontaneous and current-evoked bistable behaviour of simple spikes which is correlated with changes in membrane potential [59]. In other words, the membrane potential of Purkinje cells transits between a "hyperpolarized" state that exhibits only complex spikes and a more "depolarized" state that is associated with both simple and complex spike activity. It has been reported that membrane bistability *in vivo* can not only be triggered by current injections, but also by sensory stimulations [60]. Furthermore, Loewenstein et al., (2005) have suggested that the information coming from the IO through the climbing fibre is essential in shifting the membrane potential and toggles the PC from one state to another. Therefore, bistable behaviour of PCs might serve to gate the processing of sensory information in the cerebellar cortex [60], selecting which information is now relevant and which not.

In this thesis, we studied the electrophysiology of PCs with a focus on the hypothesis suggested by Loewenstein et al. (2005) - whether or not the input from the cf can cause a shift in membrane potential of these cells [60] and to what extent this behaviour is important for cerebellar function (Chapter 3). In the same chapter, we also studied the specific circumstances that can induce this bistablity, such as types of anaesthetics or genetic mutations that enhance inhibition (*tottering* mutant: *Tg*) [61].

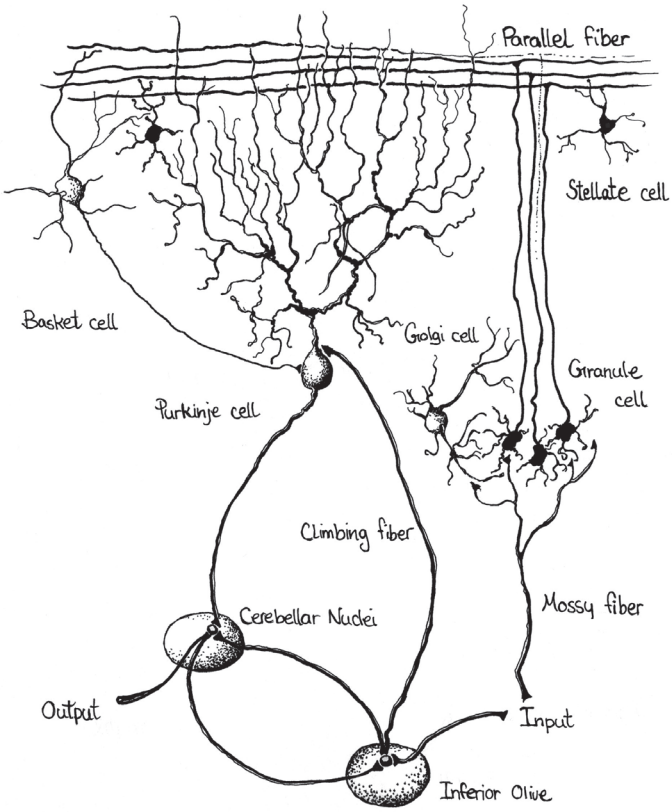

Figure 3. Schematic representation of cerebellar cortex, cerebellar nuclei and inferior olive. Purkinje cells receive excitatory inputs from climbing fibres (cf) that originate from olivary cells as well as multiple inputs from parallel fibres (pf) that originate from granule cells. Purkinje cells receive inhibitory inputs from basket and stellate cells, while Granule cells receive inhibitory inputs from Golgi cells.

Cerebellar Nuclei

With the exception of Purkinje cells in vestibulocerebellum, which relay their signals to the vestibular nuclei (VN), Purkinje cells send processed information through their axons to the cerebellar nuclei (CN), where they have a strong inhibitory effect on the activity of the final part of olivo-cerebellar loop. The deep cerebellar nuclei are divided in three subnuclei: the medial or fastigial nucleus, the interposed nucleus (which has been subdivided into anterior and posterior portions) and the dentate nucleus (Figure 4). They receive projections from various origins, but the three prominent inputs are 1) inhibitory inputs from Purkinje cells of the cerebellar cortex, 2) excitatory inputs from climbing fibre collaterals and 3) inputs from extracerebellar sources.

Cells of the cerebellar nuclei have a large variety of shapes and sizes and Purkinje cell axon terminals contact both the soma and dendrites of them all [62, 63]. Each cerebellar nuclei neuron has up to 30 Purkinje cell terminals, all of which are GABAergic [64, 65]. GABA-ergic inhibitory postsynaptic potentials (IPSPs) in cerebellar nuclei neurons cause a pause or reduction in activity [66]. The excitatory inputs on

these neurons come from climbing fibre collaterals originating from the inferior olive and mossy fibre collaterals that arise from a number of extracerebellar sources, including brain stem nuclei and spinocerebellar afferents [67]. As expected, activation of these terminals elicit excitatory postsynaptic potentials (EPSPs) and enhance the firing activity [68, 69].

Cerebellar nuclei neurons display spontaneous action potentials with an average frequency of 20-40 Hz [69, 70]. This spontaneous firing rate and pattern can be modulated by both the inhibitory and excitatory inputs projecting to these cells. Except for a small number of GABA-ergic interneurons [71, 72], most cells project their axons outside the cerebellar nuclei to a number of areas. On a whole, cerebellar nuclei neurons (except the interneurons) can be divided into two groups, medium to large-sized excitatory neurons that use glutamate and/or aspartate as a neurotransmitter and small inhibitory GABA-ergic neurons. The glutamatergic/aspartergic cells project to various nuclei in the brainstem (including the red nucleus, the mesodiencephalic junction (MDJ), the basilar and reticular pontine nuclei, the reticular formation of the medulla oblongata, and the VN), the spinal cord and several thalamic areas [8, 36, 73-75]. These projections carry information concerning the motor output. The GABAergic cells form direct projections to the inferior olive and contacts the olivary cells' glomeruli. This connection completes the olivo-cerebellar loop and is an important negative feedback mechanism [76] on the activity of olivary cells. It should not be forgotten that the excitatory output of cerebellar nuclei can also reach the IO via the MDJ.

There are different hypotheses on the function of the nuclei-olivary pathway: 1) The nuclei-olivary pathway has a critical role in balancing and controlling the activity of the olivo-cerebellar-olivary circuit, as many negative feedback systems do. This hypothesis is based on observations that the nuclei-olivary pathway regulates Purkinje cell firing [76]. Blocking the nuclei-olivary pathway results in an increased olivary discharge followed by decreased spontaneous simple spike activity in Purkinje cells, while activation of this pathway increases the simple spike firing rate [77]. 2) The nuclei-olivary pathway is important for associative cerebellar learning. Medina [78] revealed that this pathway controls the process that removes associations that were coupled to motor skills (extinction) that are no longer related. 3) The nuclei-olivary pathway can regulate the electrotonic coupling among olivary cells. This hypothesis suggests that olivary coupling can be modulated by inhibitory input from the cerebellar nuclei [34, 35] and excitatory input from mesodiencephalic junction (MDJ) [36, 37]. Both of these synapses terminate near gap junctions (at olivary glomeruli) and may therefore influence the electrotonic coupling between olivary cells [79-81]. Modulating the synaptic transmission of both of these inputs resulted in an altered complex spike synchrony at the PC level [31, 82], which supports the idea that these inputs can modulate the degree of coupling in the inferior olive by the inclusion or exclusion of particular cells in the ensemble of coupled neurons [83].

At the level of the cerebellar nucleus, we investigated neurotransmission between Purkinje cells and cerebellar nucleus cells in normal (wt) mice and mice that suffer from ataxia (*tottering mutant: Tg*) due to an altered motor output signal at the level of the Purkinje cells [61]. In this study, we investigated the consequences of altered

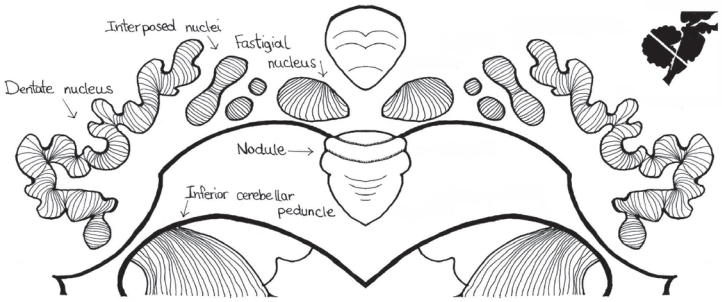

Figure 4. Anatomy of deep cerebellar nuclei. All cells of the deep cerebellar nuclei receive Purkinje cell inputs. The most lateral deep cerebellar subnucleus is the dentate nucleus. The middle cerebellar subnucleus is the interpositus nucleus and is composed of the globose and emboliform nucleus. The most medial nucleus is the fastigial nucleus.

Purkinje signalling and enhanced bistability on cerebellar nuclei cells in order to gain insight into how altered information flow through the olivo-cerebellar circuit can lead to behaviour deficits (chapter 4).

Scope of thesis

In general, the aim of our study is to investigate how each element of the olivo-cerebellar module processes incoming information and how alteration at each level of the module can affect the final output of the cerebellum. In the IO, we focused on the electrophysiological properties of olivary cells and the way they process sensory information (chapter 2.1). Additionally, we tried to uncover the role of gap junctions and electrotonic coupling in determining the output of the IO and, as a result, the cerebellum (chapter 2.2). We also investigated the role of climbing fiber input in PC bistability and the possible functional role of this phenomenon in motor behaviour (chapter 3). To further study the effect of irregularity in PC signalling, we examined mutant mice (*tg*) with a mutation in P/Q type calcium channels that display enhanced bistability, specifically focussing on the effect of the mutation on the morphology of PC-CN terminals and the activity of CN neurons (chapter 4). Chapter 5 is the general discussion.

Approaches

1) Electrophysiological techniques

In this thesis, a variety of electrophysiological techniques were used to investigate the cellular properties as well as the functional role of different parts of the olivo-cerebellar circuit in processing sensory input. Until now, most of our knowledge of the cellular behaviour of the elements in the olivo-cerebellar circuit was based on *in vitro* studies under circumstances where all afferents and efferents are cut off and the cells are surrounded by an artificial environment (i.e. artificial cerebral spinal fluid). Considering that neurons probably behave differently under such conditions, it is essential to additionally investigate the properties of these neurons while they are still within of an intact circuitry and in their natural habitat. The classical approach to studying neuronal activity in intact systems is extracellular recordings. By inserting a microelectrode into the brain and placing it close to the membrane of

the cell, electrical signals can be measured (Figure 5, No. 2). This technique reveals information about the spiking and synaptic activity of neurons in the recorded area, while only minimally interfering with intracellular processes within the recorded cells, and can also be performed in an awake, behaving animal.

Recently, we developed the ability to measure neuronal activity in an intact network by using the *in-vivo* whole-cell patch clamping, wherein the microelectrode is in contact with the interior of the cell (Figure 5, No. 1). This allows for not only recording and identifying the intrinsic dynamics of the cell, but also manipulating the currents flowing through ion channels. This technique enables us to investigate electrophysiological properties of cells such as resting membrane potential, input resistance, membrane capacitance, synaptic potentials and spiking behaviour which cannot be measured by extracellular electrode, and is, therefore, a very valuable new tool that will give us a better understanding of network behaviour, synaptic integration and information processing.

2) Genetic tools

To investigate two important properties of the olivo-cerebellar circuit, we studied two mutant mice: connexin 36 (Cx36) knockouts for the role of electrical coupling in olivary cells, and *tottering* (*Tg*) mutants for the role of irregular firing in Purkinje cells.

Cx36 mutant mice have a mutation in the gene encoding connexin 36 protein, which is necessary for formation of olivary gap junctions. *In-vitro* studies revealed that lack of Cx36 generally leads to an absence of electrotonic coupling in olivary cells, changes in subthreshold activities as well as in the temporal coding of spiking activity [84-86]. Despite all of the electrophysiological changes shown *in vitro*, knockout mice seem to have relatively normal motor behaviour, are not ataxic, perform normally on the accelerating rotarod and walk regularly. This calls into question the extent to which this mutation affects the electrophysiological characteristics of olivary cells *in vivo* and what, if any, role gap junctions play in neuronal synchrony and motor behaviour.

The *tottering* mutant mice carry a mutation in the CACNA1A gene that encodes the α1a-subunit of P/Q-type voltage gated calcium channels. *Tg* knockout mice suffer from severe neurological disorders including ataxia, motor seizures and behavioural absence seizure [87]. This mutation causes an increased calcium influx in Purkinje cells and therefore an increased irregularity of both spontaneous and modulated simple spike firing. The membrane potential of *tg* Purkinje cells exhibit robust bistable behaviour, which makes these mice excellent candidates for studying the downstream effects of bistability and irregular PC firing on olivo-cerebellar function.

3) Behavioural tools

Two sets of behavioural tests have been used in this thesis to investigate learning and memory: eyeblink conditioning and the Erasmus ladder test. Eyeblink conditioning is a well-known behavioural task for studying associative learning and memory. This classical conditioning consists of a conditioned stimulus (CS), such as an auditory stimulus, which is paired to an eyeblink-eliciting unconditioned stimu-

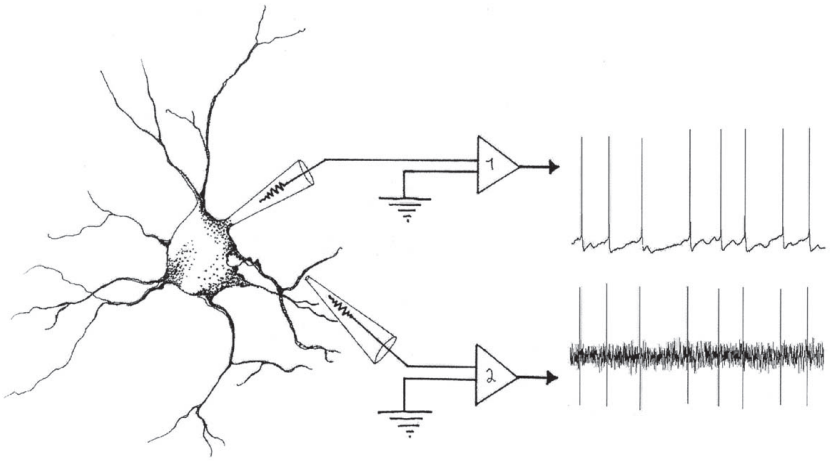

Figure 5. Electrophysiological recording techniques. In extracellular configuration the glass pipette is placed next to the soma of the cell (No. 2), whereas in whole cell configuration the electrode is attached to the membrane and the pipette solution and the cell interior are equilibrated. Right: two examples of recorded signals, one from an extracellular (bottom) and one from an intracellular pipette (top).

lus (US). The US signal will reach the PCs through the IO and climbing fibers while the CS information will reach the PC through the mossy fibres, granule cells and parallel fibres. By pairing the conditioned and unconditioned stimuli a couple of times, animals learn to associate these two stimuli and start to blink before the onset of US.

The Erasmus ladder test is another non-invasive associated learning task, which detects both motor performance and motor learning deficits. This horizontal ladder consists of 37 rungs divided into left and right sides. The rungs are equipped with pressure sensors and can be moved up and down under the control of a computer program. By pairing the change in the pattern of the rungs to a CS such as a tone, one can measure motor learning by examining the change in step-time. Motor performance can also be measured with Erasmus ladder by counting the number of descended rungs touched, i.e. the frequency of missteps.

4) Morphological tools

Ultrastructural studies were performed on PC terminals in the cerebellar nuclei, and the possible morphological alterations due to a mutation in P/Q type calcium channels were studied. Immunohistochemistry for Calbindin (a calcium binding protein) followed by the ABC method provided us with clear sections of labelled PC terminals that were then photographed and analysed using an electron microscope.

References

1. *Fine, E.J., C.C. Ionita, and L. Lohr, The history of the development of the cerebellar examination. Semin Neurol, 2002. 22(4): p. 375-84.*
2. *Ito, M., Cerebellar control of the vestibulo-ocular reflex. Annu Rev Neurosci, 1982. 5: p. 275-96.*
3. *Thompson, R.F., Neural mechanisms of classical conditioning in mammals. Philos Trans R Soc Lond B Biol Sci, 1990. 329(1253): p. 161-70.*
4. *Thach, W.T., H.P. Goodkin, and J.G. Keating, The cerebellum and the adaptive coordination of movement. Annu Rev Neurosci, 1992. 15: p. 403-42.*
5. *Ito, M., Cerebellar circuitry as a neuronal machine. Prog Neurobiol, 2006. 78(3-5): p. 272-303.*
6. *Ruigrok, T.J., Cerebellar nuclei: the olivary connection. Prog Brain Res, 1997. 114: p. 167-92.*
7. *Graybiel, A.M., et al., A cerebello-olivary pathway in the cat. Brain Res, 1973. 58(1): p. 205-11.*
8. *Legendre, A. and J. Courville, Origin and trajectory of the cerebello-olivary projection: an experimental study with radioactive and fluorescent tracers in the cat. Neuroscience, 1987. 21(3): p. 877-91.*
9. *Martin, G.F., C.K. Henkel, and J.S. King, Cerebello-olivary fibers: their origin, course and distribution in the North American opossum. Exp Brain Res, 1976. 24: p. 219-36.*
10. *Dietrichs, E. and F. Walberg, The cerebellar nucleo-olivary projection in the cat. Anat Embryol (Berl), 1981. 162(1): p. 51-67.*
11. *Schmahmann, J.D., Disorders of the cerebellum: ataxia, dysmetria of thought, and the cerebellar cognitive affective syndrome. J Neuropsychiatry Clin Neurosci, 2004. 16(3): p. 367-78.*
12. *Thach, W.T., Context-response linkage. Int Rev Neurobiol, 1997. 41: p. 599-611.*
13. *Whitworth, R.H., Jr. and D.E. Haines, On the question of nomenclature of homologous subdivisions of the inferior olivary complex. Arch Ital Biol, 1986. 124(4): p. 271-317.*
14. *Nelson, B.J. and E. Mugnaini, The rat inferior olive as seen with immunostaining for glutamate decarboxylase. Anat Embryol (Berl), 1988. 179(2): p. 109-27.*
15. *Devor, A. and Y. Yarom, Electrotonic coupling in the inferior olivary nucleus revealed by simultaneous double patch recordings. J Neurophysiol, 2002. 87(6): p. 3048-58.*
16. *Urbano, F.J., J.I. Simpson, and R.R. Llinas, Somatomotor and oculomotor inferior olivary neurons have distinct electrophysiological phenotypes. Proc Natl Acad Sci U S A, 2006. 103(44): p. 16550-5.*
17. *Llinas, R., R. Baker, and C. Sotelo, Electrotonic coupling between neurons in cat inferior olive. J Neurophysiol, 1974. 37(3): p. 560-71.*
18. *Llinas, R. and Y. Yarom, Electrophysiology of mammalian inferior olivary neurones in vitro. Different types of voltage-dependent ionic conductances. J Physiol, 1981. 315: p. 549-67.*
19. *Schweighofer, N., K. Doya, and M. Kawato, Electrophysiological properties of inferior olive neurons: A compartmental model. J Neurophysiol, 1999. 82(2): p. 804-17.*
20. *Llinas, R. and Y. Yarom, Properties and distribution of ionic conductances generating electroresponsiveness of mammalian inferior olivary neurones in vitro. J Physiol, 1981. 315: p. 569-84.*
21. *Manor, Y., et al., Low-amplitude oscillations in the inferior olive: a model based on electrical coupling of neurons with heterogeneous channel densities. J Neurophysiol, 1997. 77(5): p. 2736-52.*
22. *McCormick, D.A. and H.C. Pape, Properties of a hyperpolarization-activated cation current and its role in rhythmic oscillation in thalamic relay neurones. J Physiol, 1990. 431: p. 291-318.*
23. *Bobker, D.H. and J.T. Williams, Serotonin augments the cationic current Ih in central neurons. Neuron, 1989. 2(6): p. 1535-40.*
24. *Bal, T. and D.A. McCormick, Synchronized oscillations in the inferior olive are controlled by the hyperpolarization-activated cation current I(h). J Neurophysiol, 1997. 77(6): p. 3145-56.*
25. *King, J.S., The synaptic cluster in the inferior olivary nucleus. J Comp Neurol, 1976. 165(3): p. 387-400.*
26. *Condorelli, D.F., et al., Cloning of a new gap junction gene (Cx36) highly expressed in mammalian brain neurons. Eur J Neurosci, 1998. 10(3): p. 1202-8.*
27. *Sohl, G., et al., The murine gap junction gene connexin36 is highly expressed in mouse retina and regulated during brain development. FEBS Lett, 1998. 428(1-2): p. 27-31.*
28. *De Zeeuw, C.I., E.L. Hertzberg, and E. Mugnaini, The dendritic lamellar body: a new neuronal organelle putatively associated with dendrodendritic gap junctions. J Neurosci, 1995. 15(2): p. 1587-604.*
29. *Lang, E.J., Organization of olivocerebellar activity in the absence of excitatory glutamatergic input. J Neurosci, 2001. 21(5): p. 1663-75.*
30. *Llinas, R. and K. Sasaki, The Functional Organization of the Olivo-Cerebellar System as Examined by Multiple Purkinje Cell Recordings. Eur J Neurosci, 1989. 1(6): p. 587-602.*
31. *Lang, E.J., I. Sugihara, and R. Llinas, GABAergic modulation of complex spike activity by the cerebellar*

nucleoolivary pathway in rat. J Neurophysiol, 1996. 76(1): p. 255-75.
32. *Benardo, L.S. and R.E. Foster, Oscillatory behavior in inferior olive neurons: mechanism, modulation, cell aggregates. Brain Res Bull, 1986. 17(6): p. 773-84.*
33. *Llinas, R. and R.A. Volkind, The olivo-cerebellar system: functional properties as revealed by harmaline-induced tremor. Exp Brain Res, 1973. 18(1): p. 69-87.*
34. *De Zeeuw, C.I., et al., Microcircuitry and function of the inferior olive. Trends Neurosci, 1998. 21(9): p. 391-400.*
35. *Nelson, B.J., et al., Comparative study of glutamate decarboxylase immunoreactive boutons in the mammalian inferior olive. J Comp Neurol, 1989. 286(4): p. 514-39.*
36. *De Zeeuw, C.I. and T.J. Ruigrok, Olivary projecting neurons in the nucleus of Darkschewitsch in the cat receive excitatory monosynaptic input from the cerebellar nuclei. Brain Res, 1994. 653(1-2): p. 345-50.*
37. *Ruigrok, T.J. and J. Voogd, Cerebellar influence on olivary excitability in the cat. Eur J Neurosci, 1995. 7(4): p. 679-93.*
38. *de Zeeuw, C.I., et al., Ultrastructural study of the GABAergic, cerebellar, and mesodiencephalic innervation of the cat medial accessory olive: anterograde tracing combined with immunocytochemistry. J Comp Neurol, 1989. 284(1): p. 12-35.*
39. *Fredette, B.J. and E. Mugnaini, The GABAergic cerebello-olivary projection in the rat. Anat Embryol (Berl), 1991. 184(3): p. 225-43.*
40. *Sotelo, C., R. Llinas, and R. Baker, Structural study of inferior olivary nucleus of the cat: morphological correlates of electrotonic coupling. J Neurophysiol, 1974. 37(3): p. 541-59.*
41. *Bloedel, J.R. and T.J. Ebner, Rhythmic discharge of climbing fibre afferents in response to natural peripheral stimuli in the cat. J Physiol, 1984. 352: p. 129-46.*
42. *Simpson, J.I., The accessory optic system. Annu Rev Neurosci, 1984. 7: p. 13-41.*
43. *Gellman, R., A.R. Gibson, and J.C. Houk, Inferior olivary neurons in the awake cat: detection of contact and passive body displacement. J Neurophysiol, 1985. 54(1): p. 40-60.*
44. *Gellman, R., J.C. Houk, and A.R. Gibson, Somatosensory properties of the inferior olive of the cat. J Comp Neurol, 1983. 215(2): p. 228-43.*
45. *Garwicz, M., H. Jorntell, and C.F. Ekerot, Cutaneous receptive fields and topography of mossy fibres and climbing fibres projecting to cat cerebellar C3 zone. J Physiol, 1998. 512 (Pt 1): p. 277-93.*
46. *Chan-Palay, V. and S.L. Palay, Tendril and glomerular collaterals of climbing fibers in the granular layer of the rat's cerebellar cortex. Z Anat Entwicklungsgesch, 1971. 133(3): p. 247-73.*
47. *Andersson, G. and D.M. Armstrong, Complex spikes in Purkinje cells in the lateral vermis (b zone) of the cat cerebellum during locomotion. J Physiol, 1987. 385: p. 107-34.*
48. *Eccles, J.C., R. Llinas, and K. Sasaki, The excitatory synaptic action of climbing fibres on the purinje cells of the cerebellum. J Physiol, 1966. 182(2): p. 268-96.*
49. *Hausser, M. and B.A. Clark, Tonic synaptic inhibition modulates neuronal output pattern and spatiotemporal synaptic integration. Neuron, 1997. 19(3): p. 665-78.*
50. *Ekerot, C.F. and B. Larson, Termination in overlapping sagittal zones in cerebellar anterior lobe of mossy and climbing fiber paths activated from dorsal funiculus. Exp Brain Res, 1980. 38(2): p. 163-72.*
51. *Provini, L., S. Redman, and P. Strata, Somatotopic organization of mossy and climbing fibres to the anterior lobe of cerebellum activated by the sensorimotor cortex. Brain Res, 1967. 6(2): p. 378-81.*
52. *Ito, M. and M. Kano, Long-lasting depression of parallel fiber-Purkinje cell transmission induced by conjunctive stimulation of parallel fibers and climbing fibers in the cerebellar cortex. Neurosci Lett, 1982. 33(3): p. 253-8.*
53. *Simpson, J.I., Wylie, D. R., De Zeeuw, C. I. , On climbing fiber signals and their consequence(s). Behavioral and Brain Sciences 19(3): 368-383. 1996.*
54. *Marr, D., A theory of cerebellar cortex. J Physiol, 1969. 202(2): p. 437-70.*
55. *Gilbert, P.F., A theory of memory that explains the function and structure of the cerebellum. Brain Res, 1974. 70(1): p. 1-18.*
56. *Benedetti, F., P.G. Montarolo, and S. Rabacchi, Inferior olive lesion induces long-lasting functional modification in the Purkinje cells. Exp Brain Res, 1984. 55(2): p. 368-71.*
57. *Coesmans, M., et al., Bidirectional parallel fiber plasticity in the cerebellum under climbing fiber control. Neuron, 2004. 44(4): p. 691-700.*
58. *Kobayashi, Y., et al., Temporal firing patterns of Purkinje cells in the cerebellar ventral paraflocculus during ocular following responses in monkeys II. Complex spikes. J Neurophysiol, 1998. 80(2): p. 832-48.*
59. *Llinas, R. and M. Sugimori, Electrophysiological properties of in vitro Purkinje cell somata in mammalian cerebellar slices. J Physiol, 1980. 305: p. 171-95.*
60. *Loewenstein, Y., et al., Bistability of cerebellar Purkinje cells modulated by sensory stimulation. Nat Neurosci,*

2005. 8(2): p. 202-11.
61. *Hoebeek, F.E., et al., Increased noise level of purkinje cell activities minimizes impact of their modulation during sensorimotor control. Neuron, 2005. 45(6): p. 953-65.*
62. *Chan-Palay, V., Afferent axons and their relations with neurons in the nucleus lateralis of the cerebellum: a light microscopic study. Z Anat Entwicklungsgesch, 1973. 142(1): p. 1-21.*
63. *Palkovits, M., et al., Quantitative histological analysis of the cerebellar nuclei in the cat. I. Numerical data on cells and on synapses. Exp Brain Res, 1977. 28(1-2): p. 189-209.*
64. *McLaughlin, B.J., et al., The fine structural localization of glutamate decarboxylase in synaptic terminals of rodent cerebellum. Brain Res, 1974. 76(3): p. 377-91.*
65. *Ottersen, O.P. and J. Storm-Mathisen, Glutamate- and GABA-containing neurons in the mouse and rat brain, as demonstrated with a new immunocytochemical technique. J Comp Neurol, 1984. 229(3): p. 374-92.*
66. *Ito, M., M. Yoshida, and K. Obata, Monosynaptic inhibition of the intracerebellar nuclei induced rom the cerebellar cortex. Experientia, 1964. 20(10): p. 575-6.*
67. *Sastry, B.R., et al., GABA-ergic transmission in deep cerebellar nuclei. Prog Neurobiol, 1997. 53(2): p. 259-71.*
68. *Ito, M., et al., Inhibitory control of intracerebellar nuclei by the purkinje cell axons. Exp Brain Res, 1970. 10(1): p. 64-80.*
69. *Llinas, R. and M. Muhlethaler, Electrophysiology of guinea-pig cerebellar nuclear cells in the in vitro brain stem-cerebellar preparation. J Physiol, 1988. 404: p. 241-58.*
70. *Eccles, J.C., N.H. Sabah, and H. Taborikova, The pathways responsible for excitation and inhibition of fastigial neurones. Exp Brain Res, 1974. 19(1): p. 78-99.*
71. *Wassef, M., et al., Non-Purkinje cell GABAergic innervation of the deep cerebellar nuclei: a quantitative immunocytochemical study in C57BL and in Purkinje cell degeneration mutant mice. Brain Res, 1986. 399(1): p. 125-35.*
72. *Kumoi, K., et al., Immunohistochemical localization of gamma-aminobutyric acid- and aspartate-containing neurons in the rat deep cerebellar nuclei. Brain Res, 1988. 439(1-2): p. 302-10.*
73. *Bentivoglio, M. and H.G. Kuypers, Divergent axon collaterals from rat cerebellar nuclei to diencephalon, mesencephalon, medulla oblongata and cervical cord. A fluorescent double retrograde labeling study. Exp Brain Res, 1982. 46(3): p. 339-56.*
74. *Berretta, S., et al., Cerebellar influences on accessory oculomotor nuclei of the rat: a neuroanatomical, immunohistochemical, and electrophysiological study. J Comp Neurol, 1993. 338(1): p. 50-66.*
75. *Faull, R.L., The cerebellofugal projections in the brachium conjunctivum of the rat. II. The ipsilateral and contralateral descending pathways. J Comp Neurol, 1978. 178(3): p. 495-517.*
76. *Andersson, G., M. Garwicz, and G. Hesslow, Evidence for a GABA-mediated cerebellar inhibition of the inferior olive in the cat. Exp Brain Res, 1988. 72(3): p. 450-6.*
77. *Bengtsson, F., P. Svensson, and G. Hesslow, Feedback control of Purkinje cell activity by the cerebello-olivary pathway. Eur J Neurosci, 2004. 20(11): p. 2999-3005.*
78. *Medina, J.F., W.L. Nores, and M.D. Mauk, Inhibition of climbing fibres is a signal for the extinction of conditioned eyelid responses. Nature, 2002. 416(6878): p. 330-3.*
79. *Welsh, J.P., et al., Dynamic organization of motor control within the olivocerebellar system. Nature, 1995. 374(6521): p. 453-7.*
80. *Lang, E.J., et al., Patterns of spontaneous purkinje cell complex spike activity in the awake rat. J Neurosci, 1999. 19(7): p. 2728-39.*
81. *Llinas, R.R., The Squid Giant Synapse: A Model for Chemical Transmission. 1991.*
82. *Lang, E.J., GABAergic and glutamatergic modulation of spontaneous and motor-cortex-evoked complex spike activity. J Neurophysiol, 2002. 87(4): p. 1993-2008.*
83. *Llinas, R. and J.P. Welsh, On the cerebellum and motor learning. Curr Opin Neurobiol, 1993. 3(6): p. 958-65.*
84. *De Zeeuw, C.I., et al., Deformation of network connectivity in the inferior olive of connexin 36-deficient mice is compensated by morphological and electrophysiological changes at the single neuron level. J Neurosci, 2003. 23(11): p. 4700-11.*
85. *Long, M.A., et al., Rhythmicity without synchrony in the electrically uncoupled inferior olive. J Neurosci, 2002. 22(24): p. 10898-905.*
86. *Buhl, D.L., et al., Selective impairment of hippocampal gamma oscillations in connexin-36 knock-out mouse in vivo. J Neurosci, 2003. 23(3): p. 1013-8.*
87. *Fletcher, C.F., et al., Absence epilepsy in tottering mutant mice is associated with calcium channel defects. Cell,*

Chapter 2

Inferior olive: signal processing and role of gap junctions

2.1 Signal processing in the inferior olive

Abstract

In vitro whole-cell recordings of the inferior olive have demonstrated that its neurons are electrotonically coupled and have a tendency to oscillate. Yet, it remains to be shown to what extent subthreshold oscillations indeed occur in the inferior olive *in vivo* and whether its spatiotemporal firing pattern may be dynamically generated by in- or excluding different types of oscillatory neurons. Here we did whole-cell recordings of olivary neurons *in vivo* to investigate the relation between their subthreshold activities and their spiking behavior in an intact brain. The vast majority of neurons (85%) showed subthreshold oscillatory activities. The frequencies of these subthreshold oscillations were used to distinguish four main olivary subtypes by statistical means. Type I showed both sinusoidal subthreshold oscillations (SSTO's) and low threshold Ca^{2+} oscillations (LTO's) (16%); type II showed only SSTO's (13%); type III showed only LTO's (56%); and type IV did not reveal any subthreshold oscillations (15%). These subthreshold oscillation frequencies were strongly correlated with the frequencies of preferred spiking. The frequency characteristics of the subthreshold oscillations and spiking behavior of virtually all olivary neurons were stable throughout the recordings. Yet, the occurrence of spontaneous or evoked action potentials modified the subthreshold oscillation by resetting the phase of its peak towards 90 degrees. Together these findings indicate that the inferior olive in intact mammals offers a rich repertoire of different neurons with relatively stable frequency settings, which can be used to generate and reset temporal firing patterns in a dynamically coupled ensemble.

Introduction

The Inferior olive (IO) forms the sole source of the climbing fiber input to Purkinje cells in the cerebellar cortex (1). Single climbing fibers excite Purkinje cells in the cerebellar cortex resulting in a powerful, all or none, depolarization called the complex spike. *In vitro* studies have shown that olivary neurons have a unique combination of cellular properties including electrotonic coupling and a propensity to oscillate (2-5). Their tendency to oscillate is mainly due to specific Ca^{2+} conductances, which are distributed differentially over their membrane compartments (2, 6). Dendritic high-threshold and somatic low-threshold Ca^{2+} conductances can activate each other rhythmically and they can interact with a Ca^{2+}-dependent K^+ conductance resulting in the production of subthreshold oscillations with amplitudes of 3-10 mV (2). To date, it is unknown to what extent these oscillations also occur *in vivo* and how they influence the generation of patterns of complex spike activities in the intact olivocerebellar system (see also (7)).

In the intact system, olivary neurons are integrated in specific cerebellar modules (1, 8, 9). The climbing fibers of each olivary subnucleus innervate the Purkinje cells of a particular zone, which in turn project back to the same olivary subnucleus via one of the cerebellar nuclei. In this way the olivocerebellar system comprises many modules, which are each dedicated to specific motor domains and which can run in parallel if needed. The GABAergic feedback from the cerebellar nuclei to the inferior olive is peculiar in that its fibers terminate in a strategic position inside glomeruli directly apposed to the olivary dendrites that are coupled by gap junctions (10).

By inducing a large shunting current these terminals may be able to dynamically uncouple olivary neurons and thereby influence the synchrony of complex spike activities that occur in the cerebellar cortex (11-13). Such a mechanism may for example be involved during the training and execution of rhythmic, tongue or whisker movements (14, 15).

If the inferior olive is indeed involved in setting the pace and composition of motor domains by controlling the activities of ensembles of coupled neurons then the question remains how the preferred frequency of an oscillating ensemble is determined. In principle, there are two main options for controlling such a frequency (1): either olivary neurons are uniformly flexible and the preferred frequency of their oscillation can be controlled by activation of their excitatory afferents; in this constellation inhibitory input from the cerebellar nuclei could serve to merely control the size of the coupled ensemble. Or, alternatively, individual olivary neurons have a more unique, but fixed, preferred frequency of oscillation, and the preferred frequency of the ensemble is determined by including or excluding particular cells via their cerebellar GABAergic input. In the latter case, one should find different categories of olivary neurons with different, but fixed, preferred frequencies and one should not be able to change this frequency by peripheral activation.

Thus, to investigate the occurrence and stability of subthreshold oscillations of olivary neurons *in vivo*, to find out how they may influence the temporal pattern of their climbing fiber activities, and to study the impact of peripheral stimulation on these oscillations and spiking patterns, we performed whole-cell recordings of olivary neurons in the intact olivocerebellar system during peripheral sensory stimulation.

Results

Basic membrane properties. Results described in this study were obtained from 61 neurons of the inferior olive (i.e. principal olive, accessory olives and dorsal cap of Kooy) measured by *in vivo* whole-cell recording technique. The basic membrane properties measured *in vivo* were comparable to those measured *in vitro* (2, 16-18) (Table 1). The *in vivo* recorded IO neurons fired action potentials with an average frequency of 0.87 ± 0.22 Hz and a mean regularity of 0.74 ± 0.02 (coefficient of variation (CV) of spike intervals). They had a resting membrane potential of –55.6 ± 0.7 mV, a membrane capacitance of 184.0 ± 11.3 pF, and an input resistance of 45.9 ± 4.2 MΩ. Electrophysiological behavior of IO neurons was further studied by injection of positive and negative current pulses (Fig 1A and B). In contrast to previous *in vitro* studies, which often revealed a strong "depolarizing sag" as a result of activating H-currents (19, 20), our *in vivo* study only showed a depolarizing sag in a minority of the cases (18%; Fig 1A). Moreover, the same negative current injection evoked a strong rebound depolarization in a majority of the cases (61%). Increasing the amplitude of negative current resulted in an increase of rebound depolarization and eventually a somatic low-threshold Ca^{2+} spike was induced (Fig 1A), which in turn triggered a fast sodium spike. Intracellular depolarizing current pulses hardly initiated action potentials or spike-adaptation and depolarizing steps were followed by a hyperpolarizing sag in only 23% of the cells (Fig 1B).

Table 1. Overview of membrane properties of IO neurons measured *in vivo* with the whole cell patch clamp technique.

Parameter	Mean±s. e.m.	Range	n
Resting membrane potential (mV)	-55.6±0.7	-45.0 to -65.0	61
Input resistance (MΩ)	45.9±4.2	14.8 to 74.7	60
Membrane capacitance (pF)	184.0±11.3	50.5 to577.0	60
Firing rate (Hz)	0.87±0.22	0 to 13.2	61
Coefficient of variation for spike intervals	0.74±0.02	0.27 to 1.20	60
% Cells expressing depolarizing sag	18	10 out of 57	57
% Cells expressing rebound depolarization	61	34 out of 56	56
% Cells expressing afterhyperpolarization	23	11 out of 48	48
% Cells expressing spontaneous SSTO's	30	18 out of 61	61
SSTO frequency (Hz)	5.7±0.3*	3.6 to 7.5	18
SSTO amplitude (mV)	5.6±0.6*	1.5 to 8.9	18
% Cells expressing spont. LT Ca^{2+} spikes.	72	44 out of 61	61
LT Ca^{2+} spike frequency (Hz)	1.8±0.1*	1.0 to 3.1	44
LT Ca^{2+} spike amplitude (mV)	4.2±0.3*	1.5 to 8.5	44
% Cells expressing no spont. SSTO's or LT spikes	15	9 out of 61	61

*Values represent means ± S.E.M. * A single cell can have multiple subthreshold oscillation frequencies. SSTO: sinusoidal subthreshold oscillation, LT: low threshold.*

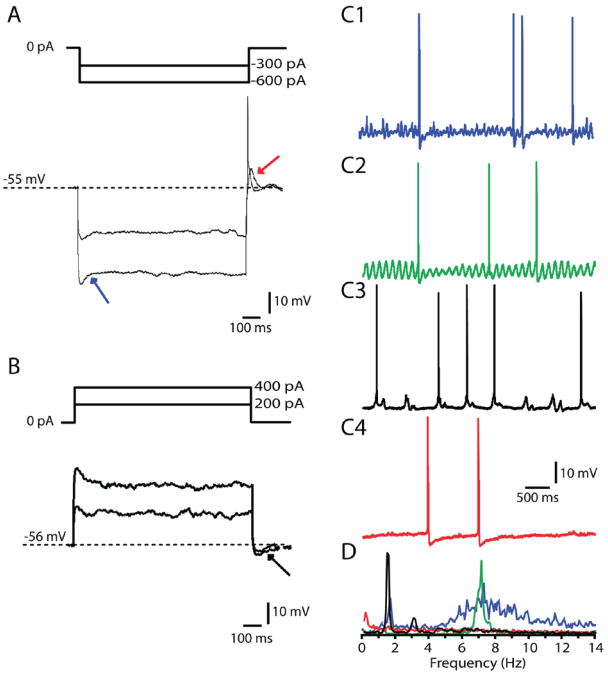

Fig. 1. Membrane properties of olivary neurons recorded in current clamp mode. (A) Hyperpolarizing current injections of 1s were applied to evoke the time-dependent inward rectification (I_H; arrow) and rebound depolarizations (arrow) as well as rebound spikes. It should be noted that type I and II neurons, which express a rebound depolarization, can initiate sinusoidal oscillations in response to this rebound depolarization. (B) Depolarizing current injections of 1s were applied to induce an after hyperpolarization (AHP; black arrow). (C) Different types of subthreshold activity in the membrane potential were observed in olivary neurons. (C1) Neuron showing a subthreshold activity composed of two different frequencies, namely 1.9 Hz and 7.2 Hz. (C2) Neuron showing sine-wave shaped oscillations of 7 Hz. (C3) Cell with low-threshold Ca^{2+} spikes, which exhibited a rhythmic behavior of 1.8 Hz. (C4) Cells without any substantial subthreshold activity. (D) Power spectra of the recordings shown in C1, C2, C3 and C4.

Whole-cell recordings of IO neurons *in vivo* exhibited various patterns of resting membrane potential activity (Fig. 1C). In contrast to *in vitro* studies in which subthreshold sine-wave-shaped oscillations and rhythmic low-threshold Ca^{2+} spikes virtually only occur in hyperpolarized neurons and in which they rarely occur together in the same neuron (2, 6), our *in vivo* recordings revealed that IO neurons can also exhibit these two types of oscillations spontaneously and relatively frequently together. We observed four different types of patterns of subthreshold activities: a) Typical rhythmic 4 to 8 Hz sinusoidal subthreshold oscillations (SSTO's) with a mean amplitude of 5.6 ± 0.6 mV (Fig. 1C2); b) rhythmic 1 to 3 Hz low-threshold Ca^{2+} oscillations (LTO's) with a mean amplitude of 4.2 ± 0.3 mV (Fig. 1C3); c) a pattern in which both oscillatory activities described above were combined (Fig. 1C1); and d) a pattern in which no subthreshold oscillations were present in the resting membrane potential (Fig. 1C4). In the first three patterns the amplitude of the oscillations could either be constant or vary in a cyclic manner. In the fourth pattern there was a subpopulation (only 3 neurons) in which no low-threshold Ca^{2+} currents were observed and in which the high firing frequencies (up to 30 Hz) could be evoked by depolarizations.

Categorization of neurons. Since the patterns of subthreshold membrane activities appeared to vary considerably among IO neurons, we investigated whether the differences described above could be established by statistical means. Using the frequency of the subthreshold membrane oscillations as a distinguishing property in a hierarchical cluster analysis, we were indeed able to readily divide the population of 61 olivary neurons into four clusters (Fig. 2A): 16% of the neurons exhibited both SSTO's and LTO's (type I); 13% exhibited only SSTO's (type II); 56% contained neurons that exhibited only LTO's (type III); and 15% did not show any subthreshold oscillation (type IV). Moreover, the identity of these clusters could be readily confirmed in a matrix in which the LTO and SSTO activities were plotted against each other in the order of their frequencies (Fig. 2B). Despite their clear characteristics at the cell physiological level, type I, II, and III neurons that were intracellularly injected with neurobiotin were indistinguishable from each other at the morphological level (Fig. 3A); they all showed the characteristic olivary dendrites that tend to curl back towards the soma (1) and they were not restricted to any particular olivary subnucleus (Fig. 2C). Due to their low occurrence type IV neurons were not labeled, but since these neurons were recorded in the medial part of the inferior olive at a depth ranging from 500-750 µm and because their activity closely resembles that of the neurons that were described by Urbano et al. (21), these neurons probably are olivary neurons from the dorsal cap of Kooy.

To determine whether the identity of an individual olivary neuron is fixed, we investigated the stability of their subthreshold oscillations over time (on average 23 minutes). Two minutes of spontaneous recordings were compared to the same episodes of recordings at least 5 to 10 minutes later. Within the two minutes timeframes themselves no transitions in subthreshold activities were observed (Fig. 4A). However, 4 out of the 61 neurons (7%) showed a change in one of the subsequent episodes with respect to the first one (Fig. 4B). Two type I cells became type III cells and two type III cells became type I cells. All these four alterations were single event transitions in SSTO activities indicating that the presence or absence of LTO's is a

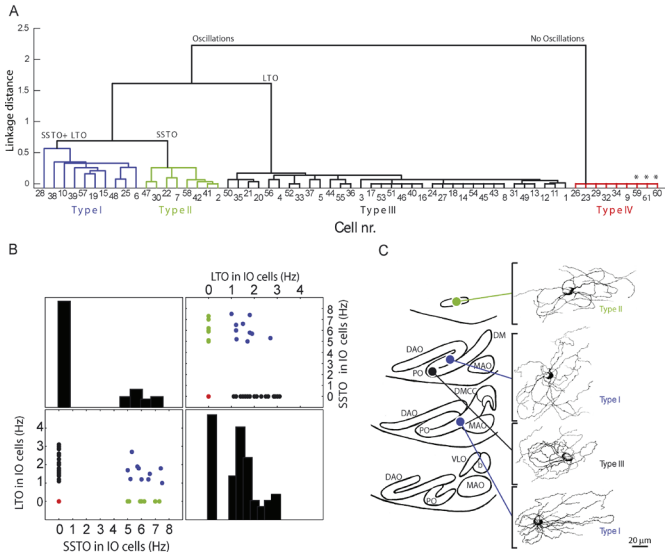

*Fig. 2. Cluster analysis based on subthreshold oscillations in membrane potential. (A) Hierarchical cluster analysis shows clustering into four distinctive groups: Type I neurons exhibit SSTO's and LTO's; type II neurons express only pure SSTO; type III neurons express only LTO; and type IV neurons exhibit no subthreshold activity. (B) Matrix plot representation of the subthreshold oscillation frequencies of olivary neurons and their classification by hierarchical cluster analysis. * Olivary neurons presumably from the dorsal cap of Kooy (21). (C) Reconstruction of Neurobiotin labeled neurons. All labeled cells (three cell types) were located in the inferior olive and revealed similar morphology. DAO, dorsal accessory olive; PO, Principal olive; DM, dorsomedial group of PO; MAO, Medial Accessory olive; DMCC, Dorsomedial cell column; VLO, Ventrolateral outgrowth; β Beta cell group.*

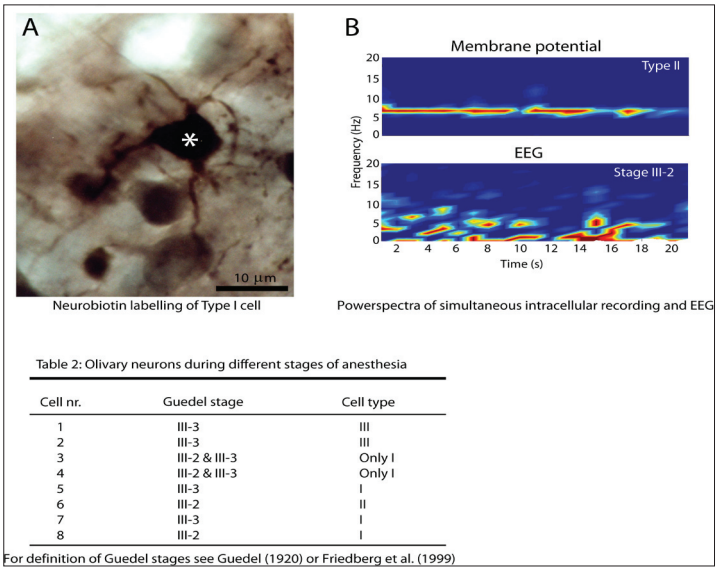

Table 2: Olivary neurons during different stages of anesthesia

Cell nr.	Guedel stage	Cell type
1	III-3	III
2	III-3	III
3	III-2 & III-3	Only I
4	III-2 & III-3	Only I
5	III-3	I
6	III-2	II
7	III-3	I
8	III-2	I

For definition of Guedel stages see Guedel (1920) or Friedberg et al. (1999)

Fig. 3. (A) Neurobiotin labeling of an in vivo whole-cell recorded olivary neuron (, type I) and neighboring dye-coupled neurons. (B) Time-frequency representation of simultaneously recorded electroencephalogram and the membrane potential of an olivary type II neuron. The depth of anesthesia was Guedel's stage III-2.*

definitive characteristic of a given cell, while those of the SSTO's can appear and disappear in rare cases. In addition, when we made whole cell recordings in animals anesthetized with a mixture of Midazolam, Medetomidine and Fentanyl (n = 21; on top of the 61 reported above) instead of Ketamine and Xylazine we observed the same consistent types of oscillations. Moreover, we did not find any evidence that the depth of Ketamine - Xylazine anaesthesia affected the characteristics of the oscillations (n = 8; on top of the cells reported above) (Fig. 3B). In the latter recordings the states and depths of anaesthesia were determined with the use of EEG recordings and qualified according to the frequency bands as described by Guedel (22, 23), and we compared Guedels' stages III-2 and III-3 during recordings that lasted at least 40 minutes (Table 2).

Post hoc analysis revealed that properties such as resting membrane potential, membrane capacitance, firing rate, coefficient of variation for spike intervals, and the occurrence of rebound depolarizations and/or hyperpolarizing sags were all not significantly different among the four cell types (Table 3). In contrast, the occurrence of H-current induced-depolarizing sags was significantly lower in type III neurons, while their shortest preferred ISI was significantly longer (all p's < 0.02), and the mean input resistance was significantly higher in type IV neurons (for comparisons with type I, II and III neurons all p's < 0.03) (Table 3).

Thus, we conclude that olivary neurons can be divided into four types with specific frequency characteristics of their subthreshold oscillations and specific membrane and response properties that are all relatively stable over time.

Table 3: Overview of membrane and response properties per olivary neuron type

					Statistical significance
	Type I	Type II	Type III	Type IV	ANOVA/ X^2-test
Distinguishing set of properties	SSTO and LTO	SSTO and No LTO	No SSTO and LTO	No SSTO No LTO	
Number of cells	10	8	34	9	
Resting membrane potential (mV)	-56.5±1.7	-54.6±1.4	-56.4±0.8	-52.3±1.9	ns
Input resistance (MΩ)	33.8±3.6	39.7±2.4	42.8±4.4	76.5±19.9	<0.02
Membrane capacitance (pF)	215±30	182±20	186±16	139±17	ns
Firing rate (Hz)	0.71±0.09	0.39±0.13	0.68±0.05	2.07±1.41	ns
Coefficient of variation for spike intervals	0.75±0.03	0.79±0.06	0.73±0.02	0.71±0.12	ns
Cells expressing depolarizing sag (%)	29	33	9	25	<0.03
Cells expressing rebound depolarizations (%)	71	67	63	38	ns
Cells expressing afterhyperpolarizations (%)	0	50	13	50	ns
Cells expressing SSTO (%)	100	100	0	0	DP
SSTO frequency (Hz)	6.2±0.3	5.9±0.3	-	-	DP
SSTO amplitude (mV)	4.9±0.7	6.8±0.5	-	-	DP
Cells expressing spontaneous LT Ca^{2+} spikes (%)	100	0	100	0	DP
LT Ca^{2+} oscillation frequency (Hz)	1.5±0.2	-	1.8±0.1	-	DP
LT Ca^{2+} oscillation amplitude (mV)	4.1±0.5	-	4.1±0.3	-	DP
Shortest preferred ISI (ms)	139.3±7.7	144.3±15.5	550.3±43.8	-	<0.01
Cells responding to peripheral stimuli (%)	67	100	88	0	<0.05
Response efficiency (%)	26.3±6.1	18.7±3.8	22.7±4.3	-	<0.02
Response latency 1st spike (ms)	37.1±7.1	36.7±3.2	51,2±5.0	-	ns
Response latency 2nd spike (ms)	411±113	172±23	516±38	-	<0.02

Values represent means ± S.E.M and indicate the levels of statistical significance according to either ANOVA or χ^2-test. SSTO: sinusoidal subthreshold oscillation, LT: low threshold, LTO: low threshold oscillation, DP: distinguishing property.

*Fig. 4. Stability of subthreshold oscillation frequencies in olivary neurons. (A) Time - subthreshold oscillation frequency representation of 120 s of spontaneous recordings from a type I, type II and type III neuron. The amplitude of the power spectra is coded in color. (B) Olivary neurons were subjected to two cluster analyses that were performed on oscillatory behavior that was obtained at 2 different time frames that were separated by 5-10 minutes. * Olivary neurons presumably from the dorsal cap of Kooy (21).*

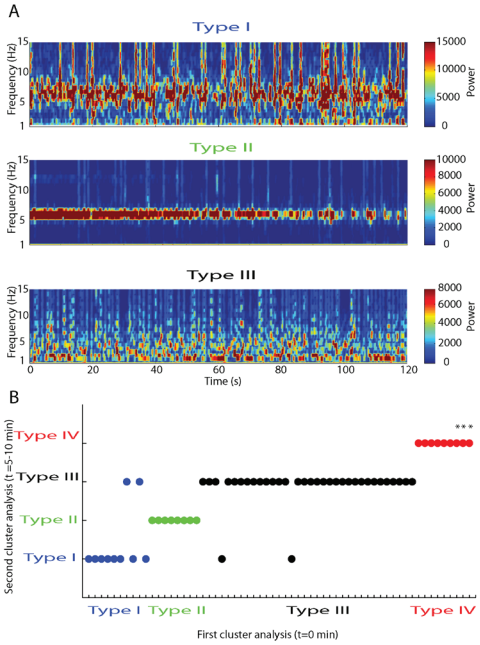

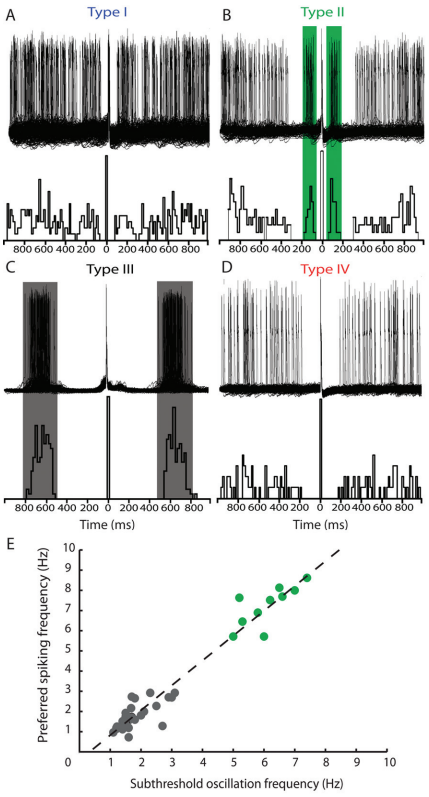

Fig. 5. Autocorrelograms showing preferred spiking patterns. (A) A type I neuron showing multiple preferred spiking patterns. (B) A type II neuron showing a preferred spiking pattern with at 80-200 ms (indicated by green box). (C) Example of a type III neuron, which shows a preferred spiking pattern at 600-800 ms (indicated by grey box). (D) A type IV neuron showing no preferred spiking pattern. (E) Correlation between olivary oscillation frequency and preferred spiking pattern frequency (linear fit: y= 1.2x-0.4, r^2=0.95).

Preferred spiking patterns. To find out whether subthreshold oscillations contribute to the firing behavior of olivary neurons, their spiking patterns were analyzed in relation to their subthreshold activities. Even though the firing frequencies among the four types were not significantly different, their patterns of preferred spiking varied (Fig. 5). Type I neurons had a dominant preferred spiking pattern with an interspike interval (ISI) of 139 ± 8 ms ranging from 120 to 190 ms in agreement with the rhythm of SSTO's (Fig. 5A). In addition, type I cells had a second preferred spiking pattern with an average ISI of 629 ± 74 ms ranging from 454 to 802 ms corresponding with the presence of LTO's. Type II neurons showed preferred spiking patterns with an interspike interval ranging from 78 to 211 ms, which was again in accordance with the wavelength of their SSTO's (Fig. 5B). In type III neurons only spiking patterns with long ISI's were found ranging from 460 to 641 ms (Fig. 5C), which was also in line with the presence of LTO's; this preferred spiking pattern was significantly different from those of neurons in the other types (Table 3; ANOVA: $p < 0.01$; Post hoc LSD: $p < 0.01$). Finally, as expected from the subthreshold activities, type IV neurons showed no preferred spiking patterns (Fig. 5D). If one directly correlates the frequencies of preferred spiking with those of the subthreshold oscillations on a cell by cell basis, the correlation becomes evident ($r2 = 0.95$) (Fig. 4E).

Response properties. Somatosensory stimulation evoked action potentials and EPSP's in vast majority (85 %) of the type I, II, and III neurons, but in none of the type IV neurons (χ2-test, $p < 0.05$; Table 2). The average response/stimulus efficiency was 23.6 ± 3.2 % (n = 20) with an average response latency of 47.2 ± 3.9 ms (n = 20). Each

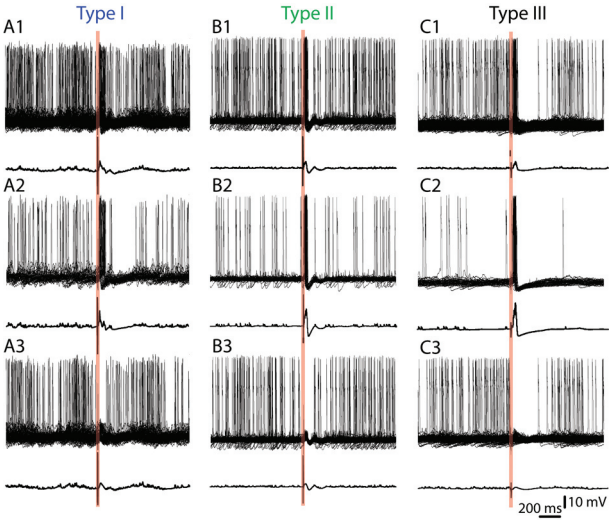

Fig. 6. Response properties after peripheral sensory stimulation. (A1) 150 traces of a type I neuron responding to peripheral stimulation and the resultant averaged trace indicated in the lower trace. (A2) Subpopulation of A1: The traces of the same neuron that responded with an action potential and their averaged trace indicated below. (A3) The complementary subpopulation of A1: The traces that did not respond with a spike and their averaged trace indicated below. B and C show the same panels as in A, but for type II and type III cells. Note that the stimulus can induce a period of inhibition not only when it does induce an action potential (see A2, B2 and C2), but also when it does not (A3, B3, and C3). In B3 it can be seen that peripheral stimulation can even reset the phase of the oscillating subthreshold responses without action potentials. Red bars indicate the time of peripheral stimuli administration.

cell type had a characteristic pattern of responding. In type I neurons stimuli evoked action potentials as well as EPSP's at short latencies of 37.1 ± 7.1 ms or long latency responses of 411 ± 113 ms (for mixture of short and long second latency responses, see Fig. 6A). In type II neurons the short latency responses were comparable to those in type I neurons, but the long latency responses (172 ± 23 ms) were significantly shorter ($p < 0.02$) (Fig. 6B). Moreover, in these neurons the stimuli did not only elicit action potentials or subthreshold potentials but they also reset the phase of the sinusoidal subthreshold oscillations; these resettings did occur both after the stimuli that evoked action potentials ánd after those that only evoked subthreshold potentials (Fig. 6B2 and Fig. 6B3). In type III neurons both the short latency responses (51.2 ± 5 ms) and long latency responses (516 ± 38 ms) were longer than those of type I and type II neurons ($p < 0.02$) (Fig. 6C). Moreover, the average inhibition period (465 ± 43 ms) that followed the stimulus evoked responses was significantly longer in these cells ($p < 0.02$). In general, the length of these inhibition periods was longer when the stimulus evoked an action potential than when it only evoked an excitatory subthreshold response (compare Fig. 6B and Fig. 6C). These results indicate a strong modulatory influence of peripheral inputs on olivary subthreshold oscillations and spiking patterns (i.e. olivary output).

Interactions oscillations and spiking behavior. The data provided above suggest that action potentials can reset the phase of the subsequent subthreshold oscillations in an accurate manner, which has also been observed *in vitro* (24). To further quantify this relationship we compared the phase of the oscillations before and after the action potentials in type II neurons (Fig. 7). The phase of the subthreshold oscillations of type II neurons was only reset after the occurrence of spontaneous or stimulus evoked action potentials when these action potentials did not occur exactly at the peak of the oscillation. The phase of their oscillations áfter the action potential was consistently reset such that the new sinusoidal peaks occurred in cycles of approximately 360 degrees after the preceding action potential (Fig. 7). This relation held true for both spontaneous action potentials and stimulus evoked action potentials, but the phase shift appeared to be somewhat greater after the stimulus evoked potentials (Fig. 7).

The interaction between spiking behavior and subthreshold oscillations was not a one way interaction: The spiking behavior did not only influence the phase of the

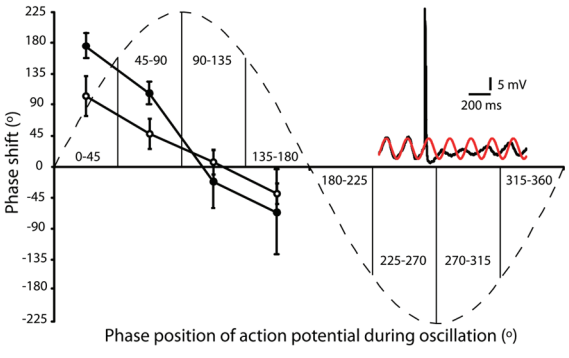

Fig. 7. Phase-response curves. The phase of the subthreshold oscillations of type II neurons was reset after the occurrence of spontaneous (open circles) or stimulus evoked (filled circles) action potentials when these action potentials did not occur exactly at the peak of the oscillation. Inset: Example of a comparison of the phase values of the subthreshold oscillations before and after the occurrence of an action potential. Red trace is a sinusoidal fit of the trace before the occurrence of the action potential followed by an extrapolation after the occurrence of the action potential.

following oscillations, but the phase of the oscillation also strongly influenced the probability for an action potential to occur. Figure 6 illustrates that there were virtually no cells spiking in the trough of the oscillation (between 180 and 360 degrees). Thus, we can conclude that spiking behavior and subthreshold oscillatory behavior of olivary neurons strongly interact *in vivo*.

Discussion

The present whole-cell recordings *in vivo* demonstrated that the vast majority of olivary neurons show subthreshold oscillations, that olivary neurons can be divided into four different categories dependent on the presence, shape and frequency of oscillation and that peripheral stimulation does not alter the characteristic stable oscillatory activities of an olivary cell other than resetting their phase. These findings have implications for the firing patterns of individual olivary neurons and they suggest that a wide variety of temporal patterns of olivary ensembles are composed by dynamically coupling or uncoupling specific types of olivary cells.

Electrophysiological composition of the inferior olive. The current *in vivo* study indicates that about 85% of the inferior olivary neurons have spontaneous subthreshold oscillations. This finding suggests that the actual level of oscillations in intact mammals is higher than observed in *in vitro* studies, in which relatively few spontaneous oscillations occur and in which hyperpolarizing current injections or electrical stimulations are usually required to induce oscillatory activity (2, 6, 20). Possibly, the reverberating loops in which the inferior olive is embedded enhance the intrinsic oscillatory properties of its neurons (25). These include the excitatory loops with the cerebellar nuclei and mesodiencephalic junction (26, 27) as well as the olivocerebellar modules comprising the olivary subnuclei, Purkinje cell zones and deep cerebellar nuclei (28). Such an extrinsic enhancing mechanism is in line with findings which indicate that serotonergic afferents to the olivary neurons as well as their level of electrotonic coupling can also modulate their propensity to oscillate (3, 29).

Apart from the non-oscillating cells, which presumably represent the neurons of the dorsal cap and ventrolateral outgrowth (21), we found 3 types of oscillating cells that could be identified based upon their spontaneous subthreshold activities and categorized accordingly using statistical cluster-analysis. They include type I cells, which show both SSTO's and LTO's and which have a wide range of preferred frequencies for both their oscillations and spiking activities varying from 1 to 8 Hz; type II cells, which show only SSTO's and which have preferred oscillatory and spiking frequencies of 5 to 8 Hz; and type III cells, which show only LTO's and which oscillate and fire at preferred frequencies of 1 to 3 Hz. *In vitro* studies, in which the SSTO's and LTO's can be studied in isolation, have shown that these oscillations in the olive are generated by rhythmic activation of dendritic high-threshold and somatic low-threshold Ca^{2+} conductances and their interaction with a Ca^{2+}-dependent K^+ conductance (3, 20). In addition, the H-current can also contribute to the olivary oscillations (20). H-current dependent depolarizing sags were frequently observed in all three main oscillating cell types, but our data show that this current does not necessarily need to be expressed in order for the oscillations to occur. Thus, while the basic membrane properties of all olivary neurons are rather similar (Table 3),

they can vary substantially in their type of subthreshold oscillations.

The different sorts of oscillations of the various cell types were reflected in the spiking patterns in that the preferred frequencies of the autocorrellograms of olivary spike activities corresponded to those obtained from the spectral analyses of the subthreshold oscillations. Likewise the temporal spiking patterns that occurred after peripheral stimulation also reflected the type of oscillatory cell they were recorded from and varied accordingly. Type II neurons (SSTO-only) responded with an action potential or an EPSP, type III neurons (LTO-only) responded with a low-threshold Ca^{2+} spike with or without an action potential followed by a long afterhyperpolarization, and type I neurons revealed a mixed response. The main response properties (rate and latency) described here for the mouse inferior olive were comparable to those found for the olive in the awake cat and rabbit (30, 31), except for type III neurons that responded with slightly longer latencies. In addition, peripheral stimulation had a clear effect on the phase of the subthreshold oscillations; it consistently reset the phase of its peak towards 90 degrees. Thus, peripheral inputs to the olive can modify the temporal code of its neurons both in relative terms (firing frequency) and absolute terms (precise moment in time).

Functional implications. Importantly, the subthreshold activity and thereby the identity of the cells appeared remarkably stable throughout the recordings. Virtually none of the recorded cells switched during the recordings from one category to the other even though many of them lasted longer than ½ an hour. We hardly ever observed the short episodic oscillatory behaviour, which has been described by Chorev et al. (7). This difference might be due to differences in species used or in methodology such as the use of sharp electrode recordings instead of whole cell recordings. We cannot exclude the possibility that the state of the animal affects the oscillations (32), but the stability was so profound that even unphysiologically strong, electrical stimulation of the tongue was not sufficient to convert the identity characteristics of the olivary neurons. These data suggest that individual olivary neurons have a rather unique, preferred frequency of oscillation, which is relatively fixed. Such an organization raises the possibility that the overall temporal structure of an ensemble of coupled olivary neurons can in principle be manipulated by including or excluding cells with particular preferred frequencies to the ensemble. Thus, since the olivary neurons can be dynamically uncoupled by the cerebellar GABAergic terminals that are apposed to the spines that are coupled by dendrodendritic gap junctions in the olivary glomeruli (1, 4, 10, 33, 34), it may well be that this input also controls both the size of and the overall preferred frequency of the olivary ensembles. In this constellation the excitatory inputs could then deliver the firing frequency and the fine-tuning for the phase of the activity in absolute time.

Materials and Methods

In vivo whole-cell recordings. C57Bl6 mice were anesthetized with a mixture of Ketamine and Xylazine (65 and 10 mg/kg i.p.), or a mixture of Medetomidine, Midazolam and Fentanyl (0.5 mg/kg, 5 mg/kg and 0.05 mg/kg i.p., respectively). The body temperature was maintained at 37°C with the use of an anal thermosensor and

a heating pad (FHC, Bowdoinham, Me., USA). To perform stable *in vivo* recordings the mouse was placed in supine position and the head was fixed (35). Neck surgery was performed to expose the ventral surface of the medulla oblongata and the dura was removed. Whole-cell recordings were performed with borosilicate pipettes (with filament; OD 1.5 mm, ID 1.2 mm, Hilgenberg, Malsfeld, Germany) filled with (in mM) 4 NaCl, 3.48 MgCl2, 9 KCl, 10 KOH, 120 K-gluconate, 10 HEPES, 17.5 Sucrose, 4 Na2ATP and 0.4 Na3GTP with pH 7.2 and osmolality at 290-310 mOsm kg-1. To label the recorded neurons 0.5% Neurobiotin was added to the internal solution. Current clamp recordings were amplified with a Multiclamp 700A (Axon instruments, Foster city, CA), filtered at 10 kHz and digitized at 20 kHz with a Digidata 1322A (Axon instruments, CA). Membrane potentials were corrected for an 8 mV junction potential. Peripheral stimulation was provided by electrical stimulation to the tongue or skin. The stimulation protocol consisted of short bipolar stimulations (2 ms, 1.25mA). Analysis was performed using Clampfit 9.0 software (Axon instruments, CA). All animal procedures were in accordance with the guidelines of the ethical committee of Erasmus MC.

Morphology. After labeling the cells with Neurobiotin, mice were transcardially perfused with 4% paraformaldehyde in 0.1 M phosphate buffer (PB). The brainstem was removed and post-fixed in perfusate and subsequently rinsed overnight at 4°C in 0.1 M PB, pH 7.4, containing 10% sucrose. The brainstem was embedded in 10% gelatine and 10% sucrose. Tissues were fixed in 10% formaldehyde and 30% sucrose solution at room temperature for 2 hours. Serial sections of 40 µm were cut on a cryo-modified sliding microtome (Leica SM2000R). Sections were incubated overnight at 4°C in avidin-biotin-peroxidase complex (Vector Laboratories, Burlingame, CA), rinsed and incubated in DAB (75 mg/100 ml). The reaction was stopped after visual inspection by rinsing in PB. Neurobiotin labeled cells were reconstructed using Neurolucida software (Microbrightfield Europe, Magdeburg).

Membrane properties and responses. Data analysis was performed on neurons with resting membrane potentials negative to -45 mV, typical olivary spike waveforms and spike amplitudes larger than 60 mV. In each neuron the following membrane properties were determined: resting membrane potential, input resistance, membrane capacitance, time-dependent inward rectification (I_H), rebound depolarizations and after hyper-polarizations. Patterns of spontaneous firing were studied in recordings from membrane potentials of at least 2 minutes. The spontaneous firing rate was determined as the inverse of the mean of all spike intervals. The coefficient of variation (CV) of spike intervals was computed by dividing the standard deviation of the spike intervals by the mean of the spike intervals. Preferred spiking patterns were studied by autocorrelograms of spontaneous spiking patterns and burst patterns were evaluated using a burst analysis method (clampfit 9.0 software, Axon Instrument, CA). Burst patterns with a significant Poisson surprise value (>5) were selected, spike times of the spikes in this burst were averaged, and this value was taken as the center point of the preferred spiking period. Subthreshold oscillations were quantified by measuring the frequency and amplitude of the oscillations. Spontaneous membrane potential recordings of at least 2 minutes were analyzed by

using a Hann windowed fast Fourier transformation to generate a power spectrum. The stability of subthreshold oscillations within a single recording was monitored by using a running Hann windowed fast Fourier transformation. Every 250 ms a power spectrum was generated by analyzing the last 819.2 ms.

Membrane responses evoked by 150 peripheral sensory stimulations were analyzed. The response efficiency was determined by dividing the amount of evoked action potentials (i.e. action potentials in the 25-100 ms time window after the stimuli) by the amount of sensory stimuli. The response latency was calculated as the average time latency of these evoked action potentials after the peripheral stimuli. The occurrence of a preferred spiking period after the stimuli-induced action potential was determined by using again the burst analysis method. The average response latency of the spikes within this preferred spiking period was calculated.

To quantify the effect of action potentials on the subthreshold oscillation, the phase difference in subthreshold oscillation before and after action potential was determined. In spontaneous membrane potential and in stimuli induced activity recordings a sine-wave was fitted in the subthreshold oscillation before a spontaneous or evoked action potential. The fitted curve was extrapolated to the oscillations succeeding the action potential. Based on this curve-fit the position of the spike and the phase shift were calculated.

Statistics/Cluster analysis. Neurons were initially grouped by visual inspection of their subthreshold activity. Hierarchical cluster analysis was used to confirm the grouping produced by this visual inspection and to generate a more reliable classification of the different groups. Hierarchical cluster analysis was performed using the frequencies of subthreshold oscillations as distinguishing variable. In this hierarchical clustering, we used standardized parameter values to compute the euclidean distance between objects. The calculated linkage distance was used to define the cell clusters. In order to reveal cluster differences in basic membrane or stimulus response properties statistic analyses were performed using ANOVA or the χ2-test's and post-hoc analysis was performed using LSD. All numerical values in the text refer to mean ± S.E.M.

Acknowledgments

We would like to thank P. Bazzigaluppi for his technical support. This work was supported by ZON-MW VENI (MDJ), NWO, ZON-MW, Neuro-Bsik (Senter), Sensopac (EU), and Prinses Beatrix Fonds (CIDZ).

References

1. *De Zeeuw, C. I., Simpson, J. I., Hoogenraad, C. C., Galjart, N., Koekkoek, S. K. & Ruigrok, T. J. (1998) Trends Neurosci 21, 391-400.*
2. *Llinas, R. & Yarom, Y. (1981) J Physiol 315, 549-67.*
3. *Llinas, R. & Yarom, Y. (1986) J Physiol 376, 163-82.*
4. *Llinas, R., Baker, R. & Sotelo, C. (1974) J Neurophysiol 37, 560-71.*
5. *Benardo, L. S. & Foster, R. E. (1986) Brain Res Bull 17, 773-84.*
6. *Llinas, R. & Yarom, Y. (1981) J Physiol 315, 569-84.*
7. *Chorev, E., Yarom, Y. & Lampl, I. (2007) J Neurosci 27, 5043-52.*
8. *De Zeeuw, C. I., Wylie, D. R., DiGiorgi, P. L. & Simpson, J. I. (1994) J Comp Neurol 349, 428-47.*
9. *Voogd, J. & Glickstein, M. (1998) Trends Neurosci 21, 370-5.*
10. *De Zeeuw, C. I., Holstege, J. C., Ruigrok, T. J. & Voogd, J. (1989) J Comp Neurol 284, 12-35.*
11. *Sasaki, K., Bower, J. M. & Llinas, R. (1989) Eur J Neurosci 1, 572-586.*
12. *De Zeeuw, C. I., Lang, E. J., Sugihara, I., Ruigrok, T. J., Eisenman, L. M., Mugnaini, E. & Llinas, R. (1996) J Neurosci 16, 3412-26.*
13. *Lang, E. J. (2002) J Neurophysiol 87, 1993-2008.*
14. *Welsh, J. P., Lang, E. J., Sugihara, I. & Llinas, R. (1995) Nature 374, 453-7.*
15. *Lang, E. J., Sugihara, I. & Llinas, R. (2006) J Physiol 571, 101-20.*
16. *De Zeeuw, C. I., Chorev, E., Devor, A., Manor, Y., Van Der Giessen, R. S., De Jeu, M. T., Hoogenraad, C. C., Bijman, J., Ruigrok, T. J., French, P., Jaarsma, D., Kistler, W. M., Meier, C., Petrasch-Parwez, E., Dermietzel, R., Sohl, G., Gueldenagel, M., Willecke, K. & Yarom, Y. (2003) J Neurosci 23, 4700-11.*
17. *Leznik, E. & Llinas, R. (2005) J Neurophysiol 94, 2447-56.*
18. *Long, M. A., Deans, M. R., Paul, D. L. & Connors, B. W. (2002) J Neurosci 22, 10898-905.*
19. *Yarom, Y. & Llinas, R. (1987) J Neurosci 7, 1166-77.*
20. *Bal, T. & McCormick, D. A. (1997) J Neurophysiol 77, 3145-56.*
21. *Urbano, F. J., Simpson, J. I. & Llinas, R. R. (2006) Proc Natl Acad Sci U S A 103, 16550-5.*
22. *Friedberg, M. H., Lee, S. M. & Ebner, F. F. (1999) J Neurophysiol 81, 2243-52.*
23. *Guedel, A. E. (1920) Signs of inhalational anesthesia (Macmillan, New York).*
24. *Leznik, E., Makarenko, V. & Llinas, R. (2002) J Neurosci 22, 2804-15.*
25. *Kistler, W. M. & De Zeeuw, C. I. (2002) Neural Comput 14, 2597-626.*
26. *De Zeeuw, C. I., Holstege, J. C., Ruigrok, T. J. & Voogd, J. (1990) Neuroscience 34, 645-55.*
27. *Ruigrok, T. J. & Voogd, J. (1995) Eur J Neurosci 7, 679-93.*
28. *Voogd, J. & Bigaré, F. (1980) The inferior olivary nucleus. Raven Press New York., 207-305.*
29. *Placantonakis, D. G., Schwarz, C. & Welsh, J. P. (2000) J Physiol 524 Pt 3, 833-51.*
30. *Gellman, R., Gibson, A. R. & Houk, J. C. (1985) J Neurophysiol 54, 40-60.*
31. *Leonard, C. S., Simpson, J. I. & Graf, W. (1988) J Neurophysiol 60, 2073-90.*
32. *Tso, M. M., Blatchford, K. L., Callado, L. F., McLaughlin, D. P. & Stamford, J. A. (2004) Neurochem Int 44, 1-7.*
33. *Devor, A. (2002) Cerebellum 1, 27-34.*
34. *Onodera, S. & Hicks, T. P. (1995) J Comp Neurol 361, 553-73.*
35. *Margrie, T. W., Brecht, M. & Sakmann, B. (2002) Pflugers Arch 444, 491-8.*

2.2 Role of gap junctions in olivary signalling

Summary

Many brain regions contain neurons that are coupled by electrical synapses allowing signals to traverse directly from one neuron to the other with minimal delay. In mammals the level of coupling in the inferior olive is probably higher than in any other brain region. Yet, the functional role of this phenomenon in cerebellar motor control remains to be determined. Here, we subjected mice that lack coupling among their olivary neurons to paradigms that require learning-dependent timing. Cx36-deficient mice showed impaired timing of both locomotion and eyeblink responses that were conditioned to a tone. The timing of spike activities generated in the olive of coupling-deficient mice was abnormal in that their latencies in response to the unconditioned stimulus were significantly more variable than those in wild types. Whole cell recordings of olivary neurons *in vivo* showed that the differences in spike timing result at least in part from altered interactions with their subthreshold oscillations. These results, combined with analyses of olivary activities in computer simulations at both the cellular and systems level, suggest that electrotonic coupling among olivary neurons is essential for proper timing of their action potentials and thereby for learning-dependent timing in cerebellar motor control.

Introduction

More than a century ago in 1906 Santiago Rámon y Cajal received the Nobel Prize for the neuron doctrine stating that neurons operate as anatomically and functionally distinct cellular units in the mammalian brain. This tenet still holds, but over the past decade the neuron doctrine has been complemented by new discoveries about the constitution, distribution and cell physiological functions of neuronal gap junctions that can establish cytoplasmic continuity among large ensembles of neurons (Bullock et al., 2005). Importantly, in 1998 groups led by Condorelli (Condorelli et al., 1998) and Willecke (Sohl et al., 1998) cloned the first gap junction protein, i.e. Connexin36 (Cx36), that is predominantly expressed by neurons. The identification of this protein allowed several groups to study the distribution of Cx36 and/or to create mouse mutants to investigate the cellular consequences of a lack of Cx36 in the brain (Bennett and Zukin, 2004; Connors and Long, 2004). To date, Cx36 and neuronal gap junctions are widely distributed in regions such as the olfactory bulb, hippocampus, cerebral cortex, (hypo)thalamus and inferior olive (De Zeeuw et al., 1995). For most of these regions the possible role of neuronal gap junctions has been determined at the cell physiological level (Deans et al., 2001; Landisman et al., 2002; Long et al., 2002 and 2005); In these *in vitro* studies a lack of Cx36 generally leads to an absence of electrotonic coupling and to changes in subthreshold activities (Buhl et al., 2003; De Zeeuw et al., 2003; Long et al., 2002). Yet, for most of the brain systems mentioned above the apparent behavioural phenotype is relatively mild and/or remains a topic for systems electrophysiological investigations (Deans et al., 2001; Guldenagel et al., 2001; Frisch et al., 2005; Long et al., 2005; but see also Deans et al., 2002 for studies on retina). With regard to the olivocerebellar system previous behavioural studies on Cx36-/- mutants showed no ataxia and a relatively normal motor performance (Kistler et al., 2002). This lack of a clear phenotype during natural motor behaviour is remarkable, because in mammals the density of gap

junctions in the inferior olive is probably higher than in any other brain region (De Zeeuw et al., 1995). Here we show that although Cx36-/- mutants have no prominent general motor deficits, they do show problems when challenged to perform a learning-dependent motor task such as conditioning their locomotion pattern or eyeblink response to a tone. In these learning tasks the timing of the motor responses is modified by conditioning the movement to a conditioned stimulus (CS) that starts before, but co-terminates with, an unconditioned stimulus (US) (Garcia and Mauk, 1998; Koekkoek et al., 2003; Perrett et al., 1993). The CS is probably conveyed by the mossy fiber - parallel fiber system to the Purkinje cells in the cerebellar cortex, while the US is conveyed by their climbing fibers originating from the inferior olive (De Zeeuw and Yeo, 2005; Hesslow et al., 1999). Thus, in the current study we investigated the hypothesis that appropriate timing of conditioned motor responses critically depends on the precise temporal coding of the activities of coupled neurons in the inferior olive (De Zeeuw et al., 1998; Leznik et al., 2002; Placantonakis et al., 2004).

Results

Deficits in locomotion conditioning

To quantify their general level of motor performance Cx36-/- mutants (C57BL/6 background; n = 16) and wild type littermates (n = 18) were trained to walk on the Erasmus ladder. The Erasmus Ladder is formed by 2 x 37 rungs positioned between a start- and end-box across which the mice can run back and forth (Figure 1A, left panel) (see also supplementary material A). Each rung on both the left and right side is equipped with a pressure sensor, which is continuously monitored. Based on instantaneous analysis of the activities of these sensors, the walking pattern of the mice can be predicted in the millisecond range, and, if wanted, interrupted by moving each individual rung up or down. Initially, the mice were trained with the even numbered rungs on the left side and the odd numbered rungs on the right side in a descended position so as to create an alternated stepping pattern with 30 mm gaps (Figure 1A, right panel). In this paradigm the Cx36-/- mutants and wild type littermates showed a similar overall average steptime, which was defined as the time needed to place the front paw from one rung to the other (358 ms ± 29 SD for Cx36-/- mutants and 339 ms ± 23.5 SD for wild types), and a comparably low number of missteps, which were identified by touches on the descended rungs ($p > 0.10$ for each session; t-test; Figure 1B). For comparison we also tested *Lurcher* mice (C57BL/6 background; n = 9), which lack Purkinje cells and which are known to show cerebellar ataxia (Porras-Garcia et al., 2005; Van Alphen et al., 2002). Indeed, these spontaneous mouse mutants showed longer steptimes (589 ms ± 49 SD; $p < 0.01$ in both cases; t-tests) and 3 to 4 times more missteps than the Cx36-/- mutants or their wild type littermates ($p < 0.0001$ and $p < 0.0001$ for each session; t-tests). Thus, in line with previous rotarod tests (Frisch et al., 2005; Kistler et al., 2002), we conclude from this test on the Erasmus Ladder that Cx36-/- mutants show, in contrast to *lurcher* mice, a relatively normal motor performance.

To find out whether the ability for motor learning is affected in Cx36-/- mice,

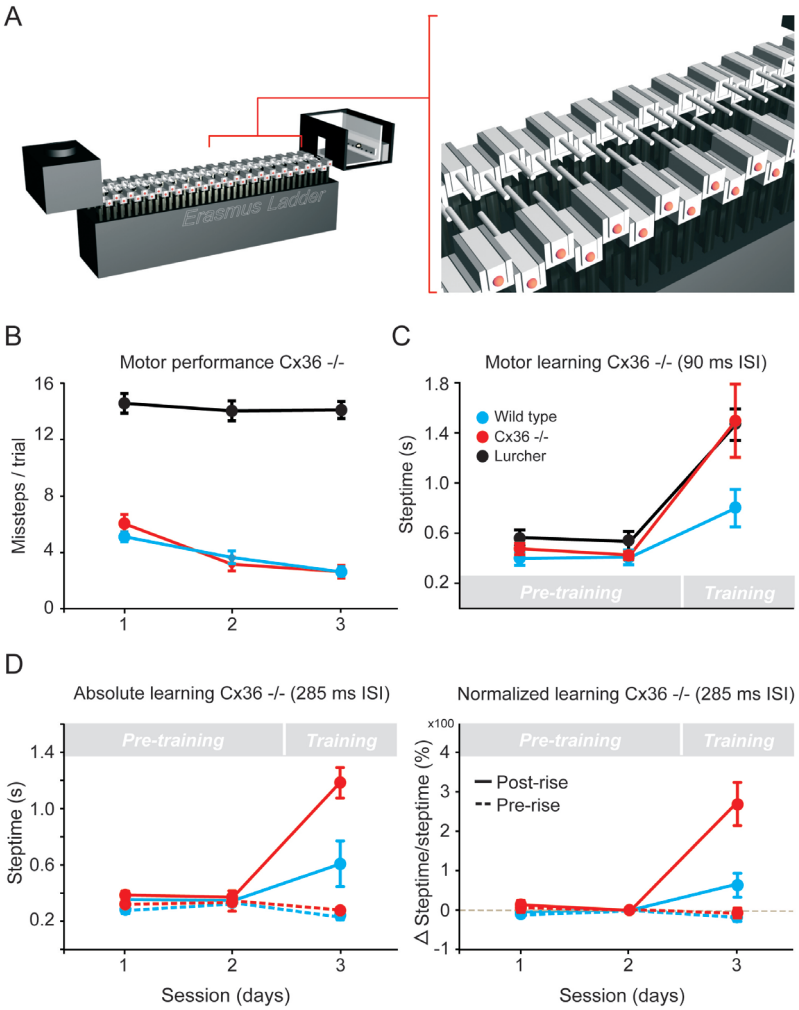

Figure 1. Erasmus Ladder test for detecting performance and learning deficits in locomotion. A, The Ladder consists of 2 x 37 horizontal rungs placed in between 2 shelter-boxes. Mice are trained to walk from one side to the other using air pressure devices placed in the bottom of the boxes. The rungs, which are all equipped with pressure sensors, can be moved up or down under the control of a linked computer system that can analyse the walking pattern instantaneously during locomotion. B, Motor performance level is revealed by the amount of descended rungs touched, which represents the number of missteps. Cx36-/- mutants (red) and wild type littermates (blue) show normal motor performance, while Lurcher mice (black) show deficits in performance during all sessions. C, Motor learning level is revealed by the change in steptime after and before conditioning (i.e. training vs pre-training). During conditioning trials a randomly selected rung rises 12 mm above the walking level to create a perturbation; this unconditioned stimulus occurs at a fixed moment (interstimulus interval; ISI) after the onset of the conditioned stimulus (a 15 kHz tone). Both Cx36-/- mutants and Lurcher mice reveal difficulties in motor learning as compared to wild types. D, While the data obtained in C have been obtained with an ISI of 90 ms, these data have been obtained with an ISI of 285 ms. Note that the deficits in learning-dependent timing are just as pronounced with this longer ISI regardless whether they are revealed in an absolute (left) or normalized (right) fashion. The normalized data show values with respect to those obtained in session 1. Also note that the steptimes in the phase preceding the rise of the rung (pre-rise) are not prolonged during the training (dotted curves). Values indicate mean ± SD.

we subjected them to a conditioning paradigm in which they were trained to make a new locomotion movement using a 15 kHz tone as the CS and a rising rung as the US (ISI of 90 ms; see also supplemental material A). A training session consisted of 8 blocks of 8 trials, which were separated by an intertrial interval of 8 to 12 s. As described above for the initial motor performance test, during the preconditioning sessions the steptime was not different among Cx36-/- mutants and wild-type littermates ($p > 0.25$; t-test). However, as soon as the conditioning procedure started, the front paw steptime in the mutants increased significantly compared to that of the wild types ($p < 0.05$; t-test). In fact, this increase in steptime was comparable to that observed in *lurchers* (Figure 1C). The difference among Cx36-/- mutants and wild types remained when we prolonged the interstimulus (CS – US) intervals from 90 ms to 285 ms ($p < 0.001$; t-test) (Figure 1D).

Since the Cx36-/- mutants lack Cx36 from early on and may therefore show compensations within the olivary neurons (De Zeeuw et al., 2003), we also tested the same conditioning Erasmus Ladder paradigm in wild type mice following application of drugs that can block olivary coupling instantaneously (Blenkinsop and Lang, 2006; Martin and Handforth, 2006; Placantonakis et al., 2006; but for potential general side effects on intrinsic or synaptic mechanisms see Cruikshank et al., 2004; Rozental et al., 2001). We either applied carbenoxolone systemically (40 mg/kg) just before two motor performance sessions and just before the first of a series of three conditioning sessions ($n = 5$), or we made intra-olivary injections with mefloquine (150 μM) one day before a series of three conditioning sessions ($n = 4$) (for impact of dosages of drugs see also Gareri et al., 2005; Margineanu and Klitgaard, 2006). In these experiments we also found a significantly greater increase in the front paw steptime of the coupling-deficient animals after, but not before, conditioning than in control animals ($n = 6$ and $n = 5$, respectively) which received injections with vehicle only ($p < 0.002$ and $p < 0.001$, respectively; t-tests) (Figures 2A, 2B and 2C). In the case of carbenoxolone the impact of the drug on conditioning tapered off more quickly than that observed after the mefloquine injections (at session 4, $p < 0.05$; t-test); this difference may be due to a relatively strong and fast clearance of carbenoxolone (Martin and Handforth, 2006; Saffitz et al., 2000).

Taken together, the experiments on the lurcher mice and on the animals subjected to intra-olivary injections described above showed that the Erasmus Ladder allows us to detect specific deficits in both cerebellar motor performance (lurcher) and cerebellar motor learning (pharmaceutical manipulation of the olive). We can therefore conclude that genetic or pharmaceutical blocking of olivary coupling mediated by Cx36 has relatively little affect on cerebellar motor performance, while it probably does affect cerebellar motor learning in that the training process is slowed down substantially.

Deficits in eyeblink conditioning

Analysis of the locomotion conditioning process described above suggests that learning-dependent timing is affected in Cx36-/- mice. However, in this paradigm the movements are analysed in discrete steps, which makes it virtually impossible to identify the exact deficits over time during continuously recorded ongoing locomotion movements. Thus, to further investigate the potential role of Cx36 in learn-

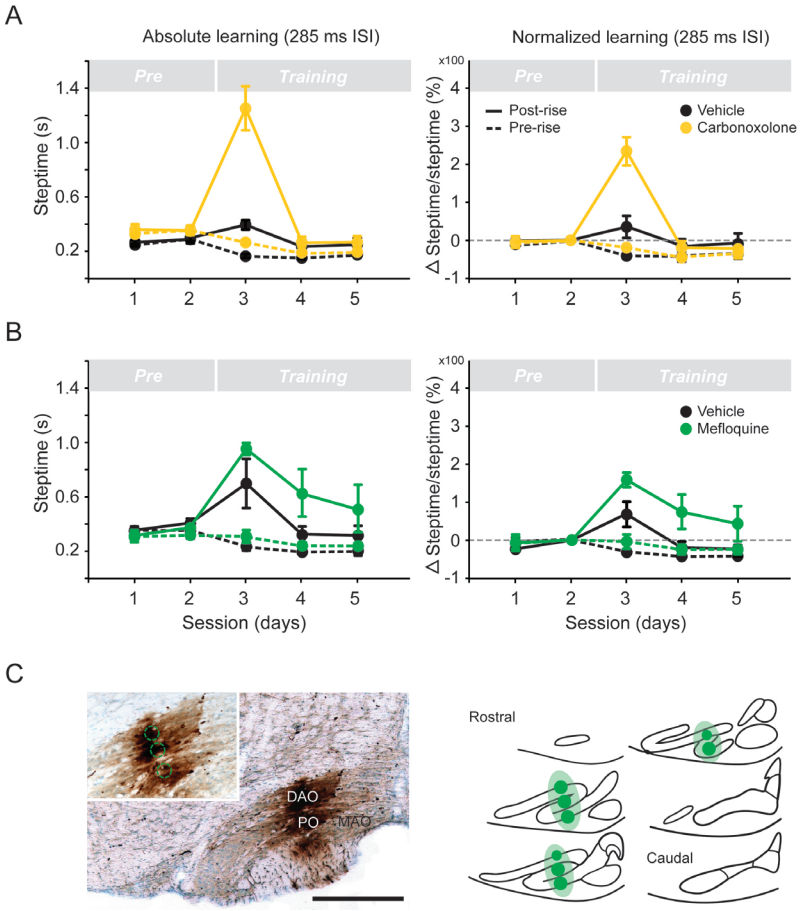

Figure 2. Systemic applications of carbenoxolone or intra-olivary injections of mefloquine affect learning-dependent timing. A, Carbenoxolone was injected ip just before the two motor performance sessions (Pre) and just before the first of a series of three conditioning sessions (Training). B, Mefloquine was injected bilaterally inside the inferior olive one day before the series of the three conditioning sessions. C, Example of one of the reconstructions of the injection site in the olive following BDA labelling. Values indicate mean ± SD.

ing-dependent timing, we compared the Cx36-/- mutants with wild type littermates in an eyeblink conditioning paradigm. For this paradigm, the motor responses can be continuously measured using the magnetic distance measurement technique (MDMT; Koekkoek et al., 2002). We subjected adult Cx36-/- mutants (n = 8) and wild type littermates (n = 8) to a conditioning paradigm using a tone as the CS and an air puff as the US at interstimulus intervals (ISIs) of 350 ms. Here too, the 8 daily training blocks consisted of 8 trials (1 US-alone, 6 paired, and 1 CS-alone). After four paired training sessions (T-1 to T-4) the percentage of conditioned responses and their average peak amplitude in wild types reached levels of 77 % and 0.48 mm, respectively, while those in Cx36-/- mice had values of 78 % and 0.56 mm. These values were not significantly different ($p > 0.9$ and $p > 0.5$; MANOVA for repeated measures; adjusted for multiple comparisons via Bonferroni correction). In contrast,

the timing properties of the conditioned responses differed dramatically among the wild types and Cx36-/- mutants as the training proceeded. While in wild types the average latency to peak amplitude of the conditioned eyelid responses was appropriately fixed at the moment when the US occurs, the timing in mutants got worse during the four training sessions (Figure 3A; see also supplementary material B). At the end of the training the average latency to peak amplitude in the mutants preceded the moment of the US by 196 ms (± 27 SD), which was significantly different from that in wild types (80 ms ± 24 SD; $p < 0.005$; t-test) (see also Figure 3D). These data indicate that coupling-deficient mutants cannot appropriately time their movements when challenged in a conditional task.

Still, these eyeblink experiments on the global Cx36 null-mutants do not directly demonstrate that the behavioural phenotype can be attributed solely to a lack of coupling in the inferior olive. GABAergic neurons in many brain regions including those in the cerebellar nuclei also show a prominent expression of Cx36 (Degen et al., 2004; Van Der Giessen et al., 2006), and a lack of this expression may therefore in principle also affect any cerebellar conditioning paradigm (Bengtsson and Hesslow, 2006). To address this potential caveat, we generated mutant mice in which the expression of Cx36 is ablated in the GABAergic neurons of the brain, while that in the relevant olivary neurons, which are all non-GABAergic, is normal (Figures 3B and 3C). These mutants (n = 4), which were cross-breedings of floxed-Cx36 mutants and Parvalbumin-Cre mice, lacked expression of Cx36 in for example the GABAergic neurons of the thalamus, olfactory bulb, cerebral cortex, hippocampus and cerebellar nuclei that express Parvalbumin (see also Seto-Ohshima et al., 1989), whereas the neurons in the dorsal accessory olive that are involved in eyeblink conditoning showed a normal level of Cx36. The Pv-Cre/cx36lox cross-bred mutants showed the same conditioned eyeblink responses as the wild types, i.e. without any deficits in their timing (Figures 3A and 3D). These data indicate that in the global Cx36-/- knockout it is most likely the deficits in the olive that are responsible for the abnormalities in learning-dependent timing. For the same argument, it is also particularly relevant to find out whether the coupling among the stellate cells in the cerebellar cortex is affected in both the global and floxed-Cx36 mutant mice (Mann-Metzer and Yarom, 1999). We therefore investigated the constitution of the gap junctions between these cells. It turned out that the vast majority of these interneuronal gap junctions is formed by Connexin45 (see eg. Fig. 5 in Van Der Giessen et al., 2006) rather than Cx36 (analysis of material from Degen et al., 2004). Thus, we conclude that Cx36-/- mutants show deficits in learning-dependent timing and that this behavioural deficit is likely due to an impairment of electrotonic coupling in the inferior olive.

Abnormal temporal pattern of climbing fiber responses

If the deficits in learning-dependent timing are due to a lack of coupling between the olivary neurons, one expects that the timing properties of the activities in these neurons are disrupted in Cx36-/- mutants. To investigate these properties we recorded the climbing fiber activities of Purkinje cells in the cerebellar cortex that reveal the olivary signals of the US during eyeblink conditioning (Hesslow, 1994; Mauk et al., 1986). The climbing fiber activities of Purkinje cells, also called complex

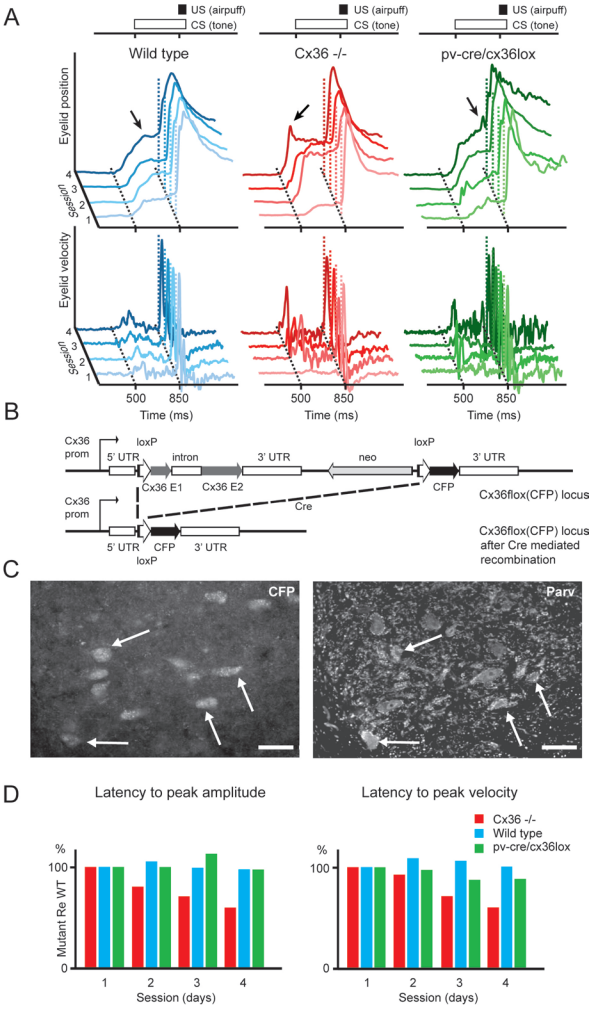

Figure 3. A lack of coupling by Cx36 gap junction proteins in the inferior olive, but not in the cerebellar nuclei, results in impaired learning-dependent timing. A, Representative examples of eyeblink traces in a wild type (blue), global Cx36-/- mutant (red), and Cx36del(lacZ)/flox(CFP) : Parvalbumin-Cre control mouse (green). They all show conditioned eyeblink responses after 4 training sessions using a tone as the conditioned stimulus (CS) and an air puff as the unconditioned stimulus (US). However, while the timing of the learned response in wild types and floxed-Cre control mice improves over the sessions, that in the global Cx36-/-mutants gets worse (see arrows). B, Genetic design of floxed-Cx36 mutants crossbred with Parvalbumin-Cre mice, which were used as controls. C, The Cx36del(lacZ)/flox(CFP) : Parvalbumin-Cre control mice showed CFP staining in their cerebellar nuclei neurons demonstrating that Cx36 has been floxed in these neurons and thus not expressed. Immunostaining for parvalbumin of the same sections (right panel) showed that most of the cerebellar nuclei neurons indeed express parvalbumin (arrows) and that they would otherwise in the non-floxed situation express Cx36. Thus, the Cx36del(lacZ)/flox(CFP) : Parvalbumin-Cre control mice do not express Cx36 in their cerebellar nuclei, while their expression in the relevant olivary subnuclei is normal (data not shown). Punctate labelling in neuropil of the right panel reflects staining of axonal fibers. D, While the latency to peak amplitude (left panel) in the global knock outs of Cx36 (red) got worse during the training sessions, that in the Cx36del(lacZ)/flox(CFP) : Parvalbumin-Cre control mice (green) was indistinguishable from that in their unaffected littermates (blue). Similarly, the average latency to peak velocity (right panel) in the mutants was also significantly reduced ($p < 0.01$; t-test).

spikes, generally reflect the temporal coding of olivary neurons rather precisely, because they are generated in an all-or-none fashion (Thach, 1967). We found that the Purkinje cells that respond well to air puff stimulation are in the mouse situated in an area covering both lobulus simplex in the hemisphere and the adjacent part of lobule VI in the posterior lobe (Figure 4A). In awake wild types (n = 9) the air puff stimulation evoked virtually only short-latency climbing fiber responses; these responses had an average peak latency of 29 $\pm$ 9 ms (SD; averaged over the 9 animals) over 879 successful stimulations (> 70% successful). In contrast, in all Purkinje cells recorded in the Cx36-/- mutants (n = 10) the same peri-oribital stimulation evoked both short-latency responses (average to peak of 30 $\pm$ 7 ms) and long-latency responses (101 $\pm$ 17 ms) (Figure 4B). Of all successful stimulations (n = 1036; > 75% successful) in the mutants 60% and 34% resulted in pure short-latency and pure long-latency responses, respectively, while 6% resulted in both a short-latency and long-latency response. These differences in the temporal distribution patterns following peripheral stimulation were highly significantly different among wild types and mutants ($p < 0.001$; t-tests). Similarly, during spontaneous activity in the awake state the Cx36-/- mutants showed significantly ($p < 0.01$; t-test) more doublets of two or three climbing fiber responses occurring within 200 ms (12 $\pm$ 6 %, SD) than wild types (5 $\pm$ 2 %, SD) (Figure 4C, upper panel), while their mean interspike interval within a doublet was significantly smaller (123 $\pm$ 11 ms in Cx36-/- mutants re 140 $\pm$ 12 ms in wild types; $p < 0.01$; t-test) (Figure 4C, middle panel). This difference was also reflected by a generally increased coefficient of variation for spike intervals ($p < 0.02$; t-test) (Figure 4C, bottom panel). All these differences in complex spike activities were not influenced by differences in average firing frequencies, because the average complex spike frequency was not significantly different among wild types and Cx36-/- mutants (0.94 $\pm$ 0.19 re 1.00 $\pm$ 0.26; $p > 0.4$; t-test; cf. Marshall et al., 2007 for differences in anaesthetized state). Likewise, the shape of the climbing fiber responses and the average number of spikelets within the complex spikes (Figure 4B) as well as the average firing rate (67 $\pm$ 13 re 69 $\pm$ 14) and coefficient of variation (0.68 $\pm$ 0.2 re 0.57 $\pm$ 0.2) of simple spike activities of the mutants were also not different from those in wild types. Thus, Purkinje cells in awake mice lacking Cx36 show robust differences in the temporal pattern of their climbing fiber responses, but not in the average firing frequencies of their ongoing activities.

Altered correlation between spiking activities and subthreshold oscillations

To explain the differences in latencies and spiking patterns following peri-orbital stimulation described above, we investigated the activities of olivary neurons using whole cell recordings *in vivo* in anaesthetized animals (for numbers of cells and details see Table 1). The majority of the neurons in wild types showed pronounced subthreshold oscillations that either had a clear sinusoidal appearance, a more complex rhythmic shape, which probably corresponds to the activation of low threshold calcium conductances (Llinas and Yarom, 1981), or both types of subthreshold activities (Figure 5A) (see also Khosrovani et al., 2007). In the mutants the same types of oscillating cells were observed, but they showed significantly more cells that did not oscillate ($p < 0.01$; χ^2-test) and the occurrence of their oscillations depended significantly stronger on the membrane potential ($p < 0.01$; t-test) as previously described

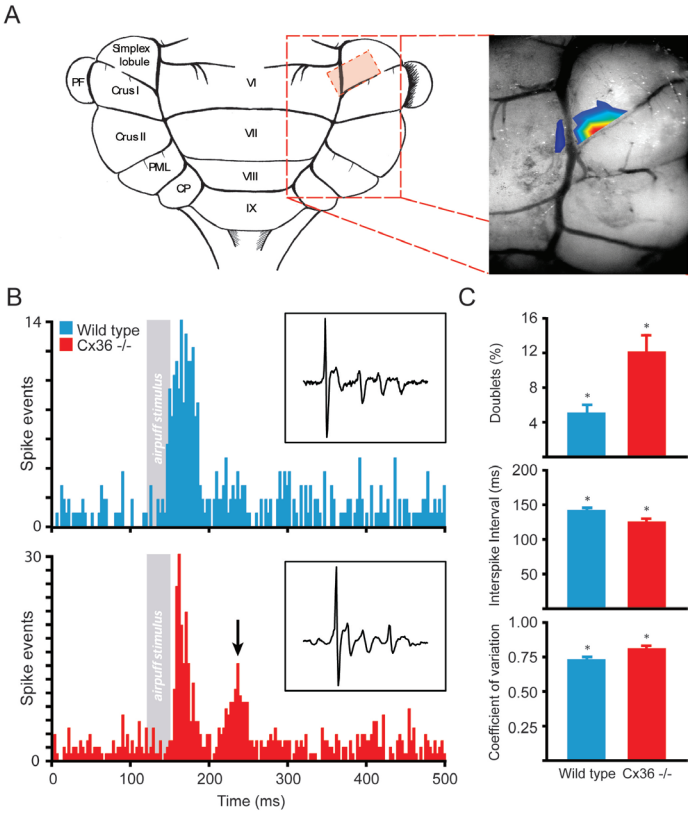

Figure 4. A lack of coupling of inferior olivary neurons results in altered timing of climbing fiber activities in the cerebellar cortex. A, Purkinje cells that responded well to air puff stimulation (i.e. US) were situated in an area covering the lobulus simplex in the hemisphere and the adjacent part of lobule VI in the posterior lobe. Colour codings correspond to the percentage of the Purkinje cells that responded with complex spike activities to air puff stimulation; red, yellow, green, light blue and dark blue indicate success rates of 50%, 40%, 30%, 20% and 10%, respectively. B, Air puff stimulation evoked only short-latency climbing fiber responses in awake wild types (blue) (latency of 29 ± 9 ms), while in the Cx36-/- mutants (red) the same peri-oribital stimulation evoked both short-latency (30 ± 7 ms) and long-latency responses (101 ± 17 ms) (arrow). Note that in both cases units on Y-axis represent two spikes. Insets show typical complex spike responses in wild types (top) and mutants (bottom) in a 8 ms trace; no differences were observed in the shape. C, During spontaneous activity in the awake state the Cx36-/- mutants showed significantly more doublets of two or three complex spikes occurring within 200 ms ($p < 0.01$; t-test), a significantly smaller mean interspike interval within these doublets ($p < 0.01$; t-test), and a general increased coefficient of variation for spike intervals ($p < 0.02$; t-test). Values indicate mean ± SD.

for *in vitro* conditions (Long et al., 2002; De Zeeuw et al., 2003) (Figures 5B and 5C). Power spectra of the oscillating subthreshold activities showed that the frequencies of the oscillations occurred in both wild types and mutants mostly in the range of 1 to 3 Hz or in the range of 6 to 9 Hz (Figure 5D). Similarly, action potentials of olivary cells in both wild types and mutants showed a so-called capacity to reset the subthreshold oscillation (see also Leznik et al., 2002; Leznik and Llinas, 2005; Khosrovani et al., 2007). Still, the olivary activities differed in that the oscillations of the wild type neurons often showed dynamic crescendo amplitudes starting directly after the generation of an action potential (crescendo amplitudes were defined

as at least a 3-fold increase of the amplitude over 5 cycles), while those in the mutants showed significantly more ($p < 0.05$; t-test) constant amplitudes (Figure 5A). Moreover, the relationship between the preferred frequencies of the subthreshold oscillations and those of the olivary spiking activities was less tight in the Cx36 null-mutant (mean residual scores of 1.33 re 0.63; $p < 0.01$; t-test) (Figure 5D). Interestingly, this reduced correlation is in line with the observation that the olivary spikes occurred significantly more often ($p < 0.05$; t-tests) during the peak period of an oscillation in wild types than in mutants (peak period is defined as the period plus or minus 90 degrees from the peak) (right panel in Figure 5C; see also arrows in Figure 5A). These differences in interactions between spike generation and subthreshold oscillations also occurred following peripheral stimulation as used in the conditioning paradigms described above (Figure 5E). Following peripheral stimulation the frequency of the subsequent oscillations in the mutant cells was significantly less stable ($p < 0.02$; t-test) than in the wild types (for quantification of first four cycles after stimulus see Figure 5F). Thus, peripheral sensory stimulation can indeed induce and modify the subthreshold activities and such modulation can influence the timing of subsequent spiking activities of olivary neurons when they are appropriately coupled. Therefore, the altered timing of the climbing fiber signals mediating the US in the coupling-deficient Cx36-/- mutants can at least in part be explained by altered interactions with their subthreshold oscillations.

How may a lack of coupling among olivary neurons in the Cx36-/- mutant lead to altered spiking?

If the lack of coupling between olivary neurons indeed leads to altered timing of their action potentials due to altered interactions with their subthreshold oscillations, we should be able to find similar relations and characteristics in a simulation of olivary neurons. To this end we used a modified version of a two-compartmental olivary cell model by Schweighofer et al. (1999) (Figure 6 and supplementary material C including videos). Since direct responses to depolarizing pulses in the olive are generally not delayed for periods of time near 100 ms (Simpson et al., 1996; Khosrovani et al., 2007), while long-latency responses due to reverberating loops can be readily found when the network is affected (Ruigrok and Voogd, 1995; De Zeeuw et al., 1998), the secondary response found in Cx36-deficient mice is probably caused by another input. Therefore, we applied to both the normal and coupling-deficient situation depolarizing currents timed ~100 ms apart, of which the second was assumed to be caused by a reverberating loop. In both wild type and Cx36-/- mutant cells, the modelled reverberating loop stimulation was in itself, i.e. without the priming induced by the first input, never strong enough to generate an action potential.

The single-cell behaviour of the model closely resembled that of its biological counterpart as described in the current and previous work (De Zeeuw et al. 2003). Both cell models oscillate at ~9 Hz, have preferred firing windows on the upward slopes of sub-threshold oscillations, exhibit differentially damped oscillations after an action potential and undergo a phase change (resetting effect) upon stimulation (Figure 6A). The Cx36-deficient cells exhibited sub-threshold oscillations with a slightly larger amplitude than that of the wild type cells and had an increased

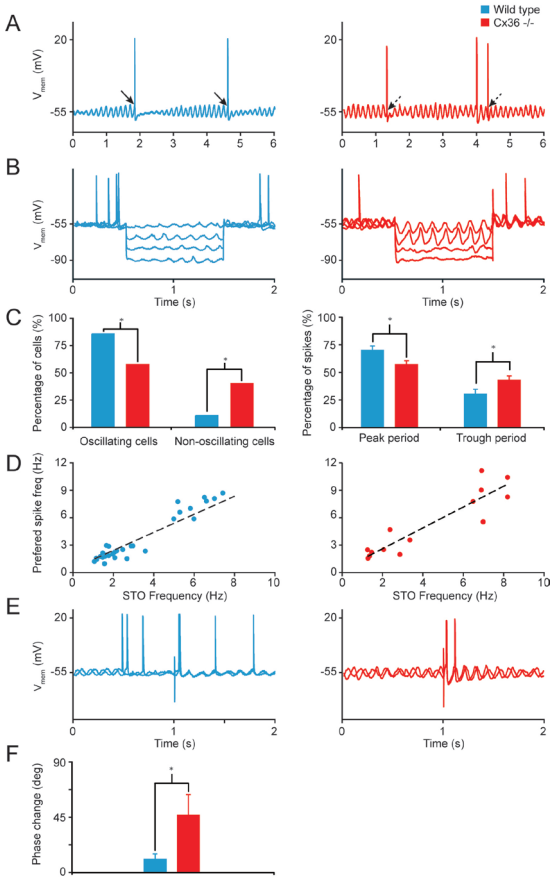

Figure 5. A lack of electrotonic coupling in the inferior olive results in altered interactions between subthreshold oscillations and generation of spiking activities. A, Examples of whole cell recordings of olivary neurons in a wild type (blue) and Cx36-/- mutant (red) in vivo. Most of the olivary spikes in the wild type occurred around the peak of the oscillations (solid arrows), while those in the mutant frequently also occurred in the trough area (dashed arrows). B, Subthreshold oscillations also occurred during hyperpolarizing steps (100 pA) in both wild types and mutants; however, as observed in vitro (Long et al., 2002; De Zeeuw et al., 2003) the oscillations in the mutants depended stronger on the membrane potential. C, Left panel; percentages of oscillating and non-oscillating cells differed significantly among wild types and Cx36-/- mutants; asterisks indicate significance level $p < 0.01$ (χ^2-test). Right panel; when oscillating the percentage of spikes that occurred in the peak period was significantly lower in Cx36-/- mutants, while that in the trough period was significantly higher ($p < 0.05$; t-tests). These periods are defined as the peak amplitude plus or minus 90 degrees and the through amplitude plus or minus 90 degrees, respectively. Percentages indicated are mean values, while error bars indicate SD. D, Power spectra showed that the frequencies of both the oscillations and spikes occurred in both wild types and mutants mostly in the range from 1 to 3 Hz and from 6 to 9 Hz. However, the correlation between the preferred frequency of the oscillations and that of the spiking activities was significantly stronger in the wild types ($p < 0.01$; t-test). E, Examples of action potentials and subthreshold oscillations in wild types (left) and Cx36-/- mutants (right) before and after peripheral stimulation. In both types of animals the peripheral stimulation had a resetting effect in that the oscillations after the occurrence of the stimulus were in phase with each other, while they were out of phase before the oscillations. However, while the phase of the subthreshold oscillation remained stable in the wild type, that in the mutant was unstable. Stimulus artefacts are set at 1. F, The average phase change within the first four cycles of 10 different traces of an individual cell following peripheral stimulation was significantly greater in Cx36-/- mutants than in wild types ($p < 0.02$; t-test; error bar indicates SD).

chance of generating doublets (12% instead of 0% in simulated wild types). Due to dendritic leak currents, the wild type cells were less excitable and had smaller firing windows.

In the multiple-cell simulations electrotonic coupling allowed the ensembles of wild type cells to gradually build up a charge as pulses come in and to synchronize their action potentials on the first input (Figures 6B and 6C, left panels) (see also video in supplementary material C). Still, the coupled wild type neurons did not respond to the reverberant input. In contrast, the Cx36-/- network depended on increased excitability to be able to respond with at least some level of synchrony, reacting as quickly as possible as pulses to different cells arrive in presumably rapid succession (Figure 6B, right panel). Simulations of Cx36-deficient networks showed a dual response as the reverberating loop stimulation was in this case sufficiently effective (Figures 6B and 6C, right panels). Thus when the first input arrived outside the firing window, the second pulse could elicit a response in an uncoupled cell, but not in coupled cells (Figure 6C) (see also videos in supplementary material C). Due to the rebound spikes, dual responses and a wide spread in timing of the action potentials in the Cx36-deficient cells, the sub-threshold oscillations of ensembles of these cells did not synchronize, despite single-cell resetting effects. As a result, the variance in timing of these networks' responses remained high.

How may altered spiking patterns lead to changes in learning-dependent timing?

Our data on evoked climbing fiber activities and the model of olivary activities described above indicate that the temporal firing patterns of olivary cells are destabilized when the cells are not coupled by functional gap junctions. Considering that electrotonic coupling of olivary neurons by Cx36 gap junctions also synchronizes climbing fiber activities of ensembles of Purkinje cells within the same parasagittal zone (Marshall et al., 2007; but cf. Kistler et al., 2002), one can appreciate that the overall defect in the temporal patterns of complex spike activities within the olivocerebellar modules must be substantial. To find out how impaired synchrony of climbing fiber responses may lead to deficits in learning-dependent motor timing, we created and tested a model of the olivocerebellar system controlling conditioned responses (Figure 7; see also extensive supplementary material D). The model is in line with the hypothesis that plasticity associated with learning a conditioned eyeblink response is distributed among the cerebellar cortex and cerebellar nuclei, which may encode the timing of the response and store a representation of the amplitude of the response, respectively (Koekkoek et al., 2003; Mauk and Donegan, 1997; Perret et al., 1993; Raymond et al., 1996). Since a properly functioning cerebellar cortex has been shown to be required for the acquisition and expression of a well-timed conditioned response (Perret et al., 1993), the inability of Cx36-deficient mice to learn an appropriately timed eyeblink response might be partly due to incorrect guidance of plasticity in the cerebellar cortex, which is known to be under climbing fiber control (Coesmans et al., 2004). We therefore investigated the possibility of a causal link between absence of properly synchronously timed climbing fiber activities and impaired cortical plasticity in a network model of an olivocerebellar module (De Zeeuw et al., 1998; De Zeeuw and Yeo, 2005). The model initially analyzes the stability of the strengths of parallel fiber to Purkinje cell synapses during periods when

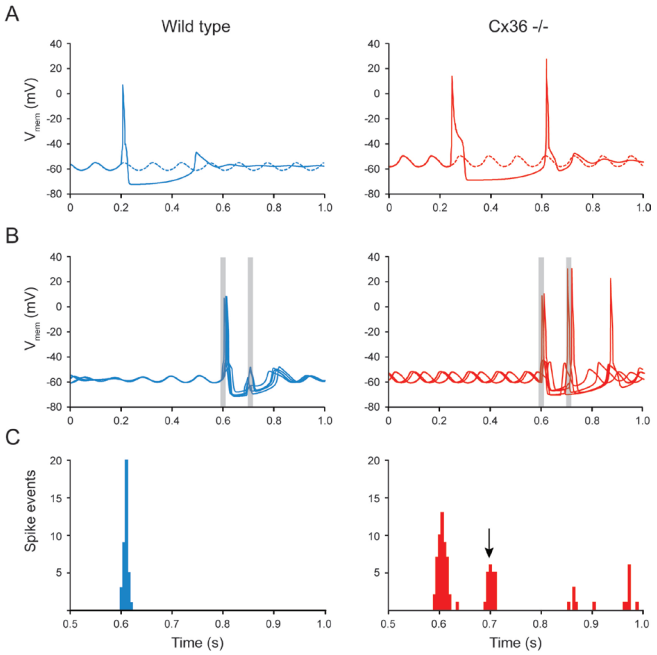

Figure 6. Simulations of wild type (left panel; blue) and Cx36 knock-out (right panel; red) inferior olivary cells using a two-compartmental computational model. A, 1000 ms trace of a wild type cell and a Cx36-deficient cell. Five μA/cm² depolarizing currents are applied for 15 ms. The wild type cell generates a spike and shows temporarily damped oscillations afterwards. The Cx36-deficient cell responds with a doublet, despite the fact that stimulation occurred in the trough. B, 5 traces of 1000 ms from one of the wild type cell ensemble simulations and a Cx36-deficient cell simulation. Due to the random initialization and coupling, the sub-threshold oscillations in the wild type cells are damped at first and increase in amplitude as they become more synchronized (compare to experimental data shown in left panel of Figure 5A). Two depolarizing 15-ms currents (gray bars) are applied at 600 ± 10 ms (SD) (4.5 μA/cm²) and 700 ± 10 ms (SD) (2.5 μA/cm²). Exact onset of the currents was randomly determined per cell. The spike responses of the wild type cells occur in a narrow time window and the second input does not give rise to any action potentials. Thus the wild type network retains its synchronized oscillations. In contrast, due to a lack of coupling the Cx36-deficient cells do not synchronize their oscillations. Their spike responses are not timed closely together, the second pulse also gives rise to action potentials, and doublets occur. Because of these factors, the Cx36-deficient network does not synchronize. C, Temporal distribution of spikes in the wild type and Cx36-deficient networks. The first depolarizing current was applied at 600 ± 10 ms and the second at 700 ± 10 ms. The coupled wild type networks synchronize the first volley of spikes and do not respond to the second pulse. In the Cx36-deficient network the first band consists of approximately the same number of spikes as the wild type response indicated above, but due to a lack of coupling, the spikes are not as synchronized. Because of the increased excitability Cx36-deficient cells also exhibit responses to the second pulse and an increased number of doublets.

active learning is not taking place and when plastic changes of synaptic strengths may occur due to uncorrelated parallel fiber and climbing fiber background activity. Subsequently, the impact of synaptic instability is explored in the situation when associative conditioning occurs, as post-learning (in)stability of parallel fiber synaptic strength might be directly related to the retention of cortical memory. The following basic assumptions form the guiding principles of the model: 1) The olivo-cerebellar system is topographically organized, with Purkinje cells, neurons of the cerebellar nuclei and neurons of the inferior olive connected in discrete closed-loop

modules in which the Purkinje cells converge onto the nuclei (Voogd and Glickstein, 1998) (Figure 7A); 2) the strengths of parallel fiber to Purkinje cell synapses can reversibly increase or decrease, depending for each activated granule cell on the width of the time interval to the climbing fiber stimulus (Coesmans et al., 2004; Wang et al., 2000); and 3) neurons tend to be more active as their excitatory inputs increase and less active as their inhibitory inputs increase (Kenyon et al., 1998).

Based upon these general assumptions, one can deduce that adaptive changes of synaptic strengths within the olivo-cerebellar feedback loop can provide a feedback to control activity in the inferior olive around a stable equilibrium value (Kenyon et al., 1998), and that such equilibrium in activities of olivary neurons may in turn be necessary for synapses in the loop to remain stably fixed at their current strength. In the cerebellar loop it is probably not directly possible for a Purkinje cell to provide a one-to-one feedback to its own climbing fiber, due to the strong convergence of Purkinje cells onto deep cerebellar nuclei neurons (Figure 7A). To enhance the efficiency of this feedback specific sets of olivary neurons may be selectively coupled. In other words, selective coupling of olivary neurons, which together innervate the complete microzone of the Purkinje cells that converge onto the cerebellar nuclei neurons that provide the GABAergic input to the very same olivary neurons, can stabilize the activities in an entire olivocerebellar module.

Thus, the model shows how gap junction coupling in the inferior olive could help to stabilize the weights of parallel fiber to Purkinje cell synapses by synchronizing climbing fiber feedback to Purkinje cells (Figure 7B). When the activity of inferior olivary neurons is not synchronized, as is the case in Cx36-deficient mutants, incorrect feedback through the cerebellar loop causes parallel fiber to Purkinje cell synaptic strengths to drift and finally saturate at their minimum or maximum strengths (Figures 7C and 7D). Such a situation prevents efficient induction and maintenance of synaptic plasticity, which is required for learning and retention of a timed motor response. More specifically, impairment of cortical plasticity might lead to inadequate modulation of the activities in the cerebellar nuclei (Medina and Mauk, 2000). The development of a rectangular 'amplitude' response in the nuclei might then prevent an optimal closure of the eyelid at the moment when the unconditioned stimulus is about to take place (Figure 7E; compare to experimental data shown in Figure 3A) (see also Perret, 1993; Medina and Mauk, 2000).

Discussion

Revealing the electrophysiological mechanisms that underlie the behavioural phenotypes of Cx36-deficient animals remains a topic of intense investigations (Bennett and Zukin, 2004; Buhl et al., 2003; Connors and Long, 2004; Deans et al., 2001; Frisch et al., 2005; Guldenagel et al., 2001; Kistler et al., 2002; Landisman et al., 2002; Long et al., 2005). Here, we showed that a lack of electrotonic coupling in the inferior olive leads to abnormal firing patterns of its neurons, which in turn can contribute to deficits in the timing of conditioned motor responses. The behavioural deficits in the global Cx36-/- mutants could be prominently revealed in different paradigms in which either a locomotion response or an eyeblink response was conditioned to a tone. In both cases conditioned responses occurred, but the timing that had to be learned to make the response optimal was aberrant. In the locomotion test on the

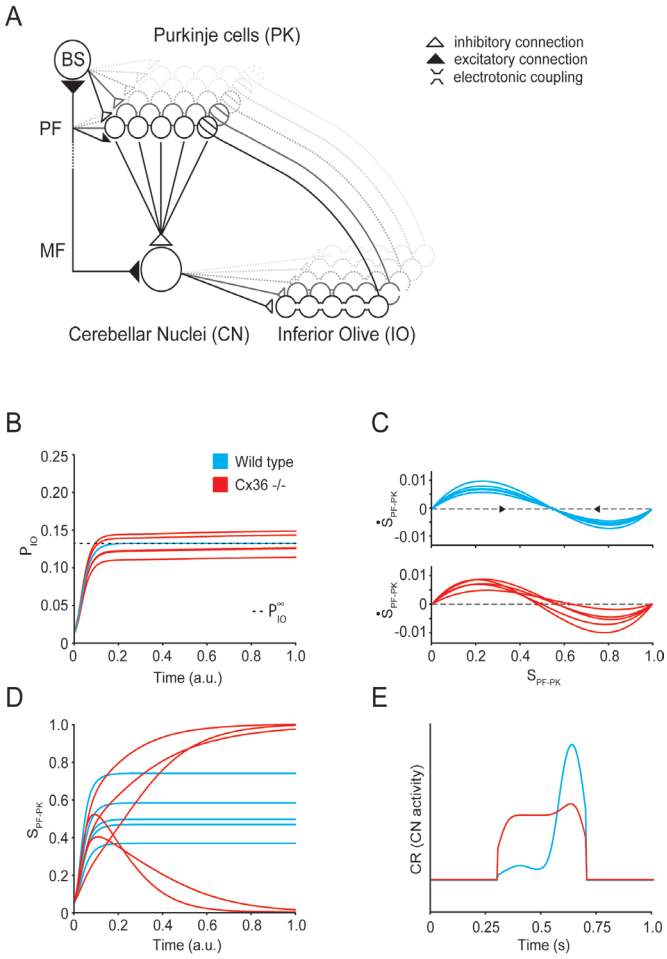

Figure 7. Impact of altered olivary coupling and spiking on learning-dependent timing in a network simulation. For panels A–D, a mathematical model was used to analyze the stability of parallel fiber to Purkinje cell synapses as a function of the average background spike probabilities of parallel fibers and climbing fibers. Panel E displays results from a real-time simulation, which incorporates the findings of the mathematical model in a conditioning paradigm. In the simulations synaptic weights are adjusted according to coincidence rules for parallel fiber and climbing fiber activity. Neural spike probabilities are represented as linear sums of inhibitory and excitatory synaptic inputs; synaptic inputs are defined as the product of presynaptic average activity and synaptic strength. The level of climbing fiber activity is regulated by feedback control through the olivo-cerebellar loop (Kenyon, 1998). A, Connectivity within a cerebellar module; Purkinje cells (PK), neurons of the cerebellar nuclei (CN) and coupled neurons of the inferior olive (IO) form a closed loop (De Zeeuw et al., 1998). A key feature is the strong convergence of Purkinje cells onto CN neurons. MF, PF, and BS indicate mossy fibers, parallel fibers and basket cell / stellate cells, respectively. B, Measure for the spike probability of 5 IO neurons as a function of time. Two different situations are investigated in the model: a synchronized IO, in which IO neurons activate collectively due to electrotonic coupling (wild-types, blue), and an asynchronous IO, in which each individual neuron fires independently at its own rate (Cx36-/- mutants, red). Wild type curves all settle at the same equilibrium value P^{∞}_{IO}, while mutant curves remain above or below this value. C, Phase plots of the average PF to PK synaptic strength S of 5 Purkinje cells in the network. The derivative of S represents the plastic change of S at each time step due to synaptic plasticity. Plasticity is driven by PF activity, i.e. PF activity determines the rate at which plasticity occurs, while the ratio of depression versus potentiation depends on the frequency of climbing fiber

activation. Synaptic strengths are stable when the derivative of S equals zero. Top panel: a synchronous IO produces synchronous climbing fiber activation, such that all Purkinje cells share a common stable state. Bottom panel: in an asynchronous IO, each neuron fires at its own specific rate, resulting in different depression versus potentiation ratios in each Purkinje cell. Thus in this situation each individual Purkinje cell strives for a different state of the network in order to stabilize its synaptic strengths. D, Development of synaptic strengths in time for a synchronous IO (blue) and an asynchronous IO (red). Wild-type Purkinje cells all receive the same stabilizing climbing fiber input, at which depression and potentiation exactly cancel each other over time. Their synaptic strengths therefore remain stable. Cx36-/- mutant Purkinje cells receive climbing fiber inputs that are either above or below equilibrium resulting in too much depression or too much potentiation, respectively. Synapses therefore saturate at their minimum or maximum strengths. E, Eyeblink responses of wild-types (blue) and Cx36-/- mutants (red) resulting from a real-time simulation of the architecture in panel A. An additional plasticity rule was incorporated at the MF to CN synapse, allowing for the development of the 'block' response in the CN. In wild-types inhibitory input from the cortex modulates the 'block' activity in the CN to produce a well-timed response. In Cx36-/- mutants saturation of PF to PK synaptic strengths prevents induction and maintenance of the right levels of depression and potentiation, resulting in insufficient cortical modulation. Details are provided as supplementary material (part D).

Erasmus Ladder Cx36-/- mutants were impaired in learning to avoid a bar that rose after a fixed period after the onset of the tone. Likewise, in the eyeblink test the coupling-deficient mutants showed after four training sessions a mismatch in their latency to peak amplitude of approximately 200 ms with respect to the onset of an air-puff. This period stands in marked contrast to the 10 to 20 ms delay that can be observed in the basic eye movement responses of Cx36 null-mutants to optokinetic stimulation (Kistler et al., 2002) or in the tremorgenic, limb and body movements of coupling-deficient rats treated with replication-incompetent lentiviral vectors (Placantonakis et al., 2004). The behavioural deficits in learning-dependent timing in the Cx36-/- mutants were robust despite secondary compensations that may occur (De Zeeuw et al., 2003). Moreover, we observed the same type of deficits in the conditioning process following application of carbenoxolone and mefloquine, which are known to block olivary coupling in an acute fashion (Blenkinsop and Lang, 2006; Martin and Handforth, 2006; Placantonakis et al., 2006). Although one cannot rule out short-term compensations or side effects with this approach either (Rozental et al., 2001; Cruikshank et al., 2004), still the behavioural effects were significant and similar to those in the global mutants, while they cannot be due to the potential long-term compensations that may occur in the Cx36-/- mutants. Importantly, the effects of mefloquine could be readily observed after injection into the inferior olive itself indicating that it is probably the coupling in the olive that is essential for learning-dependent timing of motor responses. These data in turn were supported by the finding that the abnormal timing of the conditioned eyeblink responses in the global Cx36-/- mutants was not observed in floxed Cx36 knockouts, in which Cx36 is normally expressed in the relevant olivary subnuclei, but not in most other Cx36 expressing neurons in the brain. Together, these findings indicate that the role of coupling between inferior olivary neurons becomes apparent when the olivocerebellar system is challenged in a cerebellar motor learning task and that it serves to facilitate learning-dependent timing in response to unexpected events rather than timing of movements per se.

In combination with modelling studies of both olivary neurons and the olivocerebellar system as a whole our electrophysiological recordings demonstrated that a lack of precision in the timing of the climbing fiber responses mediating the US signals (present data) as well as a reduction in synchrony of climbing fiber activi-

ties during spontaneous activity (Marshall et al., 2007; but cf. Kistler et al., 2002) are probably responsible for the behavioural deficits in the coupling-deficient Cx36-/- mutants. The lack of precision in timing is due to increased variety in the responses after the US, which in turn probably results from altered interactions with the subthreshold oscillations in the inferior olive of Cx36-/- mutants. Our whole cell recordings of olivary neurons *in vivo* did not only demonstrate that Cx36-/- mutants show less frequently subthreshold oscillations and that the stability of the remaining oscillations is reduced, but also that the incidence of spikes occurring in the trough of these oscillations is significantly higher, while the correlation between their preferred spiking pattern and the frequency of their oscillations is generally weaker. The robust appearance of subthreshold oscillations of olivary neurons has recently also been shown *in vivo* in rats with the use of sharp electrode recordings (Chorev et al., 2007), while the contribution of electrotonic coupling to the occurrence of subthreshold oscillations in olivary cells has recently also been addressed in rats with the use of lentiviral knockdown of Cx36 or pharmacological blockage of gap junctions (Leznik and Llinas, 2005; Placantonakis et al., 2006). Thus, together with the current findings we conclude that coupling supports the oscillations in the inferior olive *in vivo* and that the impact of oscillations on spiking patterns is reduced in uncoupled olivary neurons, which results in a more random timing of their spikes in relation to the oscillations.

The question remains as to how dynamic regulation of electrotonic coupling in the olive may contribute to learning-dependent timing (Bengtsson and Hesslow, 2006; De Zeeuw et al., 1998; Llinas and Sasaki, 1989; Schweighofer et al., 1999). Llinas and colleagues have provided strong evidence that the GABAergic input from the cerebellar nuclei, which terminates strategically at the coupled dendrites in olivary glomeruli (De Zeeuw et al., 1998), can uncouple the olivary neurons (Lang et al., 1996; Llinas and Sasaki, 1989). According to our model such a mechanism would counteract learning-dependent timing of the conditioned responses, because it desynchronizes the climbing fiber inputs that mediate the signals of the US. Interestingly, Mauk and colleagues recently demonstrated that the GABAergic projection to the olive is necessary for extinction of the conditioned responses by reducing the firing rate of the relevant olivary neurons below resting level (Medina et al., 2002). Thus, in this respect the mechanism of uncoupling and the mechanism of reducing the firing rate of olivary neurons may serve the same effect in that they both actively counteract the conditioning process.

Experimental Procedures

Knockout animals

Global Cx36-/- mutants and wild type mice were generated and characterized as described by Guldenagel et al. (2001). The mutants that lacked Cx36 in their cerebellar nuclei neurons were cross-breedings of floxed-Cx36 mutants and parvalbumin-Cre mice. In contrast to the mouse published in Degen et al. (2004), the current conditional Cx36 deficient mouse has the 5′ loxP site inserted in the 5′UTR of Cx36 and not in the intron, leading to functional expression of the floxed Cx36 allele. Furthermore, after Cre mediated deletion a cyan fluorescent protein (CFP) was expressed instead of the floxed Cx36 allele (Figure 3B). Transfection of embryonic stem cells,

creation of cell cultures, screening for homologously recombined HM-1 cell clones, and injections of blastocyst were performed as described by Theis et al. (2000). Subsequently Cx36+/flox(CFP) mice were mated to Cx36+/del (lacZ) : Parvalbumin-Cre mice to obtain cerebellum deleted offspring with the genotype Cx36del(lacZ)/flox(CFP) : parvalbumin-Cre. For the experiments described in the present study offspring from a parvalbumin-Cre founder with multicopy integration of the transgene was used. All experiments mentioned here and below were conducted in accordance with the European Communities Council Directive (86/609/EEC) and approved by the Dutch, British and/or German national ethics committee.

Immunofluorescence

Cx36-/flox : parvalbumin-Cre mice and Cx36-/flox(CFP) littermate controls were anesthetized and perfused with 4% paraformaldehyde in PBS. The brains were removed and cut on a vibratome (Leica, U.K.), and the sections were immersed in rabbit anti-GFP (1:1000, Invitrogen, U.K). Sections were washed in PBS and incubated in donkey anti-rabbit Cy3 (1:1000, Jackson ImmunoResearch, USA) prior to mounting (Vector Labs, U.K). Cy3 was viewed with a custom filter set and Alexa^{488} with FITC filters (Nikon E600 microscope) and images were captured directly from the slide using an Acquis Image Capture system (Synoptics, U.K).

Erasmus Ladder

The Erasmus Ladder is a fully automated system to screen both motor performance and motor learning capabilities of mutant mice in a non-invasive manner at a high-throughput level (for details see supplementary material A). It consists of a horizontal ladder in between two shelter boxes, which are equipped with two pressurized air outlets (Pneumax, 171E2B.T.A.0009) to control the moment of departure and speed of the mouse. The ladder has 2 x 37 rungs for the left and right side, which are separated 2 mm apart. The rungs are 12 mm long and 3 mm in diameter, and the distance between two rungs on one side is 15 mm. All rungs are equipped with pressure sensors (produced at Erasmus MC), which are continuously monitored and which can be used to register and analyse the walking pattern of the mouse instantaneously. Moreover, based upon the prediction of the walking pattern the rungs can be moved up or down by a high-speed pneumatic slide (Pneumax, 2141.52.00.36.91) with a maximum of 13 mm at any moment in time. The computer system (National Instruments, PXI-1000B) that runs the real-time system to record sensor data, adjust air pressure, predict future touches, calculate interventions, reposition slides and store data, operates in a fixed cycle of 2 ms. In the conditioning procedures a 15 kHz tone (Voltcraft 7202), which gradually increases over 20 ms to 100 dB and which lasts up to 300 ms, was used as the CS, while a rising rung, which ascends 12 mm, was used as the US. The trials were separated by a random inter-trial interval ranging from 8 to 12 sec.

Pharmacological interventions were done with either Carbenoxolone injections i.p. or Mefloquine injections into the olive, and the results obtained with the use of these applications were compared to the effects of vehicle alone injections. Carbenoxolone injections (40 mg/kg in 0.9% NaCl) were applied half an hour before each of the motor performance sessions and before the first conditioning session.

Bilateral Mefloquine injections (150 μM in 0,2% DMSO) were applied in a surgical procedure directly after the last motor performance session, which meant one day before the first conditioning session. Dosages were chosen so as to make sure that impact on coupling was warranted, while side-effects were minimized (see also Blenkinsop and Lang, 2006; Cruikshank et al., 2004; Gareri et al., 2005; Margineanu and Klitgaard, 2006). For this surgery the mice were anaesthetized with a mixture of ketamine/xylazine (80 mg/kg and 2 mg/kg) and placed in a stereotaxic headholder, while their body temperature was kept at 37-38 °C using a heating pad. Following a dorsal craniotomy the atlanto-occipital membrane and dura were opened, and the inferior olive was identified using electrophysiological recordings (Ruigrok and Voogd, 2000). Subsequently, the recording pipette was replaced by a glass pipette (tip diameter: 10-12 μm) filled with Mefloquine or in two additional cases for histological verification a mixture of Mefloquine and 2% BDA (Molecular Probes, Leiden, The Netherlands), and pressure injections of 50-100 nl were made within the olivary complex (see Figure 2C). After the conditioning sessions, the animals were anaesthetized with an overdose of pentobarbital (200 mg/kg i.p.) and perfused transcardially with flushes of saline and paraformaldehyde (4% in phosphate buffer). The brains were collected, embedded in gelatin, cut at 40 μm transverse sections and mounted (Ruigrok and Apps, 2007). In case of the BDA injections selected sections were processed according to a BDA protocol using ABC-elite™ (Vector Laboratories) and DAB histochemistry (Pijpers et al., 2005).

Eyeblink conditioning

Wild type and mutant mice were prepared for eyeblink conditioning according the MDMT procedure (Koekkoek et al., 2002; Koekkoek et al., 2005). Mice were anaesthetized using nitrous oxide and isoflurane, and a dental acrylic pedestal was placed on the skull. On each day the MDMT measurement system was attached to the pedestal, while a magnet was glued on the lower eyelid. Mice were subjected to either a paired or a randomly paired procedure; both procedures lasted 4 days during each of which 1 session (64 trials grouped in 8 blocks) was conducted. The trials were separated by a random inter-trial interval ranging from 20 to 40 sec. Eyelid movements were considered as a significant eyelid response when its amplitude was greater than the mean + 3 SD's of the amplitude of the movements that occurred in the 500 ms period before the onset of the CS.

Extracellular recordings

To investigate the temporal aspects of climbing fiber activities (i.e. complex spikes) mice were prepared by placing a pedestal on the head and by placing a recording chamber above the simplex lobule and adjacent areas. During experiments the animals were immobilized using a restrainer. Extracellular Purkinje cell activities were recorded in the eyeblink region of awake animals with glass microelectrodes using a Multiclamp 700A and Digidata 1322A from Axon Instruments. Complex spike responses were recorded during 1Hz air puff stimulation to the eye and analyzed off-line. A voltage threshold was used to detect complex spikes, and the time and waveform of the voltage records were used for off-line analysis (IGOR

analysis software; WaveMetrics, OR).

Whole cell recordings in vivo

Mice were prepared for experiments under isoflurane or ketamine/xylazine anesthesia. The head was fixed by bolting a pedestal to a metal bar, the neck area was opened, and the dura was removed. Glass patch pipettes (OD 1.5 mm, ID 1.2 mm, 4-6 MΩ) containing standard intracellular solution (in mM: KCl 9, KOH 10, $MgCl_2$ 3.48, NaCl 4, KGluconate 120, HEPES 10, sucrose 17.5, Na_2ATP 4, Na_3GTP 0.4, pH 7.2, osmolarity 290-310 mOsm/kg) were advanced into the inferior olive in 1-5 µm steps (SM IV, Luigs & Neumann, Ratingen, Germany). The exposed area was covered with artificial fluid (NaCl 148, KCl 3.0, $CaCl_2.2H_2O$ 1.4, $MgCl_2.6H_2O$ 0.8, $Na_2HPO_4.7H_2O$ 0.8, $NaH_2PO_4.H_2O$ 0.2). Recordings were amplified with the use of a MultiClamp 700A and DIGIDATA 1322A (Axon Instr.). All membrane potentials were corrected for the junction potential (8 mV). In current-clamp experiments, we measured voltage responses to a series of negative current steps (100 pA). Cells expressing I_H-current were determined by the presence of an increasing depolarizing sag in more than three sequential hyperpolarization steps. Likewise, rebound depolarizations were only counted if present following more than three hyperpolarization steps. In general health of the cells was examined by checking input resistance, stability of membrane potential, and quality of the amplitude and waveform of action potentials. Correlations between the subthreshold oscillation frequencies and preferred spiking frequencies were determined by analyzing autocorrelograms (clampfit 9.0 software, Axon Instruments, CA). Bursts with a significant poisson surprise value (> 5) were correlated to the corresponding subthreshold oscillation (STO) frequency extracted from the power spectrum of the recordings.

Simulations of inferior olive

The model used for the inferior olivary cell ensemble simulations was a modified version of a two-compartmental cell model by Schweighofer et al. (1999). The h current was moved to the dendritic compartment and redefined as:

$$q_\infty(V_d) = \frac{1}{1+\exp[(V_d+80)/4]}$$

$$\tau_q(V_d) = \frac{1}{\exp(-0.086V_d - 14.6) + \exp(0.07V_d - 1.87)}$$

with V_d as the dendritic membrane potential. Per cell type, five ensembles of neurons on a 5x5 grid were simulated. Wild type cells were connected to all directly neighbouring neurons (up to 8) with gap junction conductance set at 0.04 pS/cm^2. For the mutant model, Ca^{2+} conductances were increased as suggested by earlier research (De Zeeuw et al., 2003), with the new conductances for high- and low-thresh-

old Ca^{2+} set at 4.4 pS/cm^2 and 1.3 pS/cm^2, respectively (a 10% increase compared to the wild type values). Of the two depolarizing currents used, the first (4.5 µA/cm^2, 15 ms) was applied at 600 ± 10 ms after the start of the simulation, and the second (2.5 µA/cm^2, 15 ms) at 700 ± 10 ms. The exact timing was randomly determined per cell.

Model and simulations of olivocerebellar system

In the model, variable synaptic strengths are governed by coincidence rules for parallel fiber and climbing fiber activity probabilities. Synapses are accordingly described by differential equations, which are coupled by linear relations that represent the olivo-cerebellar loop. This formulation directly allows producing the phase plots shown in Figure 7C. The equations were solved by numerical integration using MATLAB's function *ode45* , which is a 4^{th} order Runge-Kutta solver. Resulting time-trajectory plots of synaptic strengths are shown in Figure 7D. The model equations were then implemented in real-time simulations running with a 5 ms time-step (performed in MATLAB). In these real-time simulations inferior olivary neurons were simulated as spiking neurons. A training paradigm consisting of paired inputs representing conditioned stimulus and unconditioned stimulus was used to train the network, both in case of synchronous and asynchronous inferior olive activity (Figure 7E). Further details on constraints, formulas and simulations are presented in an extensive report in the supplementary material (D).

Acknowledgments

We thank E. Dalm and J. v.d. Burg for their technical assistance and R. Maex for his advise on the model. The work in the group of C.I.D.Z. was supported by the Dutch Organization for Medical Sciences (ZON-MW), Life Sciences (NWO-ALW), Senter (Neuro-Bsik), Prinses Beatrix Fonds, and the European Community (EEC; SENSOPAC). Work in the Bonn laboratory was supported by the German Research Association (Wi 270/22-5,6) to K.W. Research of the H.M. team is supported by the Schilling Foundation.

Author contributions

R.S. van der Giessen, S.K. Koekkoek, S. Khosrovani, S. van Dorp, J.R. de Gruijl and A. Cupido all contributed equally and all deserve to be shared first author, because each of them was responsible for a particular technical set of experiments involved. R.S. van der Giessen was responsible for the extracellular recordings, S.K. Koekkoek for the behavioural experiments, S. Khosrovani for the whole cell recordings *in vivo*, Alexander Cupido for the Erasmus Ladder tests, and S. van Dorp and J.R. de Gruijl for the modelling. The other authors were involved in the generation of the mouse mutants, software, design of the experiments and writing. The authors declare no competing financial interest.

Table 1. Properties of olivary neurons in wild types and Cx36 -/- mutants following whole cell recordings *in vivo* (values indicate mean ± SEM).

Parameter	Wild type	n	Cx36 -/-	n	
Cells expressing spontaneous STO's					
Resting membrane potential (mV)	-55±1	53	-55±1	16	0.31
Input resistance (MΩ)	40.1±3.8	53	45.2±4.3	14	0.24
Membrane capacitance (pF)	188.7±11.8	53	233.0±37.0	14	0.07
Firing rate (Hz)	0.64±0.05	50	0.54±0.09	14	0.15
Coefficient of variation for spike intervals	0.72±0.02	50	0.83±0.05	14	0.02
STO frequency (Hz)	3.1±0.3*	53	3.4±0.6*	16	0.32
STO amplitude (mV)	8±1*	53	8±1*	16	0.44
% Cells expressing depolarizing sag	24	58	62	14	0.01
% Cells expressing rebound depolarization	62	58	92	14	0.05
% Cells expressing afterhyperpolarization	19	45	45	12	0.26
Cells expressing no spontaneous STO's					
Resting membrane potential (mV)	-52±2	9	-58±1	12	0.11
Input resistance (MΩ)	42.3±5.2	9	48.3±15.5	12	0.32
Membrane capacitance (pF)	159.6±19.1	9	100.6±3.9	12	0.07
Firing rate (Hz)	0.54±0.11	9	0.92±0.35	12	0.10
Coefficient of variation for spike intervals	0.68±0.13	9	0.68±0.04	12	0.49
% Cells expressing depolarizing sag	0	8	0	12	1.00
% Cells expressing rebound depolarization	60	8	100	12	0.29
% Cells expressing afterhyperpolarization	40	8	0	12	0.29

Statistics: t-test or χ^2-test

** All measured subthreshold oscillations (STO's); a single cell can have multiple STO frequencies.*

References

1. *Aizenman, C. D., and Linden, D. J. (1999). Regulation of the rebound depolarization and spontaneous firing patterns of deep nuclear neurons in slices of rat cerebellum. J Neurophysiol 82, 1697-1709.*
2. *Aizenman, C. D., and Linden, D. J. (2000). Rapid, synaptically driven increases in the intrinsic excitability of cerebellar deep nuclear neurons. Nat Neurosci 3, 109-111.*
3. *Bengtsson, F., and Hesslow, G. (2006). Cerebellar control of the inferior olive. Cerebellum 5, 7-14.*
4. *Bennett, M. V., and Zukin, R. S. (2004). Electrical coupling and neuronal synchronization in the Mammalian brain. Neuron 41, 495-511.*
5. *Blenkinsop, T.A., and Lang, E. J. (2006). Block of inferior olive gap junctional coupling decreases Purkinje cell complex spike synchrony and rhythmicity. J Neurosci 26, 1739-48.*
6. *Buhl, D. L., Harris, K. D., Hormuzdi, S. G., Monyer, H., and Buzsaki, G. (2003). Selective impairment of hippocampal gamma oscillations in connexin-36 knock-out mouse in vivo. J Neurosci 23, 1013-1018.*
7. *Bullock, T. H., Bennett, M. V., Johnston, D., Josephson, R., Marder, E., and Fields, R. D. (2005). Neuroscience. The neuron doctrine, redux. Science 310, 791-793.*
8. *Chorev, E., Yarom, Y., and Lampl, I. (2007). Rhythmic episodes of subthreshold membrane potential oscillations in the rat inferior olive nuclei in vivo. J Neurosci 27, 5043-5052.*
9. *Coesmans, M., Weber, J. T., De Zeeuw, C. I., and Hansel, C. (2004). Bidirectional parallel fiber plasticity in the cerebellum under climbing fiber control. Neuron 44, 691-700.*
10. *Condorelli, D. F., Parenti, R., Spinella, F., Trovato Salinaro, A., Belluardo, N., Cardile, V., and Cicirata, F. (1998). Cloning of a new gap junction gene (Cx36) highly expressed in mammalian brain neurons. Eur J Neurosci 10, 1202-1208.*
11. *Connors, B. W., and Long, M. A. (2004). Electrical synapses in the mammalian brain. Annu Rev Neurosci 27, 393-418.*
12. *Cruikshank, S. J., Hopperstad, M., Younger, M., Connors, B. W., Spray, D. C., Srinivas, M. (2004). Potent block of Cx36 and Cx50 gap junction channels by mefloquine. Proc Natl Acad Sci U S A 101, 12364-9.*
13. *De Zeeuw, C. I., Chorev, E., Devor, A., Manor, Y., Van Der Giessen, R. S., De Jeu, M. T., Hoogenraad, C. C., Bijman, J., Ruigrok, T. J., French, P., et al. (2003). Deformation of network connectivity in the inferior olive of connexin 36-deficient mice is compensated by morphological and electrophysiological changes at the single neuron level. J Neurosci 23, 4700-4711.*
14. *De Zeeuw, C. I., Hertzberg, E. L., Mugnaini, E. (1995). The dendritic lamellar body: a new neuronal organelle putatively associated with dendrodendritic gap junctions. J Neurosci 15, 1587-604.*
15. *De Zeeuw, C. I., Simpson, J. I., Hoogenraad, C. C., Galjart, N., Koekkoek, S. K., and Ruigrok, T. J. (1998). Microcircuitry and function of the inferior olive. Trends Neurosci 21, 391-400.*
16. *De Zeeuw, C. I., and Yeo, C. H. (2005). Time and tide in cerebellar memory formation. Curr Opin Neurobiol 15, 667-674.*
17. *Deans, M. R., Gibson, J. R., Sellitto, C., Connors, B. W., and Paul, D. L. (2001). Synchronous activity of inhibitory networks in neocortex requires electrical synapses containing connexin36. Neuron 31, 477-485.*
18. *Deans, M. R., Volgyi, B., Goodenough, D. A., Bloomfield, S.A., and Paul, D. L. (2002). Connexin36 is essential for transmission of rod-mediated visual signals in the mammalian retina. Neuron 36, 703-12.*
19. *Degen, J., Meier, C., Van Der Giessen, R. S., Sohl, G., Petrasch-Parwez, E., Urschel, S., Dermietzel, R., Schilling, K., De Zeeuw, C. I., and Willecke, K. (2004). Expression pattern of lacZ reporter gene representing connexin36 in transgenic mice. J Comp Neurol 473, 511-525.*
20. *Frisch, C., De Souza-Silva, M. A., Sohl, G., Guldenagel, M., Willecke, K., Huston, J. P., and Dere, E. (2005). Stimulus complexity dependent memory impairment and changes in motor performance after deletion of the neuronal gap junction protein connexin36 in mice. Behav Brain Res 157, 177-185.*
21. *Garcia, K. S., and Mauk, M. D. (1998). Pharmacological analysis of cerebellar contributions to the timing and expression of conditioned eyelid responses. Neuropharmacology 37, 471-480.*
22. *Gareri, P., Condorelli, D., Belluardo, N., Citraro, R., Barresi, V., Trovato-Salinato, A., Mudò, G., Ibbadu, G. F., Russo, E., and De Sarro, G. (2005). Antiabsence effects of carbenoxolone in two genetic animal models of absence epilepsy (WAG/Rij rats and lh/lh mice). Neuropharmacology 49, 551-63.*
23. *Gruart, A., Pastor, A. M., Armengol, J. A., and Delgado-Garcia, J. M. (1997). Involvement of cerebellar cortex and nuclei in the genesis and control of unconditioned and conditioned eyelid motor responses. Prog Brain Res 114, 511-528.*
24. *Guldenagel, M., Ammermuller, J., Feigenspan, A., Teubner, B., Degen, J., Sohl, G., Willecke, K., and Weiler, R. (2001). Visual transmission deficits in mice with targeted disruption of the gap junction gene connexin36.*

J Neurosci 21, 6036-6044.
25. *Hesslow, G. (1994). Correspondence between climbing fibre input and motor output in eyeblink-related areas in cat cerebellar cortex. J Physiol 476, 229-244.*
26. *Hesslow, G., Svensson, P., and Ivarsson, M. (1999). Learned movements elicited by direct stimulation of cerebellar mossy fiber afferents. Neuron 24, 179-185.*
27. *Ito, M., and Kano, M. (1982). Long-lasting depression of parallel fiber-Purkinje cell transmission induced by conjunctive stimulation of parallel fibers and climbing fibers in the cerebellar cortex. Neurosci Lett 33, 253-258.*
28. *Kenyon, G.T., Medina, J.F. and Mauk, M.D. (1998). A Mathematical Model of the Cerebellar-Olivary System I: Self-Regulating Equilibrium of Climbing Fiber Activity. J Comp Neurosc 5, 17-33.*
29. *Kistler, W. M., De Jeu, M. T., Elgersma, Y., Van Der Giessen, R. S., Hensbroek, R., Luo, C., Koekkoek, S. K., Hoogenraad, C. C., Hamers, F. P.,*
30. *Gueldenagel, M., et al. (2002). Analysis of Cx36 knockout does not support tenet that olivary gap junctions are required for complex spike synchronization and normal motor performance. Ann N Y Acad Sci 978, 391-404.*
31. *Khosrovani, S., Van Der Giessen, R. S., De Zeeuw, C. I., and De Jeu, M. T. (2007). In vivo mouse inferior olive neurons exhibit heterogeneous subthreshold oscillations and spiking patterns. Proc Natl Acad Sci U S A 104, 15911-6.*
32. *Koekkoek, S. K., Den Ouden, W. L., Perry, G., Highstein, S. M., and De Zeeuw, C. I. (2002). Monitoring kinetic and frequency-domain properties of eyelid responses in mice with magnetic distance measurement technique. J Neurophysiol 88, 2124-2133.*
33. *Koekkoek, S. K., Hulscher, H. C., Dortland, B. R., Hensbroek, R. A., Elgersma, Y., Ruigrok, T. J., and De Zeeuw, C. I. (2003). Cerebellar LTD and learning-dependent timing of conditioned eyelid responses. Science 301, 1736-1739.*
34. *Koekkoek, S. K., Yamaguchi, K., Milojkovic, B. A., Dortland, B. R., Ruigrok, T. J., Maex, R., De Graaf, W., Smit, A. E., VanderWerf, F., Bakker, C. E., et al. (2005). Deletion of FMR1 in Purkinje cells enhances parallel fiber LTD, enlarges spines, and attenuates cerebellar eyelid conditioning in Fragile X syndrome. Neuron 47, 339-352.*
35. *Landisman, C. E., Long, M. A., Beierlein, M., Deans, M. R., Paul, D. L., and Connors, B. W. (2002). Electrical synapses in the thalamic reticular nucleus. J Neurosci 22, 1002-1009.*
36. *Lang, E. J., Sugihara, I., and Llinas, R. (1996). GABAergic modulation of complex spike activity by the cerebellar nucleoolivary pathway in rat. J Neurophysiol 76, 255-275.*
37. *Leznik, E., and Llinas, R. (2005). Role of gap junctions in synchronized neuronal oscillations in the inferior olive. J Neurophysiol 94, 2447-2456.*
38. *Leznik, E., Makarenko, V., and Llinas, R. (2002). Electrotonically mediated oscillatory patterns in neuronal ensembles: an in vitro voltage-dependent dye-imaging study in the inferior olive. J Neurosci 22, 2804-2815.*
39. *Llinas, R., and Sasaki, K. (1989). The Functional Organization of the Olivo-Cerebellar System as Examined by Multiple Purkinje Cell Recordings. Eur J Neurosci 1, 587-602.*
40. *Llinas, R., and Yarom, Y. (1981). Electrophysiology of mammalian inferior olivary neurones in vitro. Different types of voltage-dependent ionic conductances. J Physiol 315, 549-567.*
41. *Long, M. A., Deans, M. R., Paul, D. L., and Connors, B. W. (2002). Rhythmicity without synchrony in the electrically uncoupled inferior olive. J Neurosci 22, 10898-10905.*
42. *Long, M. A., Jutras, M. J., Connors, B. W., and Burwell, R. D. (2005). Electrical synapses coordinate activity in the suprachiasmatic nucleus. Nat Neurosci 8, 61-6.*
43. *Mann-Metzer, P., and Yarom, Y. (1999). Electrotonic coupling interacts with intrinsic properties to generate synchronized activity in cerebellar networks of inhibitory interneurons. J Neurosci 19, 3298-3306.*
44. *Margineanu, D. G., and Klitgaard, H. (2006). The connexin 36 blockers quinine, quinidine and mefloquine inhibit cortical spreading depression in a rat neocortical slice model in vitro. Brain Res Bull 71, 23-8.*
45. *Marshall, S.P., Van Der Giessen, R.S., De Zeeuw, C.I., and Lang E.J. (2007). Altered olivocerebellar activity patterns in the connexin36 knockout mouse. The Cerebellum 6, 287-299.*
46. *Martin, F.C., and Handforth, A. (2006) Carbenoxolone and mefloquine suppress tremor in the harmaline mouse model of essential tremor. Mov Disord 21, 1641-9.*
47. *Mauk, M. D., Steinmetz, J. E., and Thompson, R. F. (1986). Classical conditioning using stimulation of the inferior olive as the unconditioned stimulus. Proc Natl Acad Sci U S A 83, 5349-5353.*
48. *Mauk, M. D., and Donegan, N. H. (1997). A model of Pavlovian eyelid conditioning based on the synaptic*

organization of the cerebellum. Learn Mem 4, 130-58.
49. *Medina, J. F., and Mauk, M. D. (2000). Computer simulation of cerebellar information processing. Nat Neurosci 3 Suppl, 1205-1211.*
50. *Medina, J. F., Nores, W. L., and Mauk, M. D. (2002). Inhibition of climbing fibres is a signal for the extinction of conditioned eyelid responses. Nature 416, 330-333.*
51. *Perrett, S. P., Ruiz, B. P., and Mauk, M. D. (1993). Cerebellar cortex lesions disrupt learning-dependent timing of conditioned eyelid responses. J Neurosci 13, 1708-1718.*
52. *Placantonakis, D. G., Bukovsky, A. A., Aicher, S. A., Kiem, H. P., and Welsh, J. P. (2006). Continuous electrical oscillations emerge from a coupled network: a study of the inferior olive using lentiviral knockdown of connexin36. J Neurosci 26, 5008-5016.*
53. *Placantonakis, D. G., Bukovsky, A. A., Zeng, X. H., Kiem, H. P., and Welsh, J. P. (2004). Fundamental role of inferior olive connexin 36 in muscle coherence during tremor. Proc Natl Acad Sci U S A 101, 7164-7169.*
54. *Porras-Garcia, E., Cendelin, J., Dominguez-del-Toro, E., Vozeh, F., and Delgado-Garcia, J. M. (2005). Purkinje cell loss affects differentially the execution, acquisition and prepulse inhibition of skeletal and facial motor responses in Lurcher mice. Eur J Neurosci 21, 979-988.*
55. *Pijpers, A., Voogd, J., and Ruigrok, T. J. (2005). Topography of olivo-cortico-nuclear modules in the intermediate cerebellum of the rat. J Comp Neurol 492, 193-213.*
56. *Raymond, J. L., Lisberger, S. G., and Mauk, M. D. (1996). The Cerebellum: A Neuronal Learning Machine? Science 272, 1126-1131.*
57. *Rozental, R., Srinivas, M., Spray, D. C. (2001). How to close a gap junction channel. Efficacies and potencies of uncoupling agents. Methods Mol Biol 154, 447-76.*
58. *Ruigrok, T.J.H., and Voogd, J. (1995). Cerebellar Influence on Olivary Excitability in the Cat. Europ J Neuroscience 7, 679-693.*
59. *Ruigrok, T. J., and Voogd, J. (2000). Organization of projections from the inferior olive to the cerebellar nuclei in the rat. J Comp Neurol 426, 209-228.*
60. *Ruigrok, T. J., and Apps, R. (2007). A light microscope-based double retrograde tracer strategy to chart central neuronal connections. Nat Protoc 2, 1869-1878.*
61. *Saffitz, J. E., Laing, J. G., and Yamada, K. A. (2000). Connexin expression and turnover : implications for cardiac excitability. Circ Res 86, 723-8.*
62. *Schweighofer, N., Doya, K., and Kawato, M. (1999). Electrophysiological properties of inferior olive neurons: A compartmental model. J Neurophysiol 82, 804-817.*
63. *Seto-Ohshima, A., Emson, P. C., Berchtold M. W., and Heizmann C. W. (1989). Localization of parvalbumin mRNA in rat brain by in situ hybridization histochemistry. Exp Brain Research 75, 653-658.*
64. *Simpson, J. I., Wylie, D. R., and De Zeeuw, C. I. (1996). On climbing fiber signals and their consequences. Beh Brain Sciences 19, 380-394.27.*
65. *Sohl, G., Degen, J., Teubner, B., and Willecke, K. (1998). The murine gap junction gene connexin36 is highly expressed in mouse retina and regulated during brain development. FEBS Lett 428, 27-31.*
66. *Thach, W. T., Jr. (1967). Somatosensory receptive fields of single units in cat cerebellar cortex. J Neurophysiol 30, 675-696.*
67. *Theis, M., Magin, T. M., Plum, A., and Willecke, K. (2000). General or cell type-specific deletion and replacement of connexin-coding DNA in the mouse. Methods 20, 205-218.*
68. *Van Alphen, A. M., Schepers, T., Luo, C., and De Zeeuw, C. I. (2002). Motor performance and motor learning in Lurcher mice. Ann N Y Acad Sci 978, 413-424.*
69. *Van Der Giessen, R. S., Maxeiner, S., French, P. J., Willecke, K., and De Zeeuw, C. I. (2006). Spatiotemporal distribution of Connexin45 in the olivocerebellar system. J Comp Neurol 495, 173-184.*
70. *Voogd, J., and Glickstein, M. (1998). The anatomy of the cerebellum. Trends Neurosci 21, 370-375.*
71. *Wang, S. S., Denk, W., and Hausser, M. (2000). Coincidence detection in single dendritic spines mediated by calcium release. Nat Neurosci 3, 1266-1273.*

Chapter 3

Purkinje Cell: signal processing and bistability

Abstract

Bistability of membrane potentials has been described for various neurons in the brain. Recently, evidence has been provided that complex spikes can alter the state of the membrane potential of Purkinje cells suggesting a mechanism by which somatosensory stimulation can act as a toggle switch to control the triggering of simple spikes and thereby motor behavior. Yet, all forms of bistability have only been demonstrated under anesthesia. Using intracellular and extracellular recordings we show that bistability of Purkinje cell activity as well as the toggle phenomenon are virtually absent in wildtype animals during motor performance or motor learning in the awake state, whereas both are prominently present under anesthetics or following genetic mutations that enhance inhibition. We conclude from our study that the membrane potential of Purkinje cells is effectively constrained to the upstate level under physiological circumstances and that silent states can be evoked by manipulating their intrinsic excitability.

Introduction

Cellular bistability or multistable states of the membrane potential have been demonstrated both *in vitro* and *in vivo* for different types of neurons throughout the brain and various functions have been proposed for this phenomenon. For example, bistability found in prefrontal cortex neurons could explain the ability to rapidly generate generalized responses to novel stimuli in working memory tasks[1,2], while reports suggest that bistability in the nucleus accumbens may provide a selective gate for the transfer of information by increasing the probability of action potential firing in the upstate mode[3,4]. Similarly, bistability in Purkinje cells has been proposed to play a key role in short-term processing and storage of sensorimotor information in the cerebellar cortex[5,6]. However, all recordings of bistability to date have been obtained either in slices or in anesthetized animals. Since anesthetics can directly or indirectly affect the membrane potential[7], and since stable intracellular recordings in awake behaving animals present technical complications, it remains to be elucidated whether the functional roles of bistability proposed above hold valid in normal behaving animals under physiological conditions.

Here we investigate to what extent anesthesia can enhance bistability, whether extracellular recordings in awake behaving animals show signs of bistability and/or whether such signs emerge under sensory stimulation or motor learning paradigms. To do this we recorded intracellular and/or extracellular activity of the Purkinje cells in the mouse vestibulocerebellum, which is known to control compensatory eye movements[8-10]. In this system, relationships between sensory input, motor output, and Purkinje cell activities can be rigorously defined during both motor performance and motor learning[11-13]. Moreover, the characteristic complex spike and simple spike activities of Purkinje cells, which are controlled by their climbing fiber and parallel fiber inputs, respectively, show typical interactions which may be useful for drawing conclusions from the extracellular responses about the intracellular state. Not only do Purkinje cells consistently show a pause of about 10 to 100 ms in simple spike activity directly following a single complex spike (normally referred to as climbing fiber pause[14,15], but they also show, under anesthesia, a toggle switch

phenomenon in that single complex spikes can bring the membrane potential to either an upstate or downstate level and thereby switch the simple spike activity on or off, respectively[6]. Thus, if the toggling phenomenon is present under physiological conditions, the complex spike activities relaying error signals originating in the inferior olive[16], would almost certainly have a strong impact on motor behavior by directly modifying the simple spike firing frequency[6].

In the present study we demonstrate via combined intracellular and extracellular recordings of single Purkinje cells that one can indeed accurately and consistently deduce shifts in the membrane potential from extracellularly recorded activity. We looked for signs of bistability and toggling through comparative analysis of the inter-simple spike distribution characteristics and by quantifying the periods of quiescence in simple spike activity and their relation to the occurrence of complex spikes. Our recordings during natural visual and vestibular stimulation indicate that bistability and the toggling phenomenon are prominent under anesthesia and in mutants with altered Ca^{2+} conductance, but that they are virtually absent in awake wild type

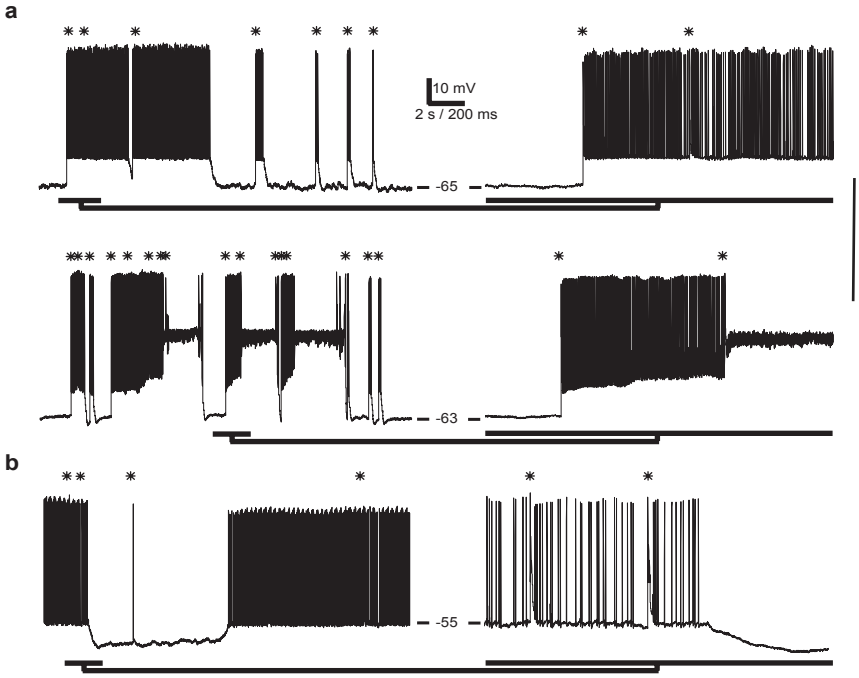

Figure 1. Membrane potential bistability of Purkinje cells in vivo under anesthesia. (a) Top panel left: whole-cell recording of a Purkinje cell in an isoflurane anesthetized mouse showing two states of membrane potential; a hyperpolarized downstate and a depolarized upstate (asterisks indicate complex spikes). Right: enlargement of a transition from down- to upstate related to a complex spike. Bottom panel left: example of a Purkinje cell in an isoflurane anesthetized mouse displaying three states: a downstate, an upstate and an even more depolarized overstate. Right: enlargement showing that both transitions to a higher state are related to the occurrence of a complex spike. (b) Purkinje cell recording from a ketamine/xylazine anesthetized mouse, typically operating mostly in the upstate (left) and showing a weaker temporal relation between the occurrence of complex spikes and transitions (right). Note that throughout all examples the upstate displays continuous firing whereas the downstate and overstate are silent, but for complex spikes.

mice, not even when we challenge the system by motor learning paradigms.

Results

Bistability is present in Purkinje cells of anesthetized mice

To confirm the occurrence of bistability of Purkinje cells, which has so far only been shown in anesthetized rats and guinea pigs[5,6], we performed whole-cell patch recordings *in vivo* in mice under isoflurane or ketamine/xylazine anesthesia. Under isoflurane all Purkinje cells (n = 6) showed a bistable or multistable membrane potential (Fig. 1a). The upstate of the membrane potential (on average -52 ± 1 mV, mean ± SEM) always occurred in conjunction with continuous firing of action potentials (mean firing frequency overall 40 ± 7 Hz; upstate 80 ± 22 Hz), whereas the downstate (-62 ± 3 mV) was completely silent but for complex spikes. In 5 out of 6 recorded Purkinje cells we observed a third state, which was even more depolarized (-37 ± 1 mV). The third state, hereafter referred to as the "overstate", was quiescent but it occasionally displayed small spikelets (~3-4 mV). While the upstate usually occurred after a downstate, the overstate always occurred after the upstate. Shifts from a particular state to a more depolarized state were often associated with the occurrence of a complex spike (from down- to upstate in 57 ± 16 % of the cases and from upstate to overstate in 57 ± 17 %; as opposed to 13 ± 8 % from up- to downstate and 17 ± 17 % from overstate to either upstate or downstate). Most of the time (68 ± 12 %) the cells were in the upstate; downstate and overstate covered 25 ± 12 % and 7 ± 5 % of the time, while their average duration lasted 1.1 ± 0.3 s and 0.8 ± 0.5 s, respectively.

Under ketamine/xylazine anesthesia 6 out of 10 Purkinje cells showed a bistable or multistable membrane potential (Fig. 1b). Here too, the upstate of the membrane potential (on average -51 ± 1 mV) was correlated with continuous firing of action potentials (mean firing frequency overall 68 ± 9 Hz, same for upstate), while the downstate (-61 ± 2 mV) and overstate (-39 ± 3 mV) were silent. Moreover, the shifts showed the same characteristics as described for the experiments under isoflurane in that the higher states usually occurred after a gradual stepwise elevation and that these elevations were relatively often associated with complex spike activities (down- to upstate 45 ± 14 % and up- to overstate 86 ± 11%). The average duration of individual downstates (1.2 ± 0.5 s) and individual overstates (1.1 ± 0.8 s) did not differ from those found under isoflurane (P = 0.91 and P = 0.74, resp.). However, the percentage of time that the membrane potential was in the downstate (3 ± 2 %) as well as the percentage of cells displaying a overstate (20%) were both significantly lower (P = 0.022 and P = 0.035, resp.) than those under isoflurane (25 ± 12 % and 83%, respectively).

These data show that Purkinje cells in mice can show multiple stable states under various forms of anesthesia, that the transitions to down- and overstate are more prominent under isoflurane than ketamine/xylazine, and that under both forms of anesthesia the complex spikes can elicit simple spike firing by shifting the membrane potential from down- to upstate.

Action potentials of intracellular recordings correspond to simple spikes of extracellular

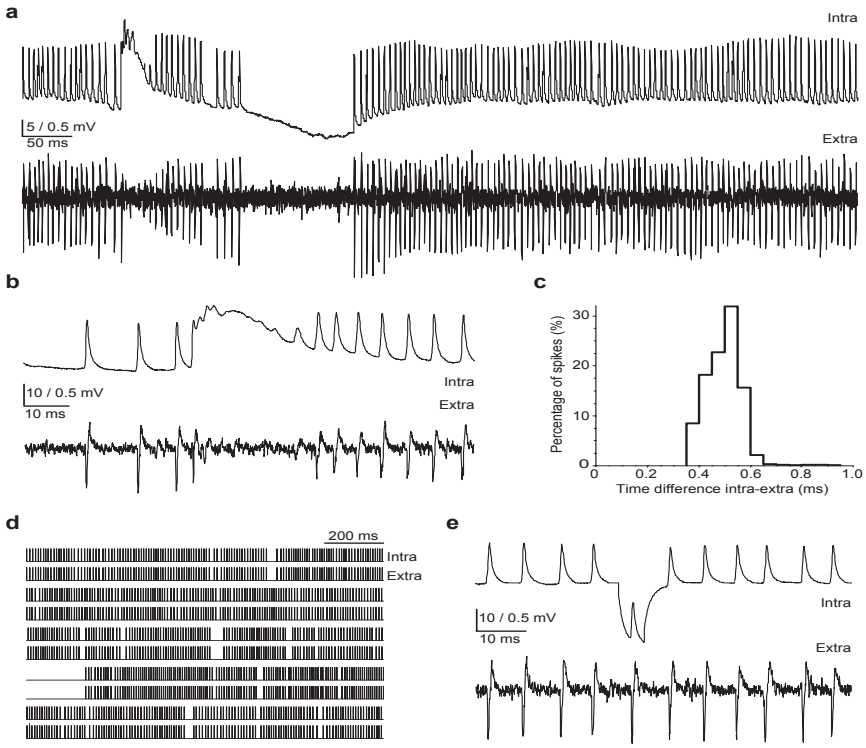

Figure 2. Dual recordings match action potentials of intracellular recordings with complex and simple spikes of extracellular recordings. (a) Simultaneous intracellular and extracellular recordings of the same Purkinje cell show a perfect match between action potentials (top) and simple spikes (bottom). (b) Enlargement of a complex spike, displaying the typical slow (calcium) wave in the intracellular recording and the complex spike waveform and climbing fiber pause in the extracellular recording. (c) Histogram of the time difference between intracellular action potentials and extracellular simple spikes. (d) Analysis of approximately 6 seconds of dual recording with each simple spike represented by a vertical bar. Together with (c) these figures demonstrate a 100% match at a time resolution of 1.0 ms. (e) Intracellular negative current injection is not seen in the extracellular recording excluding the possibility that the dual recordings result in cross-talk between the two electrodes.

recordings

While it is well established that the complex spike is an all or none response of the Purkinje cell to climbing fiber activation[15,17], much less is known about how well extracellularly recorded events correspond to the sub- and suprathreshold potentials that can be observed with the use of the whole-cell recordings such as those described above. We therefore recorded simultaneously both intracellularly and extracellularly the activity of single Purkinje cells *in vivo* under ketamine/xylazine anesthesia (n = 2) using double electrode recordings (extracellular recording electrodes were attached to patch electrodes that reached 10 μm deeper) (Fig. 2a-b). The recording traces showed a perfect match in that every simple and complex spike recorded intracellularly corresponded to a single spike recorded extracellularly and vice versa (resulting in a 100% match at a time resolution of 1.0 ms; Fig. 2c-d). Thus, during downstate silent periods identified using the intracellular data, no extracellular simple spikes were recorded. Moreover, the prolonged silent periods observed

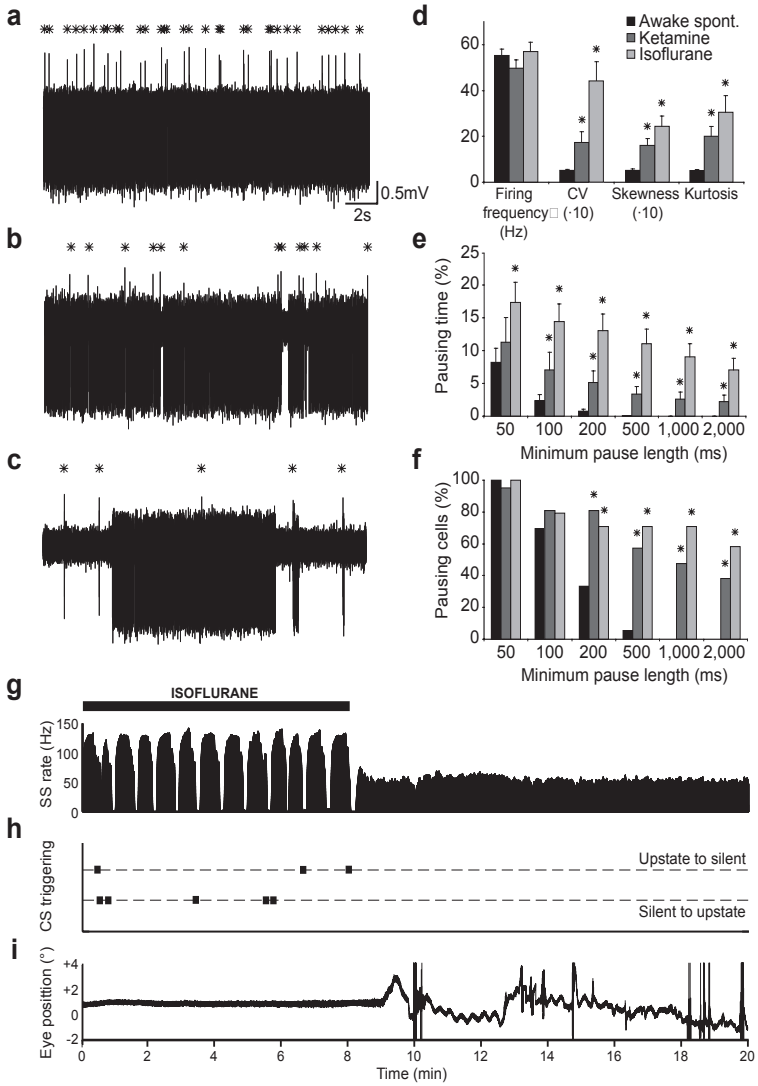

Figure 3. Simple spike pauses and signs of toggling are dramatically increased by anesthetics. (a) Typical extracellular recording of spontaneous Purkinje cell activity in an awake mouse displaying little or no signs of pauses or toggling. Asterisks indicate complex spikes. (b) Purkinje cell activity recorded extracellularly in a mouse under ketamine/xylazine anesthesia showing pauses in simple spike firing. (c) Extracellular recording of a Purkinje cell under isoflurane anesthesia displaying a highly irregular firing pattern consisting of pauses and bursts. (d) While simple firing frequency is not affected, measures for the shape of the ISSI distributions (CV, skewness and kurtosis) are significantly higher in ketamine/xylazine (n = 21) and isoflurane (n = 24) anesthetized mice compared to awake (n = 36) mice (asterisks, P < 0.05). (e-f) Histograms comparing the percentage of total recording time that individual cells were pausing (e) and the percentage of cells showing one or more pauses (f) for different minimum pause lengths. Purkinje cells in anesthetized animals display significantly more pausing than those in awake mice (asterisks, P < 0.05). (g-i) Extracellular Purkinje cell recording of a mouse starting under isoflurane anesthesia, which is ceased after 8 min. Pauses in simple spike firing frequency (g) and signs of toggling (h) that can be seen during anesthesia are no longer present after cessation of the application of isoflurane. Recordings of eye position during the experiment (i) show that eye movements start approximately 1 min after cessation of isoflurane, confirming that the mouse recovered from the anesthetics.

in the extracellular recordings corresponded exclusively to down- or overstate periods of the intracellular recordings. To exclude the possibility that cross-talk between the two electrodes caused the perfect match, we gave short negative current pulses similar in size to the spikes recorded intracellularly. These current injections resulted in a hyperpolarization in the intracellular recording, while no deflection occurred in the extracellular recording (Fig. 2e). The longest inter-simple spike interval (ISSI) in the intracellularly recorded upstate was 158 ms (median 92 ms). In contrast, the maximum duration of an ISSI during a downstate or overstate period reached a value of over 5 s (median 1079 ms), and the vast majority (> 90 %) of all downstate and overstate ISSIs were greater than 200 ms. Thus operationally we determined that any silent period observed in an extracellular recording that is longer than 158 ms, most likely reflects a downstate or overstate.

Together these data indicate that simple spikes of extracellular recordings always correspond to action potentials of intracellular recordings, and that the state of the membrane potential of a Purkinje cell can be deduced from the temporal patterns of simple spike activities that have been recorded with extracellular methods.

Extracellular recordings show low level of bistability in spontaneous awake state

Whereas whole-cell recordings in awake behaving animals impose technical problems, stable extracellular recordings of Purkinje cells are quite feasible in the awake state[13]. Thus, since the temporal pattern of simple spike activities provides,

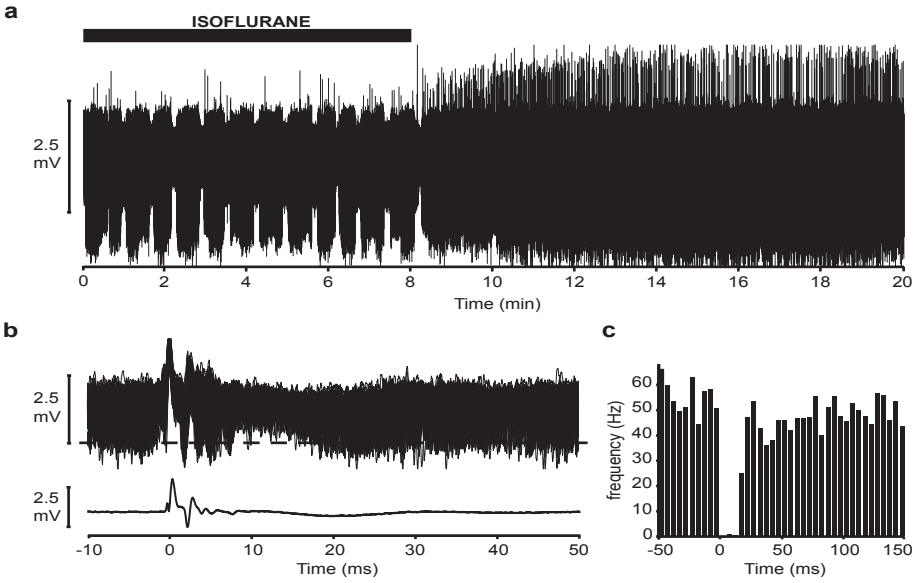

Figure 4. Purkinje cell recorded in a mouse before and after cessation of anesthesia. (a) Raw trace of the entire recording showing that pauses in simple spike firing frequency and signs of toggling that can be seen during anesthesia are no longer present after cessation of the application of isoflurane (b) Top panel: raw traces aligned in time by complex spike onset. Bottom panel: averaged signal showing the complex spike waveform. (c) Peri complex spike time histogram following waveform analysis and threshold discrimination (according to dashed line in a); note the apparent climbing fiber pause.

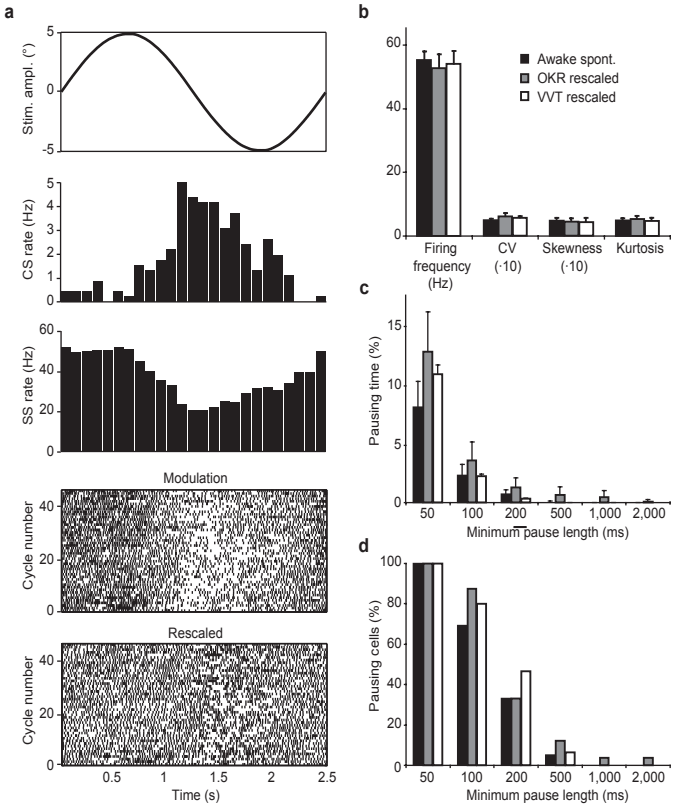

Figure 5. Subjecting the animal to a motor performance or motor learning task does not lead to significantly greater bistability in Purkinje cells. (a) To correct for the modulation (bottom, 25ms bin peri-stimulus time histogram smoothed with 50 ms Gaussian kernel) induced by optokinetic stimulation (top), the ISSI distributions were rescaled. (b) Peri-stimulus raster plots show the effect of the rescaling on the modulation (top: before, bottom: after). (c) Rescaled ISSI distributions of recordings reveal that cells do not spend significantly more time in pause when mice are subjected to optokinetic stimulation (OKR with peak velocity of 8°/s at 0.4 Hz; motor performance task) or visuovestibular training (VVT with combined optokinetic and vestibular stimulation both with an amplitude of 5° at 0.4 Hz; motor learning task) relative to spontaneously active conditions. (d) The percentage of cells with at least one pause within the examined range also did not differ between groups.

as explained above, information about the state of the membrane potential, extracellular recordings offer a means to compare the occurrence of bistability in awake animals with that in anesthetized animals. Therefore we conducted extracellular recordings of Purkinje cell activity in awake mice (n = 36 cells) as well as in mice anesthetized with either isoflurane (n = 24) or ketamine/xylazine (n = 21). As mentioned above, silent states will introduce ISSIs that are up to several orders longer in duration than ISSIs during the upstate. These long ISSIs affect the upper tail of the ISSI distribution. We examined the shape of the ISSI distribution using skewness and kurtosis as indicators of asymmetry and peakedness, respectively. We expected additional silent state ISSIs to positively skew the distribution. Because the variance of silent state ISSIs scales with their mean duration, we used the logarithm of the ISSIs. In addition, as a measure of spike train regularity, we calculated the coefficient of variation (CV), and since multiple firing states can lead to a bimodal log-ISSI dis-

tribution, we tested for unimodality using a dip test[18].

While the simple spike firing frequencies and climbing fiber pauses did not vary significantly between Purkinje cells of awake mice and mice under both types of anesthetics (both $P > 0.50$ and both $P > 0.07$, respectively), the regularity of simple spike activities in awake mice was much greater than that found in anesthetized mice (Fig. 3a-c). Their Coefficient of Variance (CV), skewness, and kurtosis were all significantly smaller (for numbers and significance levels see Table 1). Furthermore, the dip test indicated that the percentages of cells with bi-/multimodal ISSI (Fig. 7b) and firing frequency (see Supplementary Fig. 1 online) distributions, both strong indicators of multiple firing states, were significantly increased in anaesthetized mice. If bistability were present in awake animals, one would expect to find a significant number of ISSI pauses with a duration exceeding 158 ms, as seen in anesthetized mice. However, pauses longer than 158 ms hardly occurred in awake mice. Both the total percentage of time spent in a pause state and the total percentage of cells that showed one or more pauses greater than 200 ms were substantially lower in awake animals than in those anesthetized (Fig. 3d-e). All values (i.e. CV, skewness and kurtosis) were compared for Purkinje cells in the different areas Crus I and II, paramedian lobule and (para)flocculus and no differences were observed (data not shown). In addition, we found little evidence for the toggling switch phenomenon mediated by the complex spikes in awake animals (Fig. 3f). When we examined the instances at which a pause in simple spike activities of at least 100 ms occurred before or after a complex spike, we found that complex spikes rarely triggered a change in simple spike activities from silent to upstate (0.3 ± 0.1 %) and in a limited number of cases from upstate to silent (2.9 ± 1.6 %). These percentages were significantly lower than

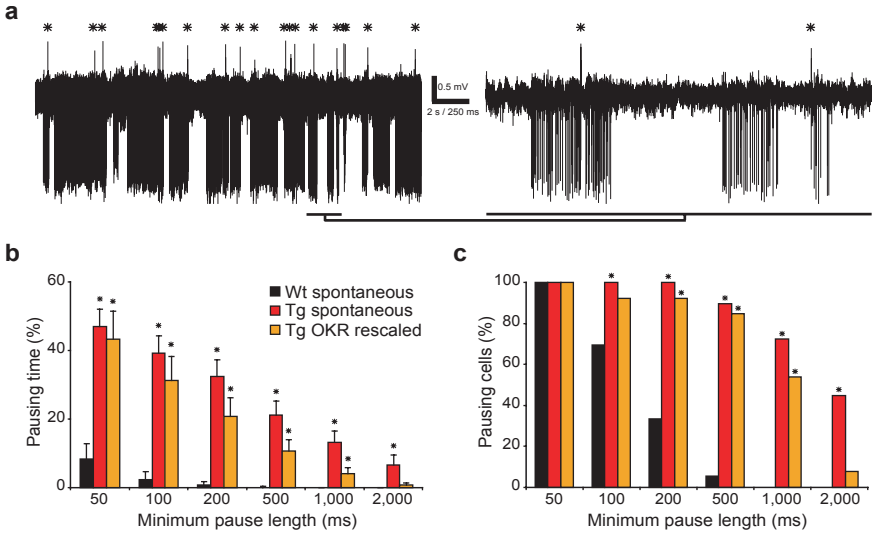

Figure 6. The tottering mutation causes changes in the simple spike temporal firing pattern comparable to the effect of anesthetics. (a) Typical extracellular Purkinje cell recording trace with irregular simple spike firing (left) and putative toggling by the second complex spike in the enlargement (right, complex spikes marked by asterisks). (b) In line with the effect of anesthetics the tottering mutation also results in Purkinje cells that spend significantly more time in pauses. This effect was found in cells from animals with and without optokinetic stimulation. (c) The percentage of pausing cells was also higher in both of these groups compared to wild type mice.

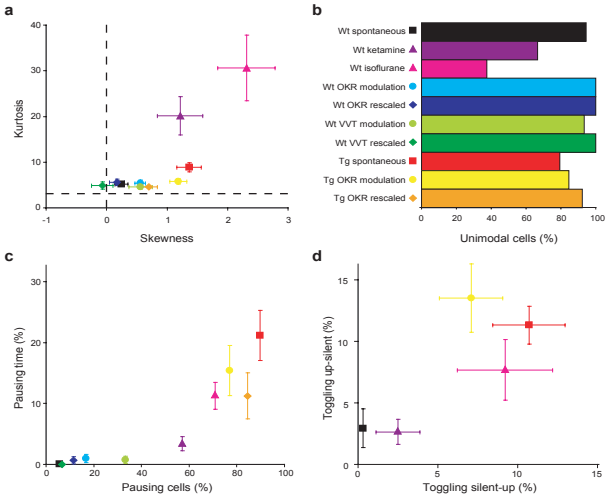

Figure 7. Silent states in Purkinje cells, suggestive for bistability, can be evoked by anesthetics or genetic mutations, but not by subjecting the animal to motor performance or motor learning tasks. (a) Skewness and kurtosis, two characteristics of the shape of ISSI distributions are both increased by anesthetics, while the tottering mutation mostly results in a higher skewness. Dashed lines indicate skewness and kurtosis value of a lognormal distribution. (b) The percentage of cells with a unimodal ISSI distribution was reduced by both anesthetics. (c) Using a minimum pause length of 500 ms (approximately 3 times the maximum ISSI found in the upstate), both the percentage of pausing time and pausing cells, as a sign for bistability, are higher as a result of either anesthetics or the tottering mutation. (d) The percentage of times a complex spike putatively triggered a change in simple spike firing in either direction, as a sign for toggling, is higher as a result of both anesthetics and the tottering mutation.

those obtained under isoflurane (silent to upstate 9.3 ± 3.0 %, $P < 0.001$; upstate to silent 7.7 ± 2.2 %, $P = 0.026$) or ketamine/xylazine (silent to upstate 2.5 ± 1.4 %, $P = 0.046$). The occasional triggering from upstate to silent by a complex spike in awake animals was, in contrast to that in anesthetized animals, found to be directly related to the simple spike firing frequency, in that signs of toggling were only seen in cells with a relatively low simple spike firing frequency (Fig. 3g). Therefore, these occasions may be artifacts.

Finally, if the use of anesthesia increases bistability, cessation of such application should bring the same Purkinje cells to a stable upstate level resulting in regular simple spike firing without pauses or inter-spike intervals longer than 158 ms and without signs of toggling by the complex spikes. We therefore investigated the extracellular activities of individual Purkinje cells (n = 2) both during and after application of isoflurane, which can be administered by respiration and stopped abruptly at will. Fig. 4 shows an example of the recordings of a Purkinje cell in the paramedian lobule. While the regular pauses and signs of complex spike toggling described above were abundantly observed during application of isoflurane, they disappeared within one minute after stopping it (Fig. 4a-c). To verify that the animal switched from an anesthetized state to an awake state after this minute, we attempted to evoke compensatory eye movements during the entire experiment. These recordings showed that sinusoidal optokinetic stimulation indeed resulted in visual reflexes approximately one minute after application of isoflurane was stopped (Fig.

4d).

Together, the extracellular recordings described above indicate that anesthetics can dramatically induce bistability in Purkinje cells and that this process is practically absent in the awake state.

Modulation of afferents to Purkinje cells does not alter their stability in awake state

While the data above demonstrate that pauses, as a sign of bistability, virtually do not occur in spontaneously active Purkinje cells in awake animals, they do not exclude the possibility that bistability may be enhanced by sensory modulation or learning paradigms. We therefore compared the temporal patterns of the simple and complex spike activities of Purkinje cell recordings from awake mice without stimulation (n = 36) with those during optokinetic stimulation (OKR modulation; n = 24) and visuovestibular training (VVT modulation; n = 15). Since optokinetic stimulation modulates the ISSIs (Fig. 5a) independent from the presence of complex spikes[19] and thereby alters the ISSI distribution, we corrected each ISSI for the average firing rate during the part of the stimulus cycle encompassed by that ISSI (Fig. 5b). This rescaling procedure removes the linear effect of the stimulus on the firing rate. The skewness and kurtosis values of the rescaled ISSI distributions recorded during both optokinetic stimulation and visuovestibular training did not differ from those during spontaneous activity in awake mice (all P-values > 0.25). Moreover, the time that the cells were in pause and percentage of cells that showed pauses also did not differ significantly among the groups (all P-values > 0.16, Fig. 5c-d). These results indicate that bistability of Purkinje cells in awake mice is neither enhanced by the sensory stimulation that modulates these cells nor by the motor performance or motor learning that is controlled by these cells.

Purkinje cells with abnormal voltage-gated calcium channels display bistable firing behavior in awake state

The findings presented above suggest that anesthesia in general causes or promotes bistability and led us to hypothesize that there could be specific factors that can influence bistability. Since isoflurane potentiates the $GABA_A$-receptor current[20,21] and is very effective in inducing bistability, we selected a mutant with enhanced inhibition to test this hypthesis. The *tottering* mouse, which suffers from a mutation in its voltage-gated P/Q-type calcium channels, appeared an interesting candidate, because its Purkinje cells show an increased susceptibility to inhibitory modulation by GABAergic interneurons[22] and show irregular simple spike firing behavior[23]. We therefore investigated bistability in *tottering* mice by analyzing the pauses and signs of toggling using extracellular recordings in the awake state (Fig. 6a-c). Purkinje cells of awake *tottering* mutants without (n = 29) and with optokinetic stimulation (n = 13) showed the same type of changes in simple spike firing patterns as the wild type animals under isoflurane anesthesia. That is, the values for ISSI distribution parameters (CV, skewness and kurtosis), pausing time, and pausing cells (minimum pause length 100-1000 ms) were all significantly higher in both these conditions than in awake wild type animals (all P-values < 0.005). Moreover, we observed numerous cases in which the complex spike activities putatively triggered simple spike activities via a toggling process. During spontaneous activity as

well as motor performance the percentages of complex spikes related to transitions between upstate and pause in awake *totterings* were significantly higher than those in awake wild types (for both upstate to silent and silent to upstate, all P-values < 0.001, Fig. 7d). These findings suggest that bistability is indeed enhanced in mutants in which inhibition is increased. To further test this hypothesis we compared the level of bistability in *totterings* with that in wild types using whole-cell recordings *in vivo* under isoflurane and ketamine/xylazine. Under ketamine/xylazine anesthesia the Purkinje cells of the *totterings* spent significantly more time in the downstate as compared to those in wild types (percentage of total time in downstate 25 ± 7 % vs. 3 ± 2 %, P = 0.022). The time spent in downstate as a result of isoflurane in normal mice, and that in *tottering* mice under ketamine is comparable. However, the use of isoflurane in *tottering* mice did not result in an additional effect on the time in downstate, which might be explained as a 'saturation' of the effect of inhibition. Together these data indicate that awake animals can show robust signs of bistability if their voltage-gated P/Q-type calcium channels are genetically affected. The fact that the influence on GABA-currents is one of the prominent features of both isoflurane application and the *tottering* mutation suggests that alterations in inhibition play an important role in bistability.

Discussion

We have demonstrated that Purkinje cells in mice shift between several membrane states when their intrinsic excitability is altered due to anesthesia or particular genetic mutations. However, Purkinje cells in healthy awake behaving animals operate virtually exclusively in the upstate of the membrane potential. This propensity holds true in mice during spontaneous activity as well as during motor performance and motor learning.

Role of membrane stability in Purkinje cells in awake behaving animals

The recent discovery that bistability can occur *in vivo* in Purkinje cells of both rats and guinea pigs under various forms of anesthesia and that climbing fiber activity evoked by sensory stimulation can trigger periods of simple spike bursts or quiescence under these circumstances has revived the debate about the possible roles of bistability of Purkinje cells[6]. In particular the findings by Loewenstein and colleagues have raised the possibility that Purkinje cell bistability may play a key role in short-term processing and storage of sensory information. We have therefore first set out experiments to investigate whether action potentials obtained with *in vivo* whole-cell recordings can be directly related to simple spike activities recorded extracellularly, and whether the temporal pattern of these simple spike activities provides information about the state of the membrane potential. By recording simultaneously whole-cell activities and extracellular activities of the same Purkinje cells under anesthesia in mice we were able to show unequivocally that both questions can be answered positively. The double recordings demonstrated that extracellular single-unit recordings accurately represent the activity measured intracellularly and that extracellularly recorded silent states and thereby bistability are characterized by long pauses (> 158 ms) and toggling by the occurrence of a complex spike between a

pause and an upstate. We subsequently employed the extracellular recording technique to investigate whether the occurrence of bistability in Purkinje cells is correlated to the presence of anesthesia and/or to the behavioral state of the animal, i.e. spontaneously active, doing a motor performance task, or being subjected to a task of cerebellar motor learning. These experiments showed that bistability in general hardly occurs in the awake state and that it can hardly be influenced by sensory stimulation or motor training paradigms in this state, while it is prominently present under isoflurane or ketamine/xylazine anesthesia (summarized in Fig. 7). These data agree with extracelular recordings in other labs that investigated simple spike and complex spike behavior in awake behaving and learning animals including those in monkeys, cats and rabbits[11,12,17,24,25]. Although most of these previous studies in awake behaving animals have also shown some irregularities in simple spike activities, detailed analyses with the current methods showed that the pauses of simple spikes hardly ever exceed 100 ms and that the silent periods after the complex spikes were perfectly in line with the normal climbing fiber pauses (data not shown), which are simply reflecting a refractory period rather than a change in the state of the membrane potential. Moreover, further inspection of the data obtained by other labs in other awake, behaving animals also showed virtually no sign of the toggling switch, which is so prominently present under anesthesia. Even simple spike activities during desynchronized sleep[26,27], hardly demonstrate any sign of bistability. Thus, although we have no access to whole-cell recordings, let alone to double intracellular and extracellular recordings, of Purkinje cells in species other than mice, it is parsimonious to conclude that Purkinje cells in awake behaving animals in general operate virtually solely in the upstate and that this state of their membrane potential is not significantly modified by sensory stimulation, motor performance or motor learning. In contrast, the Purkinje cells of *tottering* mutants, which turned out to have a very high level of bistability even in the awake state (present study), are virtually unable to exert any cerebellar control on their motor behavior[23]. Thus, one might argue that healthy Purkinje cells and a functional cerebellar cortical network are in fact designed to avoid bistability under normal physiological circumstances.

Mechanisms of bistability

Previous studies have shown that various conductances including non-inactivating sodium and calcium conductances, potassium conductances and h-currents (Ih) can play a role in generating bistability in Purkinje cells[5,6,28-31]. Our data obtained with anesthetics and genetic modification suggest that artificially enhancing the inhibitory input from the GABAergic interneurons and/or diminishing the excitatory drive through the mossy fiber - parallel fiber pathway could elicit a down state that is normally virtually absent. Isoflurane is known to potentiate the $GABA_A$-receptor current[20,21], while ketamine and xylazine act as NMDA-receptor blocker and alpha 2-adrenergic receptor agonist, respectively[32,33]. This reasoning is further supported by studies which showed that isoflurane and alpha 2-adrenergic receptor agonists can also reduce the frequency and regularity of simple spike firing *in vitro*[34-36] and that loss of inhibitory input causes Purkinje cells to fire simple spikes more regularly[37]. Moreover, our findings of an increased level of bistability in the *tottering* is also compatible with this idea, because this mutant shows a reduction in the amplitude

of the parallel fiber – Purkinje cell EPSC and an increased susceptibility to inhibitory modulation by GABAergic interneurons[22,38]. A comparable relation between enhanced inhibition and increased irregularity, characterized also by longer ISSIs, has been described in the GluRδ2 knockout mouse[39,40]. Thus, enhancing the inhibitory and/or diminishing the excitatory input to Purkinje cells at a non-physiological level may affect the various conductances such that an artificial downstate is generated, which in turn permits the complex spike to trigger or toggle a new upstate with simple spike bursts.

Methods

All experiments were conducted in accordance with the European Communities Council Directive (86/609/EEC) and were reviewed and approved by the national ethics committee.

Intracellular recordings

C57BL/6 wild type and homozygous *tottering* mice (4-5 weeks old) were prepared for experiments under isoflurane or ketamine/xylazine anesthesia[41]. In short, a pedestal was mounted on the head of a mouse using dental acrylic and the head was fixed by bolting the pedestal to a metal bar. A craniotomy (1x1 mm) was made in the occipital bone above Crus 2 and/or the vermis of the cerebellum, and the dura was carefully removed. Borosilicate glass patch pipettes (OD 1.5 mm, ID 1.2 mm, 4-6 MΩ) containing standard intracellular solution (in mM: KCl 9, KOH 10, $MgCl_2$ 3.48, NaCl 4, KGluconate 120, HEPES 10, sucrose 17.5, Na_2ATP 4, Na_3GTP 0.4, pH 7.2, osmolarity 290-310 mOsm/kg) were advanced into the top layer of the cerebellar cortex in 1-5 μm steps (SM IV, Luigs & Neumann, Ratingen, Germany), with slight positive pressure applied to the tip described elsewhere[42]. The exposed area was covered with artificial cerebrospinal fluid (NaCl 148, KCl 3.0, $CaCl_2.2H_2O$ 1.4, $MgCl_2.6H_2O$ 0.8, $Na_2HPO_4.7H_2O$ 0.8, $NaH_2PO_4.H_2O$ 0.2). Recordings were amplified (MultiClamp 700A, Axon Instr., Foster City, USA), filtered at 3-10 kHz and sampled at 10-20 kHz (DIGIDATA 1322A, Axon Instr.). Somatic and dendritic recordings with a minimal duration of 1 min were used and all membrane potentials were corrected for the junction potential (8 mV).

Extracellular recordings

C57BL/6 mice and homozygous *tottering* mice (3-12 months old) were prepared under isoflurane anesthesia for chronic neurophysiological experiments by mounting a pedestal as described above. A recording chamber was built around craniotomies in both left and right occipital bones with a maximal diameter of 3 mm[41]. For the experiment the animal was anesthetized with isoflurane or ketamine/xylazine and the head was fixed by bolting the pedestal to a metal bar. When recording from awake mice, mice were briefly anesthetized with isoflurane, restrained in a custom made pastic tube and a 20 min acclimatization period preceded the recordings. Extracellular Purkinje cell activity was recorded using borosilicate glass electrodes (OD 2.0 mm, ID 1.16 mm, 4-8 MΩ). Electrodes were advanced into the cerebellum by a hydraulic micro-drive (Narishige, Tokyo, Japan). Recordings were made from left

and right Crus I and II, paramedian lobule, and (para)flocculus. Purkinje cells were identified by the brief pause in simple spike activity following each complex spike. The raw electrode signal was amplified, filtered (CyberAmp, CED, Cambridge, UK), digitized (CED) and stored on disk for off-line analysis. Minimum duration of recordings was 2 min for spontaneous activity and 15 continuous cycles for recordings with optokinetic stimulation. Following each recording session the brain was covered with gramicidin-containing ointment and the chamber was sealed with bone wax.

Recordings under anesthesia

For intra- and extracellular recordings under anesthesia, commonly used anesthetics ketamine/xylazine and isoflurane were used. Ketamine/xylazine anesthesia was induced by an i.p. injection of 0.1 ml of a mixture containing 50 and 8 mg/kg body weight ketamine and xylazine, respectively. Anesthesia was maintained with subsequent injections of 0.05 ml of the same mixture. Isoflurane anesthesia was induced by inhalation of 4.0% isoflurane in a 2:1 mixture of NO2 and O2 for approximately 1-2 min, and was maintained with 1.0-1.5% isoflurane. Depth of anesthesia was monitored in both groups by testing corneal and pinch reflexes, observing whisker and tail movements and breathing rate. Body temperature was maintained at ~37° using a homeothermic blanket (FHC, Bowdoinham, Me., USA).

Optokinetic and vestibular stimulation

For extracellular recordings during motor performance and motor learning tasks we recorded from the left flocculus under optokinetic (and vestibular) stimulation as previously described[23]. In short, optokinetic stimulation consisted of either a planetarium or a random-dotted drum (dot size 2°) rotating sinusoidally around the vertical axis running through the animals' head with a fixed peak velocity (8°/s) at different frequencies ranging from 0.05 to 0.4 Hz. Mismatched optokinetic and vestibular stimulation consisted of a vertical axis whole body rotation in combination with horizontal axis optokinetic stimulation, both with 5° amplitude at 0.4 Hz. Stimulus velocities were measured and controlled by a 1401plus unit (CED). The left flocculus was first located by recording Purkinje cell activity during sensory motor behavior.. For optokinetic stimulation, only Purkinje cells that showed optimal complex spike modulation for stimulus rotations around the vertical axis were used. For combined optokinetic and vestibular stimulation all modulating floccular Purkinje cells were used. The position of the left eye was measured using a video set-up[43,44] (sampling rate 240 Hz; ETL-200, ISCAN, Burlington, MA, USA).

Data analysis

Off-line analysis was performed in Matlab (version 6.5, Mathworks, USA). Simple spikes and complex spikes were detected and discriminated using custom-made Matlab routines based on principal component analysis[13]. For intracellular recordings, transitions between states were detected using two thresholds, one for entering the downstate and one for entering the overstate. Only state changes with a minimum duration of 100 ms were registered. To avoid defining noise or individual complex spikes as a short upstate, we removed pairs of down-up and up-down tran-

sitions that occurred within 50 ms. In extracellular data, complex spike induced transitions were defined using two 100 ms intervals before and after each complex spike, starting at -102 and 25 ms respectively. If an interval contained simple spikes it was classified as upstate, otherwise as silent state. Complex spike toggling efficiency was defined as the fraction state changes given the total set of complex spikes. The ISSI distribution of each Purkinje cell was characterized by calculating the mean, CV (standard deviation divided by the mean), skewness and kurtosis proper. The CV indicates the relative width of the distribution; skewness indicates the asymmetry of the distribution, a positive value being a tail to the right (longer ISSIs indicating silent states); and kurtosis is a measure for the peakedness of the distribution, the higher the value the more 'peaky' the distribution is, indicating a strong preference for one firing frequency. Skewness and kurtosis were bootstrap bias corrected[45] using 2000 sets of randomly selected ISSIs. Because the ISSIs due to a silent state are several orders longer and more variable in duration than upstate ISSIs, we used the logarithm of the ISSIs to calculate the skewness and kurtosis, which makes the distributions independent of time-scale and relatively symmetric[46]. Additional silent state ISSIs will positively skew the distribution and could even render the distribution bimodal. We therefore tested all ISSI distributions for unimodality with a dip test[18] using R software (version 2.1.0, http://www.r-project.org).

In addition to comparing the shape of ISSI distributions, we also searched directly for long pauses in simple spike firing, since the downstate and the overstate are characterized by the absence of simple spike firing. We analyzed all ISSIs for each cell with different minimum silent periods that could be considered a pause (range 50 – 2000 ms). For each cell, silent states were analyzed by calculating for the entire range of pauses the percentage of total recording time the cell was pausing, and for each group the percentage of cells with at least one pause was calculated. In order to analyze Purkinje cell activity during sensory motor behavior simple spike raster plots were made. Simple and complex spike activity was modulated by optokinetically induced motor activity, which alters the ISSI distributions by inducing both shorter and longer ISSIs. Therefore we corrected each ISSI for the average firing rate during the part of the stimulus cycle that was encompassed by that ISSI using:

$$ISSI_{res}(i) = \langle ISSI \rangle \int_{u_i}^{u_{i+1}} R(\varphi_t)$$

where $ISSI_{res}(i)$ is the i^{th} rescaled inter-simple spike interval, R is the stimulus-conditional average firing rate function, φ_t is the phase of the stimulus at time t and u_i is the i^{th} simple spike time. The continuous rate function R was obtained with a kernel density estimation algorithm using a Gaussian kernel with SD=50 ms. This rescaling procedure removes the linear effect of the stimulus on the firing rate and transforms the ISSIs, in the ideal case of inhomogeneous Poisson firing, into a Poisson process with unit rate[47]. The distributions of the ISSIs before and after correction were used to calculate all used parameters, with the obvious exception of the toggling, since the rescaling disturbs the original temporal relation between complex spikes and ISSIs.

All data are presented as mean ± SEM. Statistical analysis was done using

ANOVA(for normally distributed data), Mann-Whitney (for non-parametric data) or Chi-square test (for binominal data) and values were considered significantly different when $p < 0.05$.

Acknowledgements

The authors thank Ing. J. van den Burg for excellent assistance. Research was supported by Neuro-Bsik (C.D.Z.), ZonMw (C.D.Z.), NWOALW (C.D.Z., M.F.), NWO-PIONIER (C.D.Z.), EEC (C.D.Z.), EUR (M.T.S.) and NWO-VIDI (M.F., B.W.).

References

1. *Branchereau, P., Van Bockstaele, E.J., Chan, J. & Pickel, V.M. Pyramidal neurons in rat prefrontal cortex show a complex synaptic response to single electrical stimulation of the locus coeruleus region: evidence for antidromic activation and GABAergic inhibition using in vivo intracellular recording and electron microscopy. Synapse 22, 313-31 (1996).*
2. *Durstewitz, D., Seamans, J.K. & Sejnowski, T.J. Neurocomputational models of working memory. Nat Neurosci 3 Suppl, 1184-91 (2000).*
3. *O'Donnell, P. & Grace, A.A. Synaptic interactions among excitatory afferents to nucleus accumbens neurons: hippocampal gating of prefrontal cortical input. J Neurosci 15, 3622-39 (1995).*
4. *O'Donnell, P., Greene, J., Pabello, N., Lewis, B.L. & Grace, A.A. Modulation of cell firing in the nucleus accumbens. Ann N Y Acad Sci 877, 157-75 (1999).*
5. *Williams, S.R., Christensen, S.R., Stuart, G.J. & Hausser, M. Membrane potential bistability is controlled by the hyperpolarization-activated current I(H) in rat cerebellar Purkinje neurons in vitro. J Physiol 539, 469-83 (2002).*
6. *Loewenstein, Y. et al. Bistability of cerebellar Purkinje cells modulated by sensory stimulation. Nat Neurosci 8, 202-11 (2005).*
7. *MacIver, M.B. & Kendig, J.J. Anesthetic effects on resting membrane potential are voltage-dependent and agent-specific. Anesthesiology 74, 83-8 (1991).*
8. *Ito, M. Cerebellar control of the vestibulo-ocular reflex--around the flocculus hypothesis. Annu Rev Neurosci 5, 275-96 (1982).*
9. *Lisberger, S.G. Physiologic basis for motor learning in the vestibulo-ocular reflex. Otolaryngol Head Neck Surg 119, 43-8. (1998).*
10. *De Zeeuw, C.I. et al. Gain and phase control of compensatory eye movements by the flocculus of the vestibulocerebellum. in Handbook of auditory research 375-422 (Springer Verlag, 2003).*
11. *De Zeeuw, C.I., Wylie, D.R., Stahl, J.S. & Simpson, J.I. Phase Relations of Purkinje Cells in the Rabbit Flocculus During Compensatory Eye Movements. J of Neurophysiol. 74, 2051-2063 (1995).*
12. *Simpson, J.I., Wylie, D.R. & De Zeeuw, C.I. On climbing fiber signals and their consequence(s). Beh.Brain Sciences 19, 380-394 (1996).*
13. *Goossens, H.H. et al. Simple spike and complex spike activity of floccular Purkinje cells during the optokinetic reflex in mice lacking cerebellar long-term depression. Eur J Neurosci 19, 687-97 (2004).*
14. *Armstrong, D.M. Functional significance of connections of the inferior olive. Physiol Rev 54, 358-417 (1974).*
15. *Schmolesky, M.T., Weber, J.T., De Zeeuw, C.I. & Hansel, C. The making of a complex spike: ionic composition and plasticity. Ann N Y Acad Sci 978, 359-90 (2002).*
16. *De Zeeuw, C.I. et al. Microcircuitry and function of the inferior olive. Trends Neurosci 21, 391-400 (1998).*
17. *Thach, W.T., Jr. Somatosensory receptive fields of single units in cat cerebellar cortex. J Neurophysiol 30, 675-96 (1967).*
18. *Hartigan, J.A., Hartigan, P.M. The Dip Test of Unimodality. Ann Stat 13, 70-84 (1985).*
19. *Leonard, C.S. New York University (1986).*
20. *Nakahiro, M., Yeh, J.Z., Brunner, E. & Narahashi, T. General anesthetics modulate GABA receptor channel complex in rat dorsal root ganglion neurons. Faseb J 3, 1850-4 (1989).*
21. *Hall, A.C., Lieb, W.R. & Franks, N.P. Stereoselective and non-stereoselective actions of isoflurane on the GABAA receptor. Br J Pharmacol 112, 906-10 (1994).*
22. *Zhou, Y.D., Turner, T.J. & Dunlap, K. Enhanced G protein-dependent modulation of excitatory synaptic transmission in the cerebellum of the Ca2+ channel-mutant mouse, tottering. J Physiol 547, 497-507 (2003).*
23. *Hoebeek, F.E. et al. Increased noise level of purkinje cell activities minimizes impact of their modulation during*

sensorimotor control. Neuron 45, 953-65 (2005).
24. *Norris, S.A., Greger, B., Hathaway, E.N. & Thach, W.T. Purkinje cell spike firing in the posterolateral cerebellum: correlation with visual stimulus, oculomotor response, and error feedback. J Neurophysiol 92, 1867-79 (2004).*
25. *Sato, Y., Miura, A., Fushika, H. & Kawasaki, T. Short-term modulation of cerebellar purkinjecell activity after spontaneous climbing fiber input. J Neurophysiol 68, 2051-2062 (1992).*
26. *McCarley, R.W. & Hobson, J.A. Simple spike firing patterns of cat cerebellar Purkinje cells in sleep and waking. Electroencephalogr Clin Neurophysiol 33, 471-83 (1972).*
27. *Hobson, J.A. & McCarley, R.W. Spontaneous discharge rates of cat cerebellar Purkinje cells in sleep and waking. Electroencephalogr Clin Neurophysiol 33, 457-69 (1972).*
28. *Llinas, R. & Sugimori, M. Electrophysiological properties of in vitro Purkinje cell dendrites in mammalian cerebellar slices. J Physiol 305, 197-213 (1980).*
29. *Llinas, R. & Sugimori, M. Electrophysiological properties of in vitro Purkinje cell somata in mammalian cerebellar slices. J Physiol 305, 171-195 (1980).*
30. *Li, S.J., Wang, Y., Strahlendorf, H.K. & Strahlendorf, J.C. Serotonin alters an inwardly rectifying current (Ih) in rat cerebellar Purkinje cells under voltage clamp. Brain Res 617, 87-95 (1993).*
31. *Rapp, M., Segev, I. & Yarom, Y. Physiology, morphology and detailed passive models of guinea-pig cerebellar Purkinje cells. J Physiol (Lond) 474, 101-18 (1994).*
32. *Wagner, L.E., 2nd, Gingrich, K.J., Kulli, J.C. & Yang, J. Ketamine blockade of voltage-gated sodium channels: evidence for a shared receptor site with local anesthetics. Anesthesiology 95, 1406-13 (2001).*
33. *Leppavuori, A. & Putkonen, P.T. Alpha-adrenoceptive influences on the control of the sleep-waking cycle in the cat. Brain Res 193, 95-115 (1980).*
34. *Crepel, F., Debono, M. & Flores, R. Alpha-adrenergic inhibition of rat cerebellar Purkinje cells in vitro: a voltage-clamp study. J Physiol 383, 487-98 (1987).*
35. *Parfitt, K.D., Freedman, R. & Bickford-Wimer, P.C. Electrophysiological effects of locally applied noradrenergic agents at cerebellar Purkinje neurons: receptor specificity. Brain Res 462, 242-51 (1988).*
36. *Antkowiak, B., Hentschke, H. & Kirschfeld, K. Effects of volatile anaesthetics on spontaneous action potential firing of cerebellar Purkinje cells in vitro do not follow the Meyer-Overton rule. Br J Anaesth 79, 617-24 (1997).*
37. *Hausser, M. & Clark, B.A. Tonic synaptic inhibition modulates neuronal output pattern and spatiotemporal synaptic integration. Neuron 19, 665-78 (1997).*
38. *Matsushita, K. et al. Bidirectional alterations in cerebellar synaptic transmission of tottering and rolling Ca2+ channel mutant mice. J Neurosci 22, 4388-98 (2002).*
39. *Yoshida, T., Katoh, A., Ohtsuki, G., Mishina, M. & Hirano, T. Oscillating Purkinje neuron activity causing involuntary eye movement in a mutant mouse deficient in the glutamate receptor delta2 subunit. J Neurosci 24, 2440-8 (2004).*
40. *Ohtsuki, G., Kawaguchi, S.Y., Mishina, M. & Hirano, T. Enhanced inhibitory synaptic transmission in the cerebellar molecular layer of the GluRdelta2 knock-out mouse. J Neurosci 24, 10900-7 (2004).*
41. *Goossens, J. et al. Expression of protein kinase C inhibitor blocks cerebellar long-term depression without affecting Purkinje cell excitability in alert mice. J Neurosci 21, 5813-23. (2001).*
42. *Margrie, T.W., Brecht, M. & Sakmann, B. In vivo, low-resistance, whole-cell recordings from neurons in the anaesthetized and awake mammalian brain. Pflugers Arch 444, 491-8 (2002).*
43. *Stahl, J.S., van Alphen, A.M. & De Zeeuw, C.I. A comparison of video and magnetic search coil recordings of mouse eye movements [In Process Citation]. J Neurosci Methods 99, 101-10 (2000).*
44. *Stahl, J.S. Eye movements of the murine p/q calcium channel mutant rocker, and the impact of aging. J Neurophysiol 91, 2066-78 (2004).*
45. *Efron, B. & Tibshirani, R.J. An introduction to the bootstrap, (Chapman and Hall, London, 1993).*
46. *Bhumbra, G.S. & Dyball, R.E. Measuring spike coding in the rat supraoptic nucleus. J Physiol 555, 281-96 (2004).*
47. *Brown, E.N., Barbieri, R., Ventura, V., Kass, R.E. & Frank, L.M. The time-rescaling theorem and its application to neural spike train data analysis. Neural Comput 14, 325-46 (2002).*

Chapter 4

Cerebellar nuclei: signal processing and role of calcium channels

Abstract

Homozygous *tottering* mice are spontaneous ataxic mutants, which carry a mutation in the gene encoding the ion pore of the P/Q-type voltage-gated calcium channels. P/Q-type calcium channels are prominently expressed in Purkinje cell terminals, but it is unknown to what extent these inhibitory terminals in *tottering* mice are affected at the morphological and electrophysiological level. Here we investigated the distribution and ultrastructure of their Purkinje cell terminals in the cerebellar nuclei as well as the activities of their target neurons. The densities of Purkinje cell terminals and their synapses were not significantly affected in the mutants. However, the Purkinje cell terminals were enlarged and had an increased number of vacuoles, whorled bodies and mitochondria. These differences started to occur between 3 and 5 weeks of age and persisted throughout adulthood. Stimulation of Purkinje cells in adult *tottering* mice resulted in inhibition at normal latencies, but the activities of their postsynaptic neurons in the cerebellar nuclei were abnormal in that the frequency and irregularity of their spiking patterns were enhanced. Thus, although the number of their terminals and their synaptic contacts appear quantitatively intact, Purkinje cells in *tottering* mice show several signs of axonal damage that may contribute to altered postsynaptic activities in the cerebellar nuclei.

Introduction

The spontaneous mouse mutant *tottering* (*tg*) suffers from recessive neurological disorders including ataxia, motor seizures, and behavioural absence seizures resembling petit mal epilepsy in humans (Fletcher et al., 1996). Its genotype is characterized by an autosomal recessive mutation in the gene located on chromosome 8 that encodes the α_{1A}-subunit of P/Q-type Ca^{2+}-channels in nerve, muscle and secretory cells (Fletcher et al., 1996; Pinto et al., 1998). Since P/Q-type calcium channels are abundantly present in cerebellar Purkinje cells and gate ~90% of their high-voltage-activated Ca^{2+}-influx (Llinas et al., 1989; Mintz et al., 1992), it is parsimonious to explain the juvenile onset of ataxia in *tg* mutants by deficits in their Purkinje cells. Indeed, the calcium influx in *tg* Purkinje cells is decreased by ~45% (Wakamori et al., 1998), their responses to parallel fiber stimulation are reduced by ~50% (Matsushita et al., 2002), and their simple spike firing patterns show enhanced irregularities with periods of pauses and bursts (Hoebeek et al., 2005). Moreover, Purkinje cells in *tg* show morphological aberrations in that their dendritic spines make relatively frequently multiple contacts with individual parallel fiber varicosities (Rhyu et al., 1999) and that their somata have elongated nuclei and are reduced in size (Isaacs and Abbott, 1992; Meyer and MacPike, 1971). Interestingly, many of the morphological and physiological changes in the Purkinje cell dendrites and somata precede or coincide with the occurrence of the ataxia at the end of the first month of age suggesting that these changes form a major cause of the behavioural deficits (Hoebeek et al., 2005; Rhyu et al., 1999). However, it remains possible that changes at the level of the terminals of the Purkinje cells also contribute to the ataxia in *tg* mutants, because the density of P/Q-type Ca^{2+}-channels is high in terminals (Catterall, 1999; Hillman et al., 1991) and because chronically altered firing in Purkinje cells can lead to pathological alterations in their terminals (Rossi et al., 1987). We therefore in-

vestigated the Purkinje cell terminals of *tg* mutants at both the morphological and electrophysiological level. To correlate possible morphological aberrations to the behavioural changes, we investigated the distribution and ultrastructure of Purkinje cell terminals in the cerebellar nuclei before (2-3 week old animals) and after (5 week and 6 month old animals) the onset of the ataxia. In this study the Purkinje cell terminals were identified by immunocytochemical labeling using anti-calbindin labeling (De Zeeuw and Berrebi, 1995; Teune et al., 1998). In addition, we investigated whether the contacts of the Purkinje cell terminals with their postsynaptic neurons in the cerebellar nuclei in the adult mice were functionally intact by recording the extracellular activities of the cerebellar nuclei neurons following stimulation of the Purkinje cells.

Material and methods

Animals

Data were collected from 18 *tg* mice and 17 wild type littermates (both male and female mice were included; C57BL/6J background; originally ordered from Jackson laboratory, Bar Harbor, ME, USA). All mice were genotyped at the age of p9-p12 and no oligosyndactyly was used. All preparations and experiments were done according to the European Communities Council Directive (86/609/EEC) and were reviewed and approved by the national ethics committee. For light microscopy we restricted ourselves to animals of 6 months (*tg*, N = 3; wild type, N = 3), while for electron microscopy we examined animals at the age of 2-3 weeks (i.e. for both 14 days and 20 days *tg*, N = 2 and wild type, N = 2), 5 weeks (*tg*, N = 3; wild type, N = 2) and 6 months (*tg*, N = 3; wild type, N = 3). The electrophysiological recordings were conducted in mice at the age of 6 months (*tg*, N = 5; wild type, N = 5).

Light microscopy

Three adult wild type and 3 *tg* littermates were anesthetized with an overdose of Nembutal (i.p.) and transcardially perfused with 0.12 M phosphate buffered saline (PBS, pH = 7.4) followed by 4% paraformaldehyde in phosphate buffer (PB) at room temperature. The cerebellum and brainstems were carefully removed, postfixed in 4% paraformaldehyde for two hours, placed in 10% sucrose in PB at 4°C overnight, and subsequently embedded in gelatine in 30% sucrose. The blocks were cut on a cryotome into coronal sections of 40 µm. Sections were washed in blocking solution containing 10% normal horse serum (NHS) with 0.5% triton for 1 hr and incubated in rabbit anti-Calbindin (1:7000, Swant) with 2% normal horse serum and 0.5% Triton for 48 hrs (Baurle and Grusser-Cornehls, 1994). Subsequently, the sections were incubated for 2 hrs in biotinylated Goat-anti-Rabbit IgG at room temperature (1 to 500; Vector) followed by 2 hrs in avidin-biotinylated horseradish peroxidase complex (ABC-HRP; Vector). Sections were rinsed in PB and stained with 0.5% 3,3-diaminobenzidine tetrahydrochloride and 0.01% H_2O_2 for 15 min at room temperature. Sections of *tg* mutants and wild type littermates were processed simultaneously to avoid artificial differences due to the staining procedures. For quantification of terminals in the lateral cerebellar nuclei and interposed nuclei we framed 500 µm x 500 µm and used Neurolucida systems (MicroBrightField, Colchester, VT, USA) for

analyses, which were done blind to the genotype by the investigator. The terminal numbers were averaged per animal and nucleus.

Electron microscopy

Wild type (N = 9) and *tg* mice (N = 10) were anesthetized with an overdose of Nembutal (i.p.) and transcardially perfused with 4% paraformaldehyde and 0.5% glutaraldehyde in cacodylate buffer. Brains were removed, kept overnight in 4% paraformaldehyde, and cut into 80 µm thick coronal sections on a Vibratome. The Vibratome sections were subsequently washed and blocked for 1 hr in 10% NHS followed by 48 hours of incubation in rabbit anti-Calbindin 4°C (1:7000, Swant) and 2% NHS. Subsequently, the sections were incubated overnight 4°C in biotinylated Goat-anti-Rabbit IgG (1 to 500; Vector) and avidin-biotinylated horseradish peroxidase complex (ABC-HRP; Vector). At the end of the immunostaining the sections were stained with 0.5% 3,3-diaminobenzidine tetrahydrochloride and 0.01% H_2O_2 for 15 min at room temperature. Ultimately, the sections were osmicated with 2% osmium in 8% glucose solution, dehydrated in dimethoxypropane, and stained en block with 3% uranyl acetate / 70% ethanol for 60 min and embedded in Araldite (Durcupan, Fluka, Germany). Guided by findings in semithin sections we made pyramids of the medial cerebellar nucleus, lateral cerebellar nucleus, interposed cerebellar nucleus and superior vestibular nucleus. Ultrathin sections (70-90 nm) were cut using an Ultramicrotome (Leica, Germany), mounted on copper grids, and counterstained with uranyl acetate and lead citrate. Purkinje cell terminals were photographed and analysed using an electron microscope (Philips, Eindhoven, The Netherlands). Electron micrographs were taken at magnifications ranging from 1,500x to 30,000x from single-hole EM grids, and analysed with the use of commercially available software (SIS) to study diameters and surface areas of labelled terminals and their surrounding structures in the neuropil. The surface area measurements were deduced automatically by drawing the circumference of all profiles (IBAS systems). Terminals of the lateral cerebellar nucleus and interposed cerebellar nucleus were each quantified for 10.000 μm^2 in each animal by a researcher who was blind to the genotype of the mice. Since no significant differences were observed among the two cerebellar nuclei, the data were pooled. Statistics were done with the use of unpaired Student's t-test assuming equal variances. P-values equal or smaller than 0.05 were considered significant.

Electrophysiology

Five *tg* mutants and 5 wild type littermates of ~6-8 months were anesthetized with ketamine (50 mg/kg body weight) and xylazine (8 mg/kg body weight) and subjected to extracellular, single unit recordings of neurons in the cerebellar nuclei. Borosilicate pipettes (OD 2 mm; ID 1.16 mm; 4-10 MΩ; ~1-2 µm tip diameter) filled with 2 M NaCl solution were positioned stereotactically using an electronic pipette holder (Luigs & Neumann, Ratingen, Germany). Signals were sampled at 10 KHz (Digidata 1322A, Axon Instr., Foster City, USA), amplified, filtered, and stored for offline analysis (Multiclamp 700A, Axon Instr.). Purkinje cells in the cerebellar cortex were stimulated using custom-made urethane-insulated tungsten electrodes

with two tips (separated ~25 µm). A single negative 100 µs pulse of 100-400 µA (Cornerstone BSI-950, Dagan, Minneapolis, Minnesota, USA) was used to activate the surrounding cerebellar cortical tissue. Stimulus locations were never deeper than 0.5 mm and were positioned in Lobule VI or paramedian lobule. Neurons of the cerebellar nuclei were identified by recording their characteristic activities (Rowland and Jaeger, 2005). Once a responsive area within a cerebellar nucleus was found, multiple tracks were made to record both stimulus response activity and spontaneous activity. Evoked activity was recorded for at least 70 trials of 2 sec each (at a frequency of 0.5 Hz), while spontaneous activity was recorded for at least 2 min. Histological verification of the location of recordings was done by injection of 4% Alcian blue dye.

Analysis of electrophysiological data

Off-line analysis of neuronal firing rates was performed in Matlab (Mathworks Inc. Natick, MA, USA) as previously described by Goossens et al. (2004). Firing frequency, coefficient of variance (CV; standard deviation interspike interval / mean interspike interval), and peristimulus histograms of the extracelularly recorded neuronal activities in the cerebellar nuclei were constructed using custom made routines in MATLAB (Mathworks). To identify statistically significant responses to electrical stimulation of the cerebellar cortex, we constructed an analog representation of each spike train using Gaussian local rate coding (Paulin, 1995). The sum of these Gaussians represents the instantaneous firing frequency, which we normalized. Poststimulus excursions of the mean instantaneous frequency that exceeded three times the standard deviation were marked as statistically significant responses (Rowland and Jaeger, 2005) and were used to specify the latency of the inhibition. We used a Gaussian width of 1 ms to determine the occurrence of the spike rate change, typically at < 6 ms after the stimulus onset. Statistical analysis was done using unpaired Student's t-tests (two-tailed) assuming equal variances. Differences were considered to be significant when the p-value ≤ 0.05. Data are presented as mean ± SEM.

Results

Light microscopy

Immunohistochemical calbindin stainings labelled all parts of the Purkinje cells including their cell bodies, dendrites and axons in both wild types and *tg*'s. Labelled Purkinje cell terminals were found throughout the medial cerebellar nuclei, lateral cerebellar nuclei, as well as the anterior and posterior interposed cerebellar nuclei (Fig. 1). In addition, many labelled terminals were observed in the medial vestibular nuclei and superior vestibular nuclei (Fig. 1A,B), while only few were observed in the nuclei prepositus hypoglossi (data not shown). In both wild types and *tg*'s labelled Purkinje cell terminals were mostly adjacent to cell bodies and proximal dendrites of their target neurons (see also De Zeeuw and Berrebi, 1995). No significant differences were observed among the densities of terminals in the lateral cerebellar nuclei and interposed cerebellar nuclei (data of both cerebellar nuclei pooled; p = 0.2; N = 3 for both wild type and *tg*) or between *tg*'s and wild types (p = 0.7; N = 3).

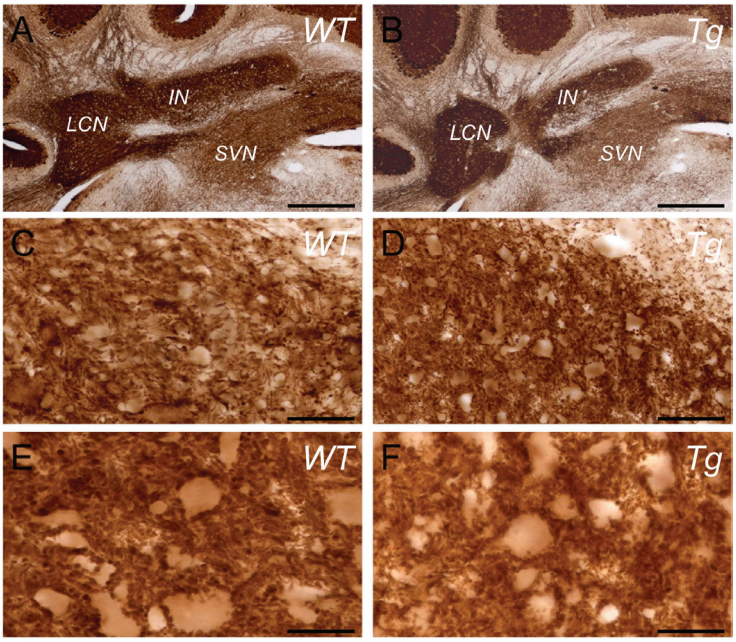

Figure 1. Distribution of calbindin labeled Purkinje cell terminals in the cerebellar and vestibular nuclei in wild types (WT) and tottering (Tg) at the light microscopic level. (A-B) Note the high densities of labeled terminals in the lateral cerebellar nucleus (LCN) and interposed nucleus (IN), and the intermediate density in the superior vestibular nucleus (SVN). (C-F) Higher magnifications of labeled Purkinje cell terminals in the interposed cerebellar nuclei. Note the abundant number of terminals apposed to the soma and proximal dendrites. Scale bars indicate 450 µm in A-B, 75 µm in C-D, and 25 µm in E-F.

Electron microscopy

-Five week old animals. The morphology and postsynaptic distribution of calbindin labelled Purkinje cell terminals were initially analyzed in animals that were at the age of 5 weeks as this is the age when ataxia is present for ~1-2 weeks (Green and Sidman, 1962). Labelled Purkinje cell terminals as well as their non-myelinated pre-terminal segments and myelinated axons could be readily identified in the various cerebellar nuclei and confirmed in the superior vestibular nucleus (Fig. 2). Purkinje cell terminals in wild types were densely packed with pleiomorphic vesicles and they established one or more symmetric synaptic contacts with the soma and/or a dendritic segment of their target neurons as described previously for rats (De Zeeuw and Berrebi, 1995; for criteria of synaptology see also De Zeeuw et al., 1989) (Fig. 2A). The vast majority of the Purkinje cell terminals included at least a few mitochondria, but some of them were filled with as many as 10 of them (see eg. Fig. 2C). Purkinje cell terminals in *tg'*s showed the same content of vesicles as well as the same type and distribution of synapses, but they were enlarged due to the presence of vacuoles and an increased number of mitochondria, many of which were bigger than in wild type (Figs. 2B and 2D).

Quantitative analyses of the Purkinje cell terminals (N = 3 and n = 204 for *tg*; N = 2 and n = 158 for wild type) of the 5 week old animals at the ultrastructural level confirmed and extended the findings described above. First, we did not find any

significant difference in the density of Purkinje cell terminals among wild types and *tg*'s ($p = 0.32$) (Fig. 2E). Next, we showed that the terminals in *tg*'s were indeed significantly enlarged ($p < 0.01$) and that more terminals contained vacuoles ($p < 0.05$) (Figs. 2E-F). Moreover, of the terminals that did contain one or more vacuoles those in the *tg* contained a higher number of vacuoles ($p < 0.05$). In contrast, the number of terminals that contained mitochondria ($p = 0.9$) as well as the number of mitochondria per terminal was not significantly increased in the cerebellar nuclei of *tg* at this age even though a trend was visible in the latter parameter ($p = 0.08$) (Fig. 2G). To find out as to whether neurotransmission and/or compensatory synaptic mechanisms may take place in Purkinje cell terminals of 5 week old *tg*'s we also quantified their number of synapses per terminal. We did not find any significant difference among wild types and mutants in this respect ($p = 0.33$).

-*Six month old animals.* The analysis of the Purkinje cell terminals in 5 week old *tg* animals showed that they were moderately but significantly enlarged and that they contained significantly more vacuoles, while their number of mitochondria tended to be slightly increased. To find out as to whether these pathologies persisted and/or deteriorated over time, we investigated the morphology of Purkinje cell terminals ($N = 3$ and $n = 172$ for *tg*; $N = 3$ and $n = 211$ for wild type) in the cerebellar nuclei of 6 month old mice. Similar to the 5 week old animals the density of Purkinje cell terminals was not significantly reduced in the cerebellar nuclei of the 6 month old *tg* mutants ($p = 0.44$), while the average surface area of their terminals was significantly larger than that in their age-matched wild type littermates ($p < 0.001$) (Fig. 3). This observation was corroborated by the findings that the average numbers of terminals that contained vacuoles and/or mitochondria were significantly larger in *tg* than those in wild type littermates ($p < 0.001$ and $p < 0.01$, respectively). In addition, the number of vacuoles per terminal as well as the mitochondria per terminal was significantly (both p-values < 0.01) increased in these terminals in the 6 month old *tg* mutants. Interestingly, the morphology of the vacuoles got worse over time in that they showed more irregular shapes and that they occupied greater surface areas than those in the 5 week old *tg*'s. The numbers of terminals that had vacuoles and mitochondria in the 6 month old *tg*'s were significantly higher than those in the 5 week old *tg*'s ($p < 0.02$ and $p < 0.01$, respectively). Moreover, Purkinje cell terminals in the cerebellar nuclei of the 6 month old mutants showed, in contrast to those in the 5 week old mutants, so-called whorled bodies (Fig. 3D). These large structures, which can also be observed in Purkinje cell terminals following olivary lesions and which might be a result of increased production of smooth endoplasmic reticulum (Rossi et al., 1987), were present in 7% of the terminals. Still, neurotransmission between the Purkinje cell terminals and their target neurons may still occur in these older *tg* mutants, because the number and structure of the synapses appeared intact as compared to wild types ($p = 0.21$). Thus, ultrastructural analyses of the cerebellar nuclei in the 6 month old animals showed that the pathology of the Purkinje cell terminals in adult *tg* mutants progresses steadily, but they also suggest that synaptic neurotransmission is possible.

-*Two week old animals.* If the morphological aberrations of the Purkinje cell terminals in *tg* contribute to their behavioural phenotype, one expects that these ab-

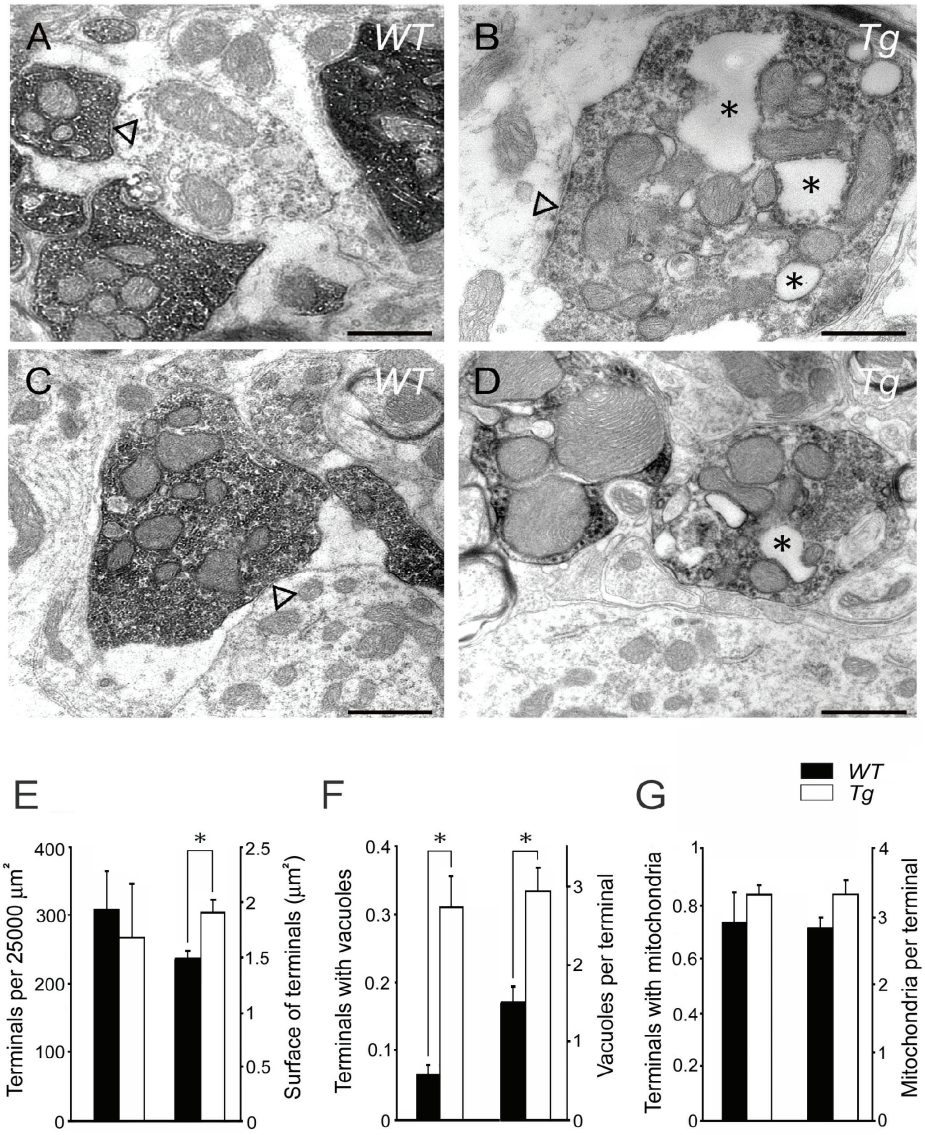

Figure 2. Electron micrographs of calbindin labeled Purkinje cell terminals taken from five week old mice. (A and B) Purkinje cell terminals in the lateral cerebellar nucleus of wild types (WT) and tottering (Tg), respectively. (C and D) Purkinje cell terminals in the superior vestibular nucleus of WT and Tg, respectively. Note that the Purkinje cell terminals in Tg contain vacuoles (asterisks) and in some cases (upper left corner in D) swollen mitochondria. The terminals in A, B and C establish symmetric synaptic contacts (open triangles). Scale bar in A indicates 550 nm, in B 350 nm, and in C and D 625 nm. (E-G) Histograms showing the morphological characteristics of Purkinje cell terminals in WT (black) and and Tg's (white) in the cerebellar nuclei (CN). (E) Densities of terminals (left) and their surface areas (right). (F) Number of terminals that have vacuoles (left), and of those terminals, the average number of vacuoles per terminal (right). (G) Number of terminals with mitochondria (left), and of those terminals, the average number of mitochondria per terminal (right). Asterisks indicate significant differences.

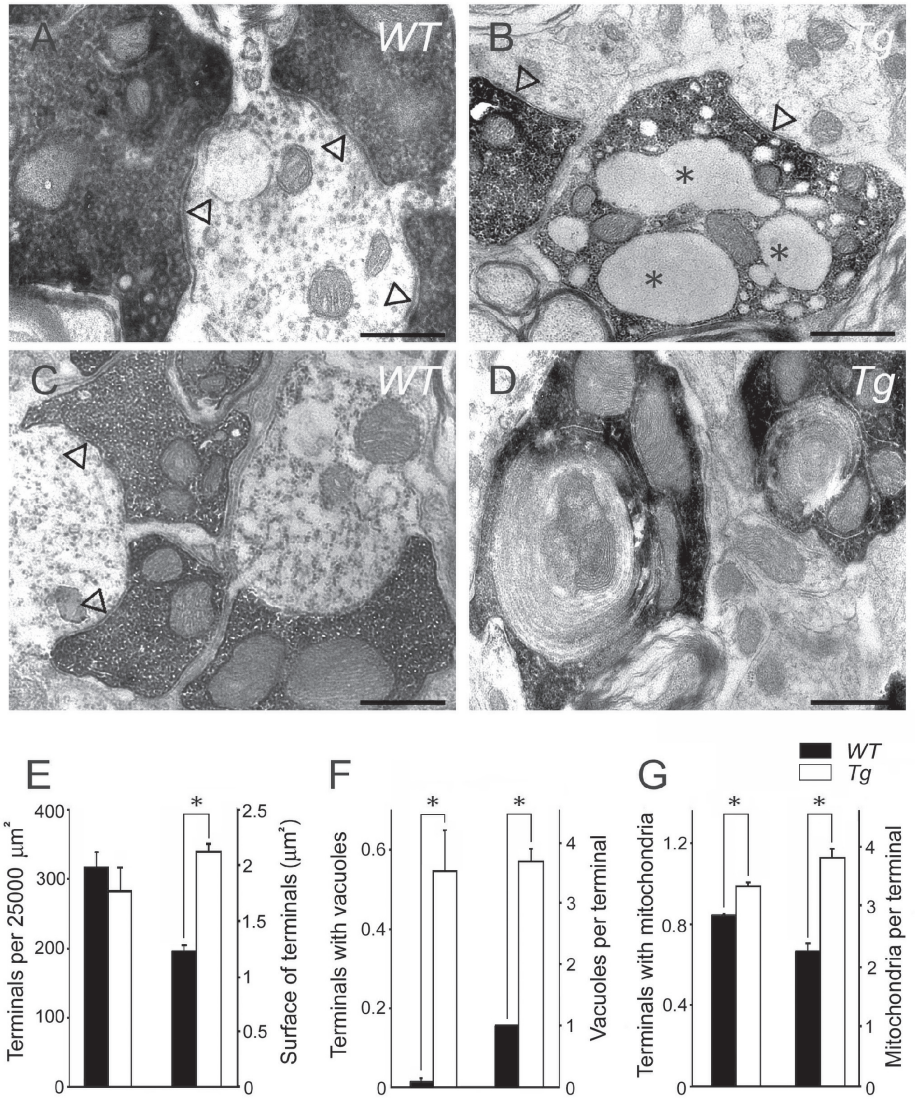

Figure 3. Electron micrographs of calbindin labeled Purkinje cell terminals taken from 6 month old mice. (A-B) Purkinje cell terminals in the lateral cerebellar nucleus of wild types (WT) and tottering (Tg), respectively. (C-D) Purkinje cell terminals in the interposed cerebellar nucleus of wild type (C) and tottering (D). Note that the Purkinje cell terminals in tottering contain vacuoles (asterisks in B) and whorled bodies (membraneous lamellar structures in D). The terminals in A, B and C establish symmetric synaptic contacts (open triangles). Scale bar in A indicates 350 nm, in B and C 625 nm, and in D 550 nm. (E-G) Histograms showing the morphological characteristics of Purkinje cell terminals in the cerebellar nuclei of 6 month old WT's (black) and Tg's (white). (E) Densities of terminals (left) and their surface areas (right). (F) Number of terminals that have vacuoles (left), and of those terminals, the average number of vacuoles per terminal (right). (G) Number of terminals with mitochondria (left), and of those terminals, the average number of mitochondria per terminal (right). Asterisks indicate significant differences.

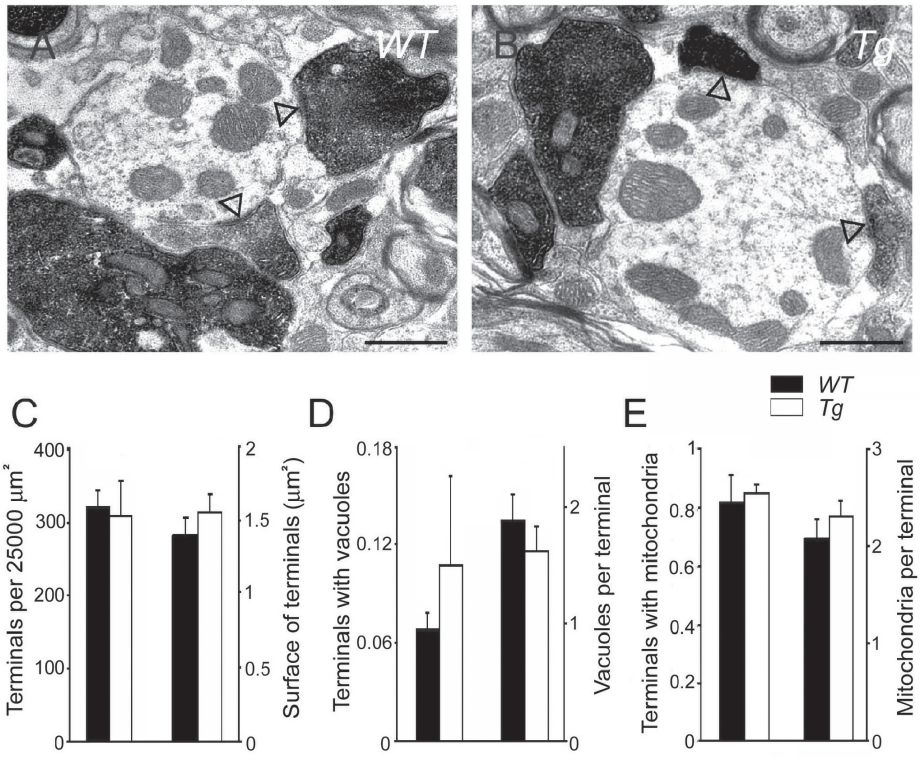

Figure 4. Electron micrographs of calbindin labeled Purkinje cell terminals taken from 2-3 week old mice. (A-B) Purkinje cell terminals in the lateral cerebellar nucleus of wild types (WT) and tottering (Tg), respectively. Note that the Purkinje cell terminals in tottering do not contain pathological inclusions and that the terminals in A and B establish symmetric synaptic contacts (open triangles). Scale bars in A and B both indicate 625 nm. (C-E) Histograms showing the morphological characteristics of Purkinje cell terminals in the cerebellar nuclei of 2-3 week old WT (black) and Tg (white). (C) Densities of terminals (left) and their surface areas (right), respectively. (D) Number of terminals that have vacuoles (left), and of those terminals, the average number of vacuoles per terminal (right). (E) Number of terminals with mitochondria (left), and of those terminals, the average number of mitochondria per terminal (right).

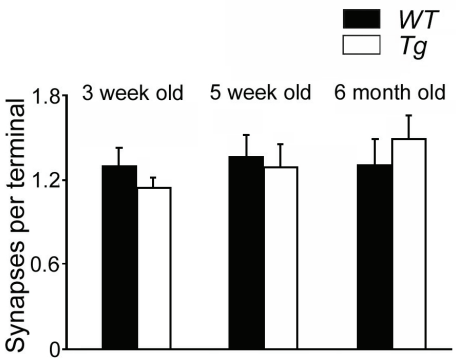

Figure 5. Histograms showing the number of synapses per terminal for 3 week old, 5 week old and 6 month old wild types (WT; black) and tottering mice (Tg; white). Note that no significant differences are found among the three different ages.

normalities start to occur in the period when the ataxia start to occur, i.e. at the age of 3 to 4 weeks (Green and Sidman, 1962). We therefore investigated whether the morphological abnormalities were already apparent at 2-3 weeks of age. Indeed, analysis of Purkinje cell terminals of these young animals did not show a significant difference among wild types (n = 116) and *tg*'s (n = 118) for any of the morphological parameters described above (Fig. 4). Thus, the density and shape of the terminals as well as those of the mitochondria inside these terminals appeared normal, and there were no signs of pathology such as high numbers of vacuoles or whorled bodies or altered numbers of synapses. The onset of the cytological abnormalities in the Purkinje cell terminals in *tg* must therefore occur between 3 and 5 weeks after birth.

Electrophysiology

The ultrastructural data described above showed that the numbers of synaptic contacts between Purkinje cells and their target neurons in the cerebellar nuclei are not affected in *tg* mutants (see also Fig. 5), while the content of the Purkinje cell terminals show signs of progressive pathology. These findings raise the questions as to whether synaptic neurotransmission is possible at the Purkinje cell terminals, and if so, whether the temporal pattern of the postsynaptic activity in the cerebellar nuclei neurons is normal. We therefore investigated the latency and duration of inhibition in the cerebellar nuclei neurons induced by activation of the Purkinje cells as well as the temporal pattern of spontaneous activities of the cerebellar nuclei neurons.

- *Latency and duration of inhibition.* Purkinje cell stimulation in the cerebellar cortex of 6 month old animals resulted in clear inhibition in the cerebellar nuclei neurons in both *tg* and wild type (Fig. 6). No differences were found among *tg* and wild type mice in the threshold for eliciting an inhibitory response ($p = 0.4$), and the latency and duration of these responses were also not significantly different. In responsive neurons the firing was interrupted with a latency of 3.1 ± 0.6 ms in *tg* and 4.2 ± 0.7 ms in wild type ($n = 7$ for both genotypes; $p = 0.21$) (Fig. 6B), while the duration of the inhibition lasted 3.0 ± 0.4 ms in *tg* and 3.3 ± 0.5 ms in wild type ($n = 7$ for both genotypes; $p = 0.58$). Apart from the initial inhibition some cells responded with a consecutive increase in firing frequency ($n = 4$ for wild type and $n = 3$ for *tg*). The latency of this excitation varied widely and was also not significantly different ($p = 0.3$) among the two genotypes (5.6 ± 2.3 ms in *tg* re 7.7 ± 2.4 ms in wild types). Thus, these data indicate that the Purkinje cell terminals are functionally intact when activated in an artificial fashion using electrophysiological stimulation.

The finding that neurotransmission at the synapses of the Purkinje cell terminals in the cerebellar nuclei can occur following artificial electrical stimulation, does not necessarily imply that this process operates normally under more natural circumstances. We therefore also recorded spontaneous activities of the cerebellar nuclei neurons that receive Purkinje cell input (Fig. 7A). Long episodes of extracellular recordings without electrical stimulation showed that the average firing frequency of these neurons in the lateral and medial cerebellar nuclei of 6 month old *tg* mice (64.7 ± 3.6 Hz; $N = 5$ and $n = 44$) is significantly higher ($p < 0.01$) than that of wild type littermates (48.5 ± 3.0 Hz; $N = 5$ and $n = 70$) (Fig. 7B). In addition, the coefficient of variance of these spiking activities in *tg* (1.44 ± 0.22) was significantly higher ($p < 0.01$) than that in wild types (0.99 ± 0.1) (Fig. 7C). These data are in line with the hy-

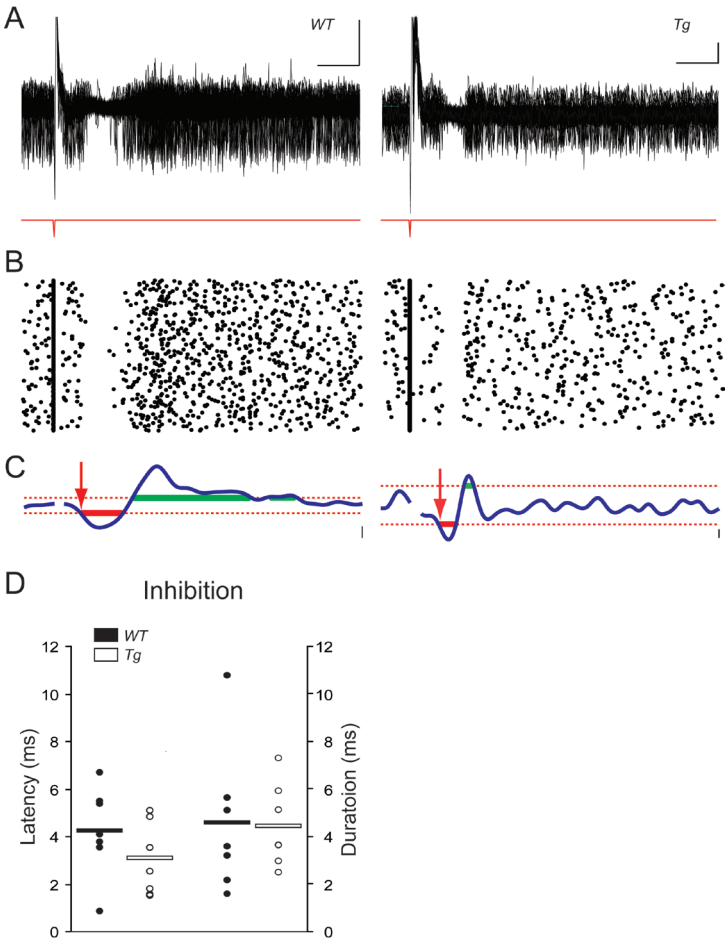

Figure 6. Cerebellar nuclei neurons responding to stimulation of Purkinje cells in the cerebellar cortex of 6 month old wild type and tottering mice. (A) Overlay of 100 traces of a single unit recording from an interposed nucleus neuron of a wild type (WT; left panel) and tottering (Tg; right panel) mouse. Note that the firing continues during the stimulus artefact. Scale bars indicate 500 µV (vertical) and 5 ms (horizontal) in the left panel and 200 µV (vertical) and 5 ms (horizontal) in the right panel. Dip in lower trace indicates stimulus pulse of 100 µs. (B) Accompanying scatter plot of single unit activity showing the same period of inhibition as in A. Note that the recording of the single unit activity is absent during the stimulus artefact. (C) Gaussian fit with a 1 ms time constant. Solid line indicates the mean Gaussian fit and the dotted horizontal lines indicate ± 3 SD used to calculate the latency. Note that both these wild type and tottering cells responded with a significant inhibition (solid line) followed by a significant excitation (solid line; see text for details). Vertical scale bars indicate 0.5 and 0.2 normalized frequency in the left and right panel, respectively. (D) Average latency (left) and duration of the inhibition (right) following stimulation of the cerebellar cortex. Dots indicate values of individual recordings and horizontal bars indicate the average values per genotype.

pothesis that under physiological conditions the inhibition imposed by the Purkinje cells onto the cerebellar nuclei neurons in *tg* is less effective and less consistent than that in wild types.

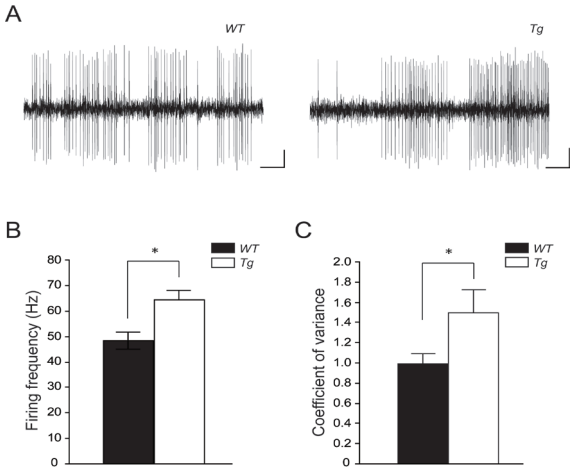

Figure 7. Activity patterns of cerebellar nuclei neurons of 6 month old wild type and tottering mice. (A) Typical examples of extracellular recordings of cerebellar nuclei neurons from the lateral dentate nucleus of a wild type (WT, left panel) and tottering (Tg, right panel) mouse. Scale bars indicate 10 mV (vertical line) and 100 ms (horizontal line). (B) Average firing frequencies found in wild type and tottering; note the increased level in tottering. (C) Average coefficients of variance found in wild type and tottering; note the increased level in tottering.

Discussion

The main finding of the present study is that Purkinje cell terminals in the cerebellar nuclei in *tg* show signs of structural damage such as an increase in size, swelling of mitochondria, presence of pathological vacuoles, and formation of large whorled bodies, while their synapses required for inhibitory neurotransmission appear intact. These morphological observations are corroborated by the finding that the activity patterns of their postsynaptic neurons in the cerebellar nuclei are faster and more irregular than those of their wild type littermates. As will be discussed below the morphological and physiological findings each have their own implications, but together they suggest that the pathology in Purkinje cell terminals in *tg* may contribute to a suboptimal neurotransmission in their cerebellar nuclei and thereby to their behavioural deficits.

The observation that the number of Purkinje cell terminals and synapses were not affected in *tg* agreed with the fact that we found normal latencies and duration values for inhibition in the cerebellar nuclei neurons following artificial stimulation of the Purkinje cell input. These findings are in line with the findings in *tg* that electrical stimulation of floccular Purkinje cells in their vestibulocerebellum can evoke short latency eye movements (Hoebeek et al., 2005) and that cortical lesions in their anterior vermis can have a positive impact on the occurrence of intermittent myoclonus-like movements (Abbott et al., 2000; Campbell et al., 1999). Thus, neurotransmission appears possible at the synapses formed by the Purkinje cell terminals and their target neurons in the cerebellar and vestibular nuclei, but the question remains to what extent the pathology in the Purkinje cell terminals impairs signal coding.

The occurrences of swollen mitochondria and pathological vacuoles and to a lesser extent also those of the whorled bodies form the most prominent pathological changes that can be found in the Purkinje cell terminals of *tg* mice. The exact mechanisms by which these three phenomena can be explained remain to be shown, but several possibilities should be addressed. First, the Purkinje cell terminals in *tg* contain the mutated P/Q-type Ca^{2+}-channels and thereby they will most likely directly

show altered dynamics and kinetics of their vesicle release, which in turn may influence the constitution of the organelles inside them (Garcia et al., 2006; Heuser et al., 1971; Hirokawa and Heuser, 1981; Sutton et al., 1999). Second, a more indirect effect may also play a mechanistic role. This possibility is raised by the finding that similar pathological phenomena can be observed in Purkinje cell terminals in response to lesions of the inferior olive (Desclin and Colin, 1980; Rossi et al., 1987). For example, Rossi and colleagues showed that the formation of vacuoles, mitochondria, smooth endoplasmatic reticulum, and whorled bodies were all affected in a dynamic fashion in particular time frames after lesioning the olive. Presumably, the changes in smooth endoplasmic reticulum that were observed by Rossi and colleagues, but not by us, were directly related to those of the whorled bodies (Ikemoto et al., 2003; Takei et al., 1994), which were in fact also more substantial in their study than in the current one (Rossi et al., 1987). Since olivary lesions result in an absence of climbing fiber activity and thereby in a substantial increase in overall simple spike activity (Strata and Montarolo, 1982), and because the simple spike activity in *tg* mice also shows periods of bursts at high frequencies (Hoebeek et al., 2005), the pathology in the Purkinje cell terminals in *tg* could be partly secondary to the altered simple spike activities. Thus, apart from the local direct effects induced by altered expression of mutated P/Q channels in the membranes of the Purkinje cell terminals, the periodical increase in instantaneous simple spike firing frequency of the Purkinje cells may trigger multiple intracellular mechanisms, which in turn could lead to the increase of the number and volume of mitochondria as well as the formation of vacuoles and whorled bodies within the same terminals.

The findings described and discussed above raise the question to what extent the pathological aberrations in the Purkinje cell terminals in *tg* interact with those in their dendrites and cell bodies, and to what extent they both contribute to the cerebellar movement disorders (Hoebeek et al., 2005; Matsushita et al., 2002; Rhyu et al., 1999). The possibility that the pathological process at the terminals interacts with that at the cell body and dendritic arbor and that they both contribute to the behavioural deficits is supported by the observation that the period in which the morphological aberrations in the terminals start to occur, i.e. between the third and fifth postnatal week, coincides with the period in which the dendrites show their first abnormalities and in which the first signs of ataxia start to occur (Green and Sidman, 1962; Rhyu et al., 1999). Moreover, it should be noted that abnormalities occurring in the axons themselves may also interact with those in the dendrites and terminals. In older *tg*'s (> 6 months) the axons also show signs of swelling with accumulations of cytoplasmic organelles, irregularly arranged microtubules, and inclusions of a lysosomal origin (Meier and MacPike, 1971; Rhyu et al., 1999), raising the possibility that propagation of action potentials down the Purkinje cell axons can also be affected in these *tg* mice. Such a deficit may be especially detrimental, because during burst activity the simple spike frequency in *tg* mice can even exceed the maximum frequency that can be transmitted down the Purkinje cell axon in a healthy rodent (Hoebeek et al., 2005; Khaliq and Raman, 2005; Monsivais et al., 2005). Thus, since the swelling and abnormalities that occur in the axons and terminals may further reduce this maximum frequency in *tg*, the synaptic efficacy of the high frequency, simple spike bursts at their cerebellar nuclei neurons will be even lower. This re-

duced efficacy may add to the more direct cell physiological deficits caused by the mutated P/Q-type voltage-gated calcium channels in Purkinje cell terminals that will affect their machinery of neurotransmitter release as has also been shown for other cerebellar GABAergic inhibitory synapses (Caillard et al., 2000; Stephens et al., 2001; Satake et al., 2004). It is therefore not surprising that we found that the activity patterns of the cerebellar nuclei neurons that are innervated by Purkinje cells showed an increased firing frequency and an increased level of irregularity. These electrophysiological findings are compatible with a reduced efficacy of synaptic inhibition from the Purkinje cells. One may argue that P/Q-type calcium channels are also expressed by cerebellar nuclei neurons themselves (Fletcher et al., 1996; Sawada et al., 2001), but this factor is less likely to have a dominant role in the behavioural deficits, because the expression and presumptive functional impact are probably relatively low (Hillman et al., 1991; see also Aizenman et al., 2000 and Gauck et al., 2001) and it can probably be compensated for by modifying the Purkinje cell input (Hoebeek et al., 2005).

In conjunction, we conclude that the abnormalities at the Purkinje cell terminals in *tg* are likely to interact with those at the dendrites, soma and axons, and that they probably all contribute to an impaired output of the cerebellar nuclei neurons and thereby to the ataxia.

Acknowledgements

The authors thank Ing. E. Haasdijk for her excellent assistance. Furthermore we like to thank Ing. J. van den Burg and M. Rutteman for technical assistance. Research was supported by Neuro-Bsik, ZonMw, EUR-Fellowship, EEC-SENSOPAC, and Prinses Beatrix Fonds.

References

1. *Abbott LC, Bump M, Brandl A, De Laune S. 2000. Investigation of the role of the cerebellum in the myoclonic-like movement disorder exhibited by tottering mice. Mov Disord 15 Suppl 1:53-59.*
2. *Aizenman CD, Huang EJ, Manis PB, Linden DJ, 2000. Use-dependent changes in synaptic strength at the Purkinje cell to deep nuclear synapse. Prog Brain Res. 124:257-273.*
3. *Campbell DB, North JB, Hess EJ. 1999. Tottering mouse motor dysfunction is abolished on the Purkinje cell degeneration (pcd) mutant background. Exp Neurol 160(1):268-278.*
4. *Catterall WA. 1999. Interactions of presynaptic Ca2+ channels and snare proteins in neurotransmitter release. Ann N Y Acad Sci 868:144-159.*
5. *Caillard O, Moreno H, Schwaller B, Llano I, Celio MR, Marty A. 2000. Role of the calcium-binding protein parvalbumin in short-term synaptic plasticity. Proc Natl Acad Sci U S A 97:13372-13377.*
6. *Desclin JC, Colin F. 1980. The olivocerebellar system. II. Some ultrastructural correlates of inferior olive destruction in the rat. Brain Res 187(1):29-46.*
7. *De Zeeuw CI, Holstege JC, Ruigrok TJ, Voogd J. 1989. Ultrastructural study of the GABAergic, cerebellar, and mesodiencephalic innervation of the cat medial accessory olive: anterograde tracing combined with immunocytochemistry. J Comp Neurol. Jun 1;284(1):12-35.*
8. *De Zeeuw CI, Berrebi AS. 1995. Postsynaptic targets of Purkinje cell terminals in the cerebellar and vestibular nuclei of the rat. Eur J Neurosci 7(11):2322-2333.*
9. *Fletcher CF, Lutz CM, O'Sullivan TN, Shaughnessy JD, Jr., Hawkes R, Frankel WN, Copeland NG, Jenkins NA. 1996. Absence epilepsy in tottering mutant mice is associated with calcium channel defects. Cell 87(4):607-617.*
10. *Gauck V, Thomann M, Jaeger D, Borst A. 2001. Spatial distribution of low- and high-voltage-activated calcium currents in neurons of the deep cerebellar nuclei. J Neurosci. 21(15):RC158.*
11. *Goossens HH, Hoebeek FE, Van Alphen AM, Van Der Steen J, Stahl JS, De Zeeuw CI, Frens MA. 2004. Simple spike and complex spike activity of floccular Purkinje cells during the optokinetic reflex in mice lacking cerebellar long-term depression. Eur J Neurosci. Feb; 19(3):687-697.*
12. *Green MC, Sidman RL. 1962. Tottering--a neuromusclar mutation in the mouse. And its linkage with oligosyndacylism. J Hered 53:233-237.*
13. *Garcia AG, Garcia-De-Diego AM, Gandia L, Borges R, Garcia-Sancho J. 2006. Calcium signaling and exocytosis in adrenal chromaffin cells. Physiol Rev. Oct;84(4):1093-1131.*
14. *Heuser J, Katz B, Miledi R. 1971. Structural and functional changes of frog neuromuscular junctions in high calcium solutions. Proc R Soc Lond B Biol Sci 178(53):407-415.*
15. *Hillman D, Chen S, Aung TT, Cherksey B, Suqimori M, Llinas RR. 1991. Localization of P-type calcium channels in the central nervous system. Proc Natl Acad Sci. Aug 15;88(16);7076-7080.*
16. *Hirokawa N, Heuser JE. 1981. Structural evidence that outline toxin blocks neuromuscular transmission by impairing the calcium influx that normally accompanies nerve depolarization. J Cell Biol. Jan;88(1):160-171.*
17. *Hoebeek FE, Stahl JS, van Alphen AM, Schonewille M, Luo C, Rutteman M, van den Maagdenberg AM, Molenaar PC, Goossens HH, Frens MA, De Zeeuw CI. 2005. Increased noise level of purkinje cell activities minimizes impact of their modulation during sensorimotor control. Neuron 45(6):953-965.*
18. *Ikemoto T, Yorifuji H, Satoh T, Vizi ES. 2003. Reversibility of cisternal stack formation during hypoxic hypoxia and subsequent reoxygenation in cerebellar Purkinje cells. Neurochem Res 28(10):1535-1542.*
19. *Isaacs KR, Abbott LC. 1992. Development of the paramedian lobule of the cerebellum in wild-type and tottering mice. Dev Neurosci 14(5-6):386-393.*
20. *Khaliq ZM, Raman IM. 2005. Axonal propagation of simple and complex spikes in cerebellar Purkinje neurons. J Neurosci Jan 12;25(2):454-63.*
21. *Llinas RR, Sugimori M, Cherksey B. 1989. Voltage-dependent calcium conductances in mammalian neurons. The P channel. Ann N Y Acad Sci. 560:103-111.*
22. *Matsushita K, Wakamori M, Rhyu IJ, Arii T, Oda S, Mori Y, Imoto K. 2002. Bidirectional alterations in cerebellar synaptic transmission of tottering and rolling Ca2+ channel mutant mice. J Neurosci 22(11):4388-4398.*
23. *Meier H, MacPike AD. 1971. Three syndromes produced by two mutant genes in the mouse. Clinical, pathological, and ultrastructural bases of tottering, leaner, and heterozygous mice. J Hered 62(5):297-302.*
24. *Mintz IM, Venema VJ, Swiderek KM, Lee TD, Bean BP, Adams ME. 1992. P-type calcium channels blocked by the spider toxin omega-Aga-IVA. Nature 366, 156-158.*
25. *Monsivais P, Clark BA, Roth A, Hausser M. 2005. Determinants of action potential propagation in cerebellar Purkinje cell axons. J Neurosci 25(2):464-472.*
26. *Paulin MG. System identification of spiking sensory neurons using realistically constrained nonlinear time*

series models. In: Advances in Processing and Pattern Analysis of Biological Signals, editd by Gath I and Inbar G. New York: Plenum, 1995, p. 183-194.

27. *Pinto A, Gillard S, Moss F, Whyte K, Brust P, Williams M, Stauderman K, Harpold M, Lang B, Newsom-Davis J, Bleakman D, Lodge D, Boot J. 1998. Human autoantibodies specific for the alpha1A calcium channel subunit reduce both P-type and Q-type calcium currents in cerebellar neurons. Proc Natl Acad Sci U S A 95(14):8328-8333.*
28. *Rhyu IJ, Abbott LC, Walker DB, Sotelo C. 1999. An ultrastructural study of granule cell/Purkinje cell synapses in tottering (tg/tg), leaner (tg(la)/tg(la)) and compound heterozygous tottering/leaner (tg/tg(la)) mice. Neuroscience 90(3):717-728.*
29. *Rossi F, Cantino D, Strata P. 1987. Morphology of Purkinje cell axon terminals in intracerebellar nuclei following inferior olive lesion. Neuroscience 22(1):99-112.*
30. *Rowland NC, Jaeger D. 2005. Coding of tactile response properties in the rat deep cerebellar nuclei. J Neurophysiol. Aug;94(2):1236-1251.*
31. *Satake S, Saitow F, Rusakov D, Konishi S. 2004. AMPA receptor-mediated presynaptic inhibition at cerebellar GABAergic synapses: a characterization of molecular mechanisms. Eur J Neurosci 19:2464-2474.*
32. *Sawada K, Sakata-Haga H, Ando M, Takeda N, Fukui Y. 2001. An increased expression of Ca(2+) channel alpha(1A) subunit immunoreactivity in deep cerebellar neurons of rolling mouse Nagoya. Neurosci Lett 316(2):87-90.*
33. *Stephens GJ, Morris NP, Fyffe RE, Robertson B. 2001. The Cav2.1/alpha1A (P/Q-type) voltage-dependent calcium channel mediates inhibitory neurotransmission onto mouse cerebellar Purkinje cells. Eur J Neurosci 13:1902-1912.*
34. *Strata P, Montarolo PG. 1982. Functional aspects of the inferior olive. Arch Ital Biol. May;120(1-3):321-29. Review*
35. *Sutton KG, McRory JE, Guthrie H, Murphy TH, Snutch TP. 1999. P/Q-type calcium channels mediate the activity-dependent feedback of syntaxin-1A. Nature. Oct 21;401(6755):800-804.*
36. *Takei K, Mignery GA, Mugnaini E, Südhof TC, De Camilli P. 1994. Inositol 1,4,5-trisphosphate receptor causes formation of ER cisternal stacks in transfected fibroblasts and in cerebellar Purkinje cells. Neuron 12(2):327-342.*
37. *Teune TM, van der Burg J, de Zeeuw CI, Voogd J, Ruigrok TJ. 1998. Single Purkinje cell can innervate multiple classes of projection neurons in the cerebellar nuclei of the rat: a light microscopic and ultrastructural triple-tracer study in the rat. J Comp Neurol 392(2):164-178.*
38. *Wakamori M, Yamazaki K, Matsunodaira H, Teramoto T, Tanaka I, Niidome T, Sawada K, Nishizawa Y, Sekiguchi N, Mori E, Mori Y, Imoto K. 1998. Single tottering mutations responsible for the neuropathic phenotype of the P-type calcium channel. J Biol Chem 273(52):34857-34867.*

Chapter 6

Discussion

Discussion

In this thesis, we investigated electrophysiological properties and the functional role of the olivo-cerebellar module. The electrophysiological and morphological results will be discussed here for each element of this olivocerebellar loop, and will be used to speculate on the general function of the olivo-cerebellar system.

Information processing by the inferior olive

Visual and somatosensory input that reaches the IO induces a powerful response in these cells [1]. Olivary cells have a unique combination of properties that can influence the way they process and gate this incoming information.

Intrinsic subthreshold oscillation. One relative unique property of olivary cells is that they exhibit subthreshold oscillations in their membrane potential. The presence of 6-8 Hz oscillations was first found *in vitro*. In some studies an even lower frequency of oscillation (close to 2 Hz) is reported [2]. However, the existence of subthreshold oscillations *in vivo* and their differences from those *in vitro* have only recently been revealed [3, 4]. Our findings, obtained by *in vivo* whole cell recording, demonstrated that indeed the vast majority of olivary neurons exhibit subthreshold oscillations (85%). This high number of oscillating cells, compared to *in vitro* studies, could be due to an intact reverberating loop mechanism that might enhance the intrinsic subthreshold oscillations in these neurons [5]. In addition to cells that express no oscillations, others exhibit a variety of shapes and frequencies of subthreshold oscillations. Next to the "classic" 6-8 Hz sinusoidal subthreshold oscillations, a lower frequency of around 2 Hz and a mixture of these two frequencies were observed. This raises the question whether different frequencies of oscillations represent different cell types or different states of cell activity. The fact that the shape and frequency of oscillations are stable over time (even up to one hour of recording), that the shape and frequency cannot be switched to a different state by various stimuli, and that these different oscillations impose significantly different preferred spiking patterns does support the idea of distinct cell types. However, no morphological differences were found among labelled cells and measurements under different anaesthetics shifted the oscillatory behaviour of the population (data not shown). Therefore, we conclude that different types of oscillations most likely represent stable activity states of olivary cells. Nevertheless, the silent cells are probably different cell types. The latter is supported by a study of Urbano and co-workers (2006) that proposes that olivary cells with no subthreshold oscillations belong to the dorsal cap and the ventrolateral outgrowth (DCK/VLO) and are in control of the oculomotor system [6], whereas principel olive (PO) cells are oscillating cells that influence the somatomotor system. These two cell types also have different electrophysiological characteristics and behave differently when exposed to Harmaline, a tremor-inducing drug. Applying Harmaline to olivary cells that express spontaneous subthreshold oscillations enhances the amplitude of oscillations and on top of that the firing activity to approximately 10 Hz [2]. This 10 Hz firing is correlated to the frequency of muscle tremor found in Harmaline injected animals [7]. The DCK/VLO cells (non oscillating cells) are not affected by Harmaline, which explains why no tremor is

found in the oculomotor system after Harmaline injection [8]. We conclude that IO neurons can be subdivided based on their subthreshold oscillatory behaviour, and that their specific spiking pattern is most likely related to their functional state.

Role of olivary gap junctions. Olivary cells are the most electrotonically interconnected cells in the brain [9, 10]. This interconnection occurs at the level of glomeruli and through gap junctions formed by connexin 36 proteins. These structures serve as bridges for ionic transmission among olivary cells [2, 11, 12]. One of the main hypotheses suggests that gap junctions play a synchronizing role among coupled cells. Slice studies confirmed that indeed there is similarity in amplitude, frequency and phase of subthreshold membrane potential oscillations in neighbouring neurons [11, 13, 14]. Although it seems that gap junctions are important for synchronization, they do not participate in the generation of these subthreshold oscillations [15]. Our data (see chapter 3) from mice that lack coupling through gap junctions revealed that olivary cells indeed act as independent oscillators. Gap junctions are only relevant for synchronization of subthreshold oscillations and not of action potentials, because of their low-pass filtering characteristics [16]. However, since action potentials normally occur during the rising part of oscillations, the synchronization of the subthreshold oscillations increases the likelihood of time-locked action potentials in a coupled network. In fact, lack of coupling among cells (such as in Cx36 mice) alters the time-locked action potential output of the IO and as a result decreased levels of complex spike synchrony were observed between neighboring Purkinje cells of Cx36 mutant mice [17].

If, though, the information coming to the IO is indeed being synchronized through gap junctions, the extension of the electronically coupled network could play a notable role. Although previous studies have reported a variety of sizes for coupled networks (depending on the method used) [18, 19], the actual size of these networks remains unknown. Additionally, it is still unclear whether cells with different frequencies of oscillation can be interconnected in one network. One could imagine that by including or excluding a particular cell (with a specific oscillatory frequency) in a mixed ensemble of coupled cells, the overall preferred frequency (and as a result the output of the IO) could be affected.

Another hypothesis on the role of gap junctions is based on the co-location of synaptic terminals and gap junctions in dendritic spines [20]. It suggests that gap junctions synchronize the synaptic input of neighboring olivary cells rather than subthreshold oscillations. When an input reaches the glomeruli it causes an all-or-none response in targeted cells that leads to synchronized firing of coupled neurons. In this way, even non-oscillating cells (DCK/VLO) that also express gap junction, can generate a synchronized output. It is not unlikely that molecules involved in plasticity processes can be transferred, through these gap junctions, to neighboring synapses (i.e. local spreading of synaptic plasticity).

Sensory input shifts the oscillations. The sensory input that reaches the IO can influence the oscillatory activity of olivary cells. Our findings provided the first evidence that sensory stimulation *in vivo* resets the onset of oscillations in the responding olivary cells. However, this input cannot alter the shape and/or frequency of oscil-

lations in an individual olivary neuron. Somatosensory stimuli did not evoke responses in cells that did not express oscillatory behaviour [6], while in the remaining cells the shape and timing of responses differ significantly based on their type of subthreshold oscillations.

When sensory information reaches the IO, it resets the timing of the subthreshold oscillations by shifting the peak of the oscillations toward the evoked action potential. This shift can be considered as a time correction for future action potentials. It is important to note that sensory input not only causes a direct effect on a group of coupled olivary cells, but might also shift the overall spiking pattern of that ensemble based on their original oscillatory frequency. From a behavioural point of view, a shift in climbing fibre input followed by a specific sensory signal could lead to more accurate timed execution of a certain movement.

Factors for controlling olivary discharge and synchrony. In addition to sensory input, IO neurons receive both inhibitory and excitatory input from CN neurons. These inputs affect olivary discharge and are also thought to modulate the degree of coupling among IO cells. However, this discharge modulation is not specific for the nuclei-olive pathway. Serotonergic input from the medullary raphe can also strongly influence the activity of olivary cells [21]. These neurons exhibit a variety of firing activities based on different states of sleep [22]. The serotonin released from these neurons can suppress the subthreshold and suprathreshold oscillatory activity of olivary cells without affecting their firing frequency [23]. Moreover, serotonin microinjection in the IO increases synchrony among PC complex spikes [24]. Therefore, one could conclude that since there is much less need for motor control during sleep, the oscillatory behaviour of olivary cells can be modulated differently based on the sleep-wake state of an animal.

Information processing by the cerebellar cortex

A clear understanding of the intrinsic dynamics and spiking behaviour of Purkinje cells is essential, since they generate the sole output of cerebellar cortex. Purkinje cells receive information predominantly from parallel and climbing fibres, causing respectively simple and complex spikes. Climbing fibre input generates a low firing activity rates (1-2 Hz), while parallel fibre input causes simple spikes with an average frequency of 40-50 Hz [25]. These inputs can be modulated given the phase of motor behaviour [26]. There are different hypotheses for information processing of each of these inputs and how they can affect one another.

Climbing fibre information controls the gain of parallel fibre information. One theory on climbing fibre function proposes that because of the low firing rate, this input has a very limited direct effect on the output of the cerebellar cortex, but does so, rather, by modifying the strength of parallel fibres [27, 28]. Moreover, by well-timed coactivation of climbing fibre and parallel fibre input, one could induce a long-term depression (LTD) in synaptic strength between parallel fibre and Purkinje cell [29, 30] resulting in lower Purkinje cell simple spike activity. The same synapse can also experience an enhanced synaptic transmission, known as long-term potentiation

(LTP), by continuous stimulation of parallel fibres. Synaptic modification can be the underlying mechanism of motor learning and memory. The complex spike then carries information related to an error or unexpected event that occurs during movement [31, 32]. The complex spike activity would counterbalance the simple spike activity evoked by parallel fibre (LTD), and these synaptic modification can leads to learning and improvement in subsequent movements and motor skills [28, 33, 34]. Alternatively, the low frequency activity of climbing fibre can by itself give a reset the simple spike activity.

The enigmatic issue of the climbing fiber toggle switch. Complex spikes can modulate the frequency of simple spike firing by causing a pause in the simple spike activity. It has been suggested that climbing fibre input can also affect the Purkinje cells in such a way that it induces toggling between different activity stages [35, 36]. Toggling of the membrane potential has been observed both *in vitro* [36-38] as well as *in vivo* in anaesthetized rats and guinea pigs [37, 39]. This transition between rest and firing state is most likely modulated by the balance between inhibitory and excitatory inputs [37, 38]. Climbing fibre input might play an essential role in this bi-directional transition [37, 39, 40]. Loewenstein and co-workers (2005) put forward the hypothesis that the sensory input transmitted by climbing fibres results in a sustained change of Purkinje cell spiking activity. They suggested that these changes in spiking activity, known as bistability, play a role in short-term processing and storage of sensory information [39]. Our whole cell recordings from mice under different anaesthetics also confirmed the existence of bistability. However, extracellular recordings from Purkinje cells in healthy, awake behaving animals both during rest and motor performance/motor learning did not show any bistability in simple spike activity. Therefore, we are convinced that bistability is very rare in awake animals, whereas anaesthetics can dramatically induce toggling in Purkinje cells. Moreover, in contrast with what has been previously reported by Loewenstein et al, in our experiments neither natural sensory stimulation, motor behaviour nor motor learning was able to induce bistability and therefore, we think that this phenomenon is not likely to play any physiological role in information transmission in the cerebellar cortex.

Climbing fibre information contains motor commands or time tags (clock function). Although it seems difficult to relate low frequency climbing fibre activity (1-2 Hz) to the control of fast limb movements, still there are reports that suggest that this is the case. For example, Welsh showed a correlation between the rhythm of complex spike activities and rhythmic body movements, such as those during rhythmic tongue movements [41, 42]. There is also evidence of climbing fibre activation around the onset of movement [26, 43] and related to speed and direction of the movement [44, 45]. Another hypothesis focuses on the role of climbing fibre input as a "clock" function [34, 46, 47] which controls the timing of peripheral acts as well as the triggering and continuation of certain behaviours. This theory is generally based on three elements: 1) rhythmic subthreshold oscillations of cells in the IO; 2) synchrony in the output of olivary cells, most likely through gap junctions; and 3) the climbing fibre activity correlated with the initiation and performance of certain movements.

Considering that electrical coupling and synchronized olivary output is one of the key elements of this timing theory, it is somewhat surprising that animals with no electrical coupling (Cx36 mice) still manage to exhibit normal motor behavior [48] - no ataxia, regular walking pattern and normal compensatory eye movement. Of course, there could be some compensatory mechanisms masking the effect of this mutation [15], but some degree of impairment in cerebellar output in these mice would still be expected.

Our data suggests that gap junctions are essential for Purkinje cell complex spike synchrony. From behavioural point of view, lack of synchrony in Cx36 mice leads to deficit in timing of unexpected motor movement. For example, during a specific motor task such as the Erasmusladder test, Cx36 mice show a significant impairment in conditioning its motor behaviour in order to anticipate on an obstacle, however at the end the animal learns to adapt to the task. But when it comes to a motor learning tasks like classical eyeblink conditioning, there is a clear impairment in timing that becomes even more pronounced over time. Both these two associative conditioning tests suggest that the synchronized well-timed output of IO is important for learning the right timing.

Information processing by the cerebellar nuclei

The cerebellar nucleus consists of inhibitory and excitatory neurons and input from Purkinje cells innervates both types of cells. The GABA-ergic neurons of the CN are part of a closed loop that project back to the IO, whereas glutamatergic excitatory cells mostly project to the mesodiencephalic junction. This nucleus can project to 1) IO via parvocellular red nucleus, the nucleus of Bechterew and the nucleus of Darkschewitsch, forming the olivo-cerebellar mesodiencephalic loop, or 2) motor neurons in the spinal cord via the Magnocellular red nucleus forming an open loop that influences motor behavior.

It is known that the small GABA-ergic neurons in CN have strong inhibitory feedback control on IO cells, which probably explains why olivary cells that are so sensitive to sensory input have so little change in discharge rate when they receive sensory input. Moreover, this input, which mostly terminates at the level of olivary glomeruli, is suggested to affect the synchrony among olivary cells. Llinas reported that altered activity of the nucleo-olivary pathway results in widespread synchronization of complex spikes in the cerebellar cortex [49]. In other words, one could think of the direct nucleo-olivo pathway as a controlling factor in decoupling ensembles of olivary cells based on a given function.

The role of the indirect nucleo-olivo pathway (via mesodiencephalic junction) is less well understood. It has been suggested that this input has a coupling effect on olivary cells and removes the decoupling inhibitory effect of the direct nucleo-olivary pathway. Although there is not enough evidence to fully confirm this hypothesis, the fact that this input also terminates next to the olivary glomeruli suggests it plays a physiological role related to gap junctions.

It is important to note that inhibitory input from Purkinje cells controls the activity of both GABA-ergic and glutamatergic cells in CN. The input from the cerebellar cortex simultaneously modulated the activity of olivo-cerebellar-olive and olivo-cerebellar mesodiencephalic loop. Moreover, Purkinje cell inhibitory input can

induce LTP [50, 51] and LTD [51-54] in CN cells. Modulation of the plasticity in the inhibitory drive to CN neurons, can affect the efficacy of the signal transmission at the level of CN which plays an important role in cerebellar control of motor coordination and learning.

One could assume that when CN neurons fire in an irregular pattern, whether it is due to dysfunction at the level of CN and/or altered input from cerebellar cortex (for example in *tg* mice), such irregularity not only directly effects the output of cerebellum (via open loop) but also causes an altered olivary discharge. Moreover, it could affect the modulation of olivary ensembles and their synchronization, which can all lead to acceleration of abnormal motor behaviour such as ataxia.

Information processing in the olivo-cerebellar module

There are many theories on how the olivo-cerebellar circuit may works, but the data presented here suggest the following. The fact that olivary cells *in vivo* express subthreshold oscillations and that the shape and frequency of oscillations influence the way they process sensory input emphasizes the important functional role of oscillations in the IO. In an ensemble of olivary cells with a similar type of synchronized subthreshold oscillations each cell has the same phase of oscillations, which results in an ensemble orchestration of firing possibilities occurring in the same time window. At the IO population level, an ensemble of 10 Hz synchronized oscillating cells generate a time locked output of approximately 100 ms. When a sensory input reaches this ensemble, it can reset this activity and cause a well timed response. At the Purkinje cell population level, this translates as 100 ms time locked CS activity. Considering that each PC expresses continuous SSs at an high firing rate (bistability does not occur in the awake behaving animal) [55] and that the PC axon does not propagate all of the spikes on the complex spike waveform [56, 57], strongly suggest that the role of CS pauses is greater than that of CSs themselves. Therefore, the time locked CS pauses may carry the information from the IO and is being recognized by CN neurons. These rhythmic pauses remove the ongoing GABA-ergic inhibition from the CN and result in time locked episodes of increased firing in the population of CN neurons. This well timed population coding of 10 Hz can activate motor neurons and control motor events. On the other hand, the same 10 Hz output of CN neurons projects back to the IO. Given that we hardly observed IPSPs during whole cell recordings from olivary neurons, and given that the GABA-ergic nucleo-olive projection innervates the peripheral dendrites in the glomeruli of the IO, I believe that CN projections may have a tonic inhibitory effect on olivary cells, and that the feedback loop (loop time approximately 100 ms) can have a decoupling role on sets of olivary cells, when/before the next oscillation starts (i.e. feedback correction speed of one cycle: ~ 100 ms).

Plans for future

Although studies done for this thesis reveal some characteristics of neurons in the olivocerebellar loop and their functional implications, there is still a lot to be elucidated. One of the major issues that still need to be studied, is the electrophysiological activity of olivary cells in the awake behaving animal. Although, we successfully explored the possibility of performing *in vivo* whole cell recording from olivary cells,

one could not exclude the dramatic effect of anesthetics on the activity of the cells, which could vary a great deal from physiological conditions.

When coupling/decoupling of olivary cells is important for proper olivocerebellar function then it is important to know the limiting factors of ensemble formation *in vivo*. The extensiveness of coupled networks in the IO and their possible changes during specific behaviours might shed some light on the capacity of the IO for motor control and need to be investigated. This might be possible with the help of imaging techniques.

At the level of cerebellar cortex, whole cell recording from Purkinje cells in awake behaving animal will give a better understanding of their role in transferring information. Additionally, the effect of inhibitory inputs from local interneurons during motor behaviour, and their synaptic plasticity in motor learning are fascinating subjects that need extra research.

At the level of CN, in light of our limited knowledge about the electrophysiological properties of these cells, organizing sets of *in-vivo* extra- and intracellular experiments based on the type of neurons (inhibitory and excitatory) and their precise location in the CN will certainly add more detail to cerebellar function. To end with, future behavioural studies and modeling will help to uncovering the function role of the intriguing olivo-cerebellar module.

References

1. *Bloedel, J.R. and T.J. Ebner, Rhythmic discharge of climbing fibre afferents in response to natural peripheral stimuli in the cat. J Physiol, 1984. 352: p. 129-46.*
2. *Llinas, R. and Y. Yarom, Oscillatory properties of guinea-pig inferior olivary neurones and their pharmacological modulation: an in vitro study. J Physiol, 1986. 376: p. 163-82.*
3. *Chorev, E., Y. Yarom, and I. Lampl, Rhythmic episodes of subthreshold membrane potential oscillations in the rat inferior olive nuclei in vivo. J Neurosci, 2007. 27(19): p. 5043-52.*
4. *Khosrovani, S., et al., In vivo mouse inferior olive neurons exhibit heterogeneous subthreshold oscillations and spiking patterns. Proc Natl Acad Sci U S A, 2007. 104(40): p. 15911-6.*
5. *Kistler, W.M. and C.I. De Zeeuw, Dynamical working memory and timed responses: the role of reverberating loops in the olivo-cerebellar system. Neural Comput, 2002. 14(11): p. 2597-626.*
6. *Urbano, F.J., J.I. Simpson, and R.R. Llinas, Somatomotor and oculomotor inferior olivary neurons have distinct electrophysiological phenotypes. Proc Natl Acad Sci U S A, 2006. 103(44): p. 16550-5.*
7. *Farmer, S.F., Rhythmicity, synchronization and binding in human and primate motor systems. J Physiol, 1998. 509 (Pt 1): p. 3-14.*
8. *McAuley, J.H., J.C. Rothwell, and C.D. Marsden, Human anticipatory eye movements may reflect rhythmic central nervous activity. Neuroscience, 1999. 94(2): p. 339-50.*
9. *De Zeeuw, C.I., E.L. Hertzberg, and E. Mugnaini, The dendritic lamellar body: a new neuronal organelle putatively associated with dendrodendritic gap junctions. J Neurosci, 1995. 15(2): p. 1587-604.*
10. *De Zeeuw, C.I., et al., Association between dendritic lamellar bodies and complex spike synchrony in the olivocerebellar system. J Neurophysiol, 1997. 77(4): p. 1747-58.*
11. *Llinas, R. and Y. Yarom, Electrophysiology of mammalian inferior olivary neurones in vitro. Different types of voltage-dependent ionic conductances. J Physiol, 1981. 315: p. 549-67.*
12. *Llinas, R., R. Baker, and C. Sotelo, Electrotonic coupling between neurons in cat inferior olive. J Neurophysiol, 1974. 37(3): p. 560-71.*
13. *Lampl, I. and Y. Yarom, Subthreshold oscillations and resonant behavior: two manifestations of the same mechanism. Neuroscience, 1997. 78(2): p. 325-41.*
14. *Llinas, R. and Y. Yarom, Properties and distribution of ionic conductances generating electroresponsiveness of mammalian inferior olivary neurones in vitro. J Physiol, 1981. 315: p. 569-84.*
15. *Long, M.A., et al., Rhythmicity without synchrony in the electrically uncoupled inferior olive. J Neurosci, 2002. 22(24): p. 10898-905.*
16. *Srinivas, M., et al., Functional properties of channels formed by the neuronal gap junction protein connexin36. J Neurosci, 1999. 19(22): p. 9848-55.*
17. *Marshall, S.P., et al., Altered olivocerebellar activity patterns. Cerebellum, 2007: p. 1-13.*
18. *Benardo, L.S. and R.E. Foster, Oscillatory behavior in inferior olive neurons: mechanism, modulation, cell aggregates. Brain Res Bull, 1986. 17(6): p. 773-84.*
19. *Llinas, R. and R.A. Volkind, The olivo-cerebellar system: functional properties as revealed by harmaline-induced tremor. Exp Brain Res, 1973. 18(1): p. 69-87.*
20. *Kistler, W.M. and C.I. De Zeeuw, Gap junctions synchronize synaptic input rather than spike output of olivary neurons. Prog Brain Res, 2005. 148: p. 189-97.*
21. *Compoint, C. and C. Buisseret-Delmas, Origin, distribution and organization of the serotoninergic innervation in the inferior olivary complex of the rat. Arch Ital Biol, 1988. 126(2): p. 99-110.*
22. *Veasey, S.C., et al., Response of serotonergic caudal raphe neurons in relation to specific motor activities in freely moving cats. J Neurosci, 1995. 15(7 Pt 2): p. 5346-59.*
23. *Placantonakis, D.G., C. Schwarz, and J.P. Welsh, Serotonin suppresses subthreshold and suprathreshold oscillatory activity of rat inferior olivary neurones in vitro. J Physiol, 2000. 524 Pt 3: p. 833-51.*
24. *Sugihara, I., E.J. Lang, and R. Llinas, Serotonin modulation of inferior olivary oscillations and synchronicity: a multiple-electrode study in the rat cerebellum. Eur J Neurosci, 1995. 7(4): p. 521-34.*
25. *Thach, W.T., Jr., Somatosensory receptive fields of single units in cat cerebellar cortex. J Neurophysiol, 1967. 30(4): p. 675-96.*
26. *Mano, N., I. Kanazawa, and K. Yamamoto, Complex-spike activity of cerebellar Purkinje cells related to wrist tracking movement in monkey. J Neurophysiol, 1986. 56(1): p. 137-58.*
27. *Marr, D., A theory of cerebellar cortex. J Physiol, 1969. 202(2): p. 437-70.*
28. *Keating, J.G. and W.T. Thach, Nonclock behavior of inferior olive neurons: interspike interval of Purkinje cell complex spike discharge in the awake behaving monkey is random. J Neurophysiol, 1995. 73(4): p. 1329-40.*
29. *Ekerot, C.F. and M. Kano, Long-term depression of parallel fibre synapses following stimulation of climbing*

fibres. Brain Res, 1985. 342(2): p. 357-60.
30. *Ito, M., M. Sakurai, and P. Tongroach, Climbing fibre induced depression of both mossy fibre responsiveness and glutamate sensitivity of cerebellar Purkinje cells. J Physiol, 1982. 324: p. 113-34.*
31. *Andersson, G. and D.M. Armstrong, Complex spikes in Purkinje cells in the lateral vermis (b zone) of the cat cerebellum during locomotion. J Physiol, 1987. 385: p. 107-34.*
32. *Gellman, R., A.R. Gibson, and J.C. Houk, Inferior olivary neurons in the awake cat: detection of contact and passive body displacement. J Neurophysiol, 1985. 54(1): p. 40-60.*
33. *Gilbert, P.F. and W.T. Thach, Purkinje cell activity during learning. Brain Res, 1977. 128(2): p. 309-28.*
34. *Llinas, R. and K. Sasaki, The Functional Organization of the Olivo-Cerebellar System as Examined by Multiple Purkinje Cell Recordings. Eur J Neurosci, 1989. 1(6): p. 587-602.*
35. *Rapp, M., I. Segev, and Y. Yarom, Physiology, morphology and detailed passive models of guinea-pig cerebellar Purkinje cells. J Physiol, 1994. 474(1): p. 101-18.*
36. *Llinas, R. and M. Sugimori, Electrophysiological properties of in vitro Purkinje cell somata in mammalian cerebellar slices. J Physiol, 1980. 305: p. 171-95.*
37. *Williams, S.R., et al., Membrane potential bistability is controlled by the hyperpolarization-activated current I(H) in rat cerebellar Purkinje neurons in vitro. J Physiol, 2002. 539(Pt 2): p. 469-83.*
38. *Hounsgaard, J. and J. Midtgaard, Intrinsic determinants of firing pattern in Purkinje cells of the turtle cerebellum in vitro. J Physiol, 1988. 402: p. 731-49.*
39. *Loewenstein, Y., et al., Bistability of cerebellar Purkinje cells modulated by sensory stimulation. Nat Neurosci, 2005. 8(2): p. 202-11.*
40. *McKay, B.E., et al., Climbing fiber discharge regulates cerebellar functions by controlling the intrinsic characteristics of purkinje cell output. J Neurophysiol, 2007. 97(4): p. 2590-604.*
41. *Welsh, J.P., et al., Dynamic organization of motor control within the olivocerebellar system. Nature, 1995. 374(6521): p. 453-7.*
42. *Welsh, J.P. and R. Llinas, Some organizing principles for the control of movement based on olivocerebellar physiology. Prog Brain Res, 1997. 114: p. 449-61.*
43. *Ojakangas, C.L. and T.J. Ebner, Purkinje cell complex and simple spike changes during a voluntary arm movement learning task in the monkey. J Neurophysiol, 1992. 68(6): p. 2222-36.*
44. *Ebner, T.J., et al., What do complex spikes signal about limb movements? Ann N Y Acad Sci, 2002. 978: p. 205-18.*
45. *Kitazawa, S., T. Kimura, and P.B. Yin, Cerebellar complex spikes encode both destinations and errors in arm movements. Nature, 1998. 392(6675): p. 494-7.*
46. *De Zeeuw, C.I., et al., Microcircuitry and function of the inferior olive. Trends Neurosci, 1998. 21(9): p. 391-400.*
47. *Braitenberg, V., Is the cerebellar cortex a biological clock in the millisecond range? Prog Brain Res, 1967. 25: p. 334-46.*
48. *Kistler, W.M., et al., Analysis of Cx36 knockout does not support tenet that olivary gap junctions are required for complex spike synchronization and normal motor performance. Ann N Y Acad Sci, 2002. 978: p. 391-404.*
49. *Lang, E.J., I. Sugihara, and R. Llinas, GABAergic modulation of complex spike activity by the cerebellar nucleoolivary pathway in rat. J Neurophysiol, 1996. 76(1): p. 255-75.*
50. *Racine, R.J., et al., Long-term potentiation in the interpositus and vestibular nuclei in the rat. Exp Brain Res, 1986. 63(1): p. 158-62.*
51. *Aizenman, C.D., P.B. Manis, and D.J. Linden, Polarity of long-term synaptic gain change is related to postsynaptic spike firing at a cerebellar inhibitory synapse. Neuron, 1998. 21(4): p. 827-35.*
52. *Morishita, W. and B.R. Sastry, Long-term depression of IPSPs in rat deep cerebellar nuclei. Neuroreport, 1993. 4(6): p. 719-22.*
53. *Morishita, W. and B.R. Sastry, Postsynaptic mechanisms underlying long-term depression of GABAergic transmission in neurons of the deep cerebellar nuclei. J Neurophysiol, 1996. 76(1): p. 59-68.*
54. *Aizenman, C.D. and D.J. Linden, Rapid, synaptically driven increases in the intrinsic excitability of cerebellar deep nuclear neurons. Nat Neurosci, 2000. 3(2): p. 109-11.*
55. *Schonewille, M., et al., Purkinje cells in awake behaving animals operate at the upstate membrane potential. Nat Neurosci, 2006. 9(4): p. 459-61; author reply 461.*
56. *Monsivais, P., et al., Determinants of action potential propagation in cerebellar Purkinje cell axons. J Neurosci, 2005. 25(2): p. 464-72.*
57. *Khaliq, Z.M. and I.M. Raman, Axonal propagation of simple and complex spikes in cerebellar Purkinje neurons. J Neurosci, 2005. 25(2): p. 454-63.*

SUMMARY / SAMENVATTING

Summary

The cerebellum is located just above the brainstem, at the base of the skull. The cerebellum is considered to be involved in the coordination of movements, correction of movements as well as learning of movements. The structure of the cerebellum can be divided into functional modules. The basic processing of information of each module seems to be rather similar. In general, each cerebellar module consists of three neuroanatomical structures: 1) the inferior olive (IO), 2) the cerebellar cortex and 3) the cerebellar nucleus (CN). Neurons from these three structures are connected to each other and form a circuit known as the olivocerebellar loop. Sensory information reaches the olivocerebellar system via 2 pathways: 1) via the IO and 2) via the mossy fiber/granule cell/parallel fiber pathway. In short, sensory input enters the IO, olivary cells integrate the information and send the processed signal to the Purkinje cells (PC) of the cerebellar cortex and, via en-passant collaterals to the cerebellar nuclear cells. The PC relays this signal via strong depolarisations known as complex spike. Sensory information that reaches the PCs via the parallel fibers generate simple spikes. PCs process the information of both sources. The PC exert a powerful synaptic inhibition onto cerebellar nuclei neurons, where the final step of cerebellar processing occurs. Neurons from these nuclei either generate the final output of the cerebellum or project their information back to the IO, creating a closed olivocerebellar loop.

Inferior olive neurons have two unique electrophysiological properties. First, the membrane potentials of IO cells exhibit subthreshold oscillations in the frequency range from 1 - 10Hz. Olivary action potentials are generated on the depolarizing peaks of these oscillations and the firing frequency of these neurons are limited and cannot reach frequencies higher than approx. 10Hz. (the baseline frequency is generally close to 1Hz). Second, these olivary neurons are electrotonically coupled through dendro-dendritic gap junctions, allowing neighbouring cells to oscillate in synchrony. In chapter 2 of this thesis, we investigated the electrophysiological properties of olivary cells in vivo and showed that in an intact circuit, olivary cells exhibit stable subthreshold oscillations. These cells can be subdivided into four clusters based on the frequency of their subthreshold oscillations. This feature raises the possibility of generating a large set of neuronal codes by composing different cell ensembles. Our results also revealed that these subthreshold oscillations are important in regulating the spiking pattern of olivary cells. These subthreshold oscillations can be shifted by spontaneous or evoked action potentials (from sensory stimulation), which affect the timing of the spiking pattern (i.e. neuronal code). This shifting mechanism of the neuronal code could be part of tuning the timing of movements.

The role of olivary electronic coupling was studied using connexin 36 knockout mice that lack the gap junctions between olivary neurons. Without any connexin 36 (no electrotonic coupling) the olivary cells act as independent oscillators, in which time-locking of action potentials on top of the peaks of the oscillations is strongly weakened. Thus, the subthreshold oscillation in uncoupled olivary cells will impose less control over the spiking patterns, which results in a more random timing of their spikes in relation to the oscillations. The lack of "subthreshold synchrony" among olivary cells in the connexin 36 mutant mice also causes decreased levels of

complex spike synchrony among PCs in the cerebellar cortex. This result might explain the impaired learning-dependent timing that was found in these mutants (see chapter 2.2).

In Chapter 3 of this thesis, we focused on the role of olivary output in transmitting information to the cerebellar cortex (via complex spikes: Cs). It has been suggested that the Cs act as a toggle switch that controls the information processing state of the PC. We showed that in an awake behaving animals, Cs neither cause membrane potential shifts nor long simple spike pauses (more than 200 ms). In fact, we showed that toggling characteristics like irregularity in PC firing and episodes of membrane potential shifts are most likely due to the use of anesthetics. However, we did observe this toggling phenotype in awake tottering mice.

The tottering mouse suffers from a mutation in P/Q type calcium channels and exhibit pronounced irregularity PC firing. This irregularity in spiking activity might lead to morphological abnormalities that we observed at the level of PC terminal in the CN (chapter 4). Because PCs expose a strong inhibition on CN neurons, it is not surprising that their irregular spiking behaviour influence the regularity of firing of CN neurons. As mentioned before, CN neurons either generate the motor output signal of the cerebellum or project a signal back to the IO. Therefore, the irregularity in their activity can not only directly affect the motor output of cerebellum but can also reverberate through the entire olivo-cerebellar loop and influence the functionality of all the units in this module; indicating the complexity that might underlie the abnormal motor behaviour, we observe in tottering mice.

In chapter 5, we discussed the electrophysiological and morphological results for each element of this olivocerebellar loop, and this discussion is used to speculate on the general function of the olivo-cerebellar system.

Samenvatting

Het cerebellum (de kleine hersenen) is gelegen net boven de hersenstam, bij de basis van de schedel. Het cerebellum is betrokken bij zowel de coördinatie, de correctie als het aanleren van nieuwe bewegingen. Het cerebellum is onderverdeeld in functionele modules. De wijze waarop informatie wordt verwerkt in deze modules verschillen onderling niet veel. Elke cerebellaire module bestaat uit drie neuroanatomische structuren: 1) de onderste olijf (oliva inferior), 2) de cerebellaire schors en 3) de cerebellaire kernen. Neuronen in deze drie gebieden zijn met elkaar verbonden en vormen olivocerebellaire circuits. Sensorische informatie komt op twee manieren het olivocerebellaire systeem binnen: 1) via de onderste olijf en 2) via de mossy vezels, granule cellen en parallel vezels. De olijfcellen integreren de informatie en geven het signaal aan de Purkinje cellen (PC) van de cerebellaire schors en via collateralen ook aan cellen van de cerebellaire kernen. De Purkinje cellen geven het signaal door via sterke depolarisaties, die “complex spikes” worden genoemd. Sensorische informatie, die via de parallel vezels de PC bereiken veroorzaken actiepotentialen, die “simple spikes” worden genoemd. De PC integreert al de binnengekomen informatie en de verwerkte signalen van de PC gaan vervolgens naar de cellen van de cerebellaire kernen. De PC hebben een inhiberend effect op de activiteit van deze cellen. Hier vindt de laatste stap van de informatieverwerking in het cerebel-

lum plaats. De neuronen uit deze cerebellaire kernen genereren de uiteindelijke output van het cerebellum of projecteren de informatie terug naar de onderste olijf, waardoor een gesloten olivocerebellair circuit ontstaat.

Olijfcellen hebben twee unieke electrofysiologische eigenschappen. Ten eerste hebben olijfcellen laagdrempelige membraanpotentiaal oscillaties met een frequentie tussen de 1 en 10Hz. De actiepotentialen, die door de olijf neuronen worden gegenereerd, zijn verankerd met de depolariserende pieken van deze oscillaties en de vuurfrequentie van deze cellen zijn gelimiteerd en kunnen niet hoger worden dan 10Hz (de basisfrequentie ligt rond 1Hz). Ten tweede, olijfcellen zijn electrotonisch met elkaar verbonden door middel van gap junctions, waardoor gekoppelde cellen synchroon kunnen oscilleren. In hoofdstuk 2 hebben we de electrofysiologische eigenschappen van olijfcellen onderzocht in vivo. Deze olijfcellen, die nog onderdeel uitmaken van complete olivocerebellair circuits, laten zeer stabiele laagdrempelige oscillaties in de membraanpotentiaal zien. Deze cellen kunnen worden onderverdeeld in vier clusters op basis van de frequentie van hun laagdrempelige oscillaties. Door de aanwezigheid van deze verschillende oscillatie frequenties kunnen er, door het samenstellen van verschillende cel ensembles, vele neuronale codes worden gegenereerd. Onze resultaten laten ook zien dat deze laagdrempelige oscillaties belangrijk zijn voor het reguleren van het vuurpatroon van de olijfcellen. De laagdrempelige membraanpotentiaal oscillaties kunnen verschuiven door spontane actiepotentialen of door sensorische stimulatie, waardoor uiteindelijk het vuurpatroon (de neuronale code) verschoven wordt. Dit verschuivingsmechanisme van de neuronale code kan van groot belang zijn voor de juiste timing van beweging.

De rol van de electrotonische koppeling in de olijfkern hebben we onderzocht met connexin 36 knockout muizen, die geen gap junctions hebben tussen de olijfcellen. Zonder connexin 36 (zonder electrotonische koppeling) oscilleert de olijfcel onafhankelijk en is de timing van de actiepontentiaal niet meer verankerd met de piek van de oscillaties. Onze resultaten laten zien dat de laagdrempelige oscillaties in ongekoppelde olijfcellen het vuurpatroon veel minder dicteert en dat de timing van de actiepotentialen meer willekeurig is geworden. Het gebrek aan "laagdrempelige synchronie" tussen olijfcellen in de connexin 36 muis zorgt ook voor minder synchroniciteit van de complex spikes van PC in de cerebellaire schors; hetgeen een goede verklaring vormt voor het feit dat deze mutanten slechter zijn in "learning-dependent timing" (zie hoofdstuk 2.2).

In hoofdstuk 3 van dit proefschrift onderzochten wij één van de functies, die werd toegedicht aan de output van olijfcellen en de overdracht van deze informatie naar de PC. Deze overdracht resulteert in PC complex spikes. Verschillend onderzoekers beweerde dat de complex spike een aan/uit-schakelaar is, die de informatieverwerking van de PC reguleert. In hoofdstuk 3 laten wij zien dat de complex spikes in een wakker dier geen stapsgewijze veranderingen in de membraanpotentiaal van PC en geen lange simple spike pauzes (meer dan 200 ms) veroorzaken. Deze aan/uit karakteristieken worden zeer waarschijnlijk veroorzaakt door het gebruik van specifieke anaesthetica. Echter, wij zien deze aan/uit karakteristieken wel in wakkere tottering muizen.

De tottering muis heeft een mutatie in P/Q type calcium kanalen, hetgeen een extreem onregelmatig spontaan simple spike vuurpatroon veroorzaakt. In hoofdstuk 4 hebben we onderzocht of deze onregelmatigheid leidt tot morfologische afwijkingen. In de cerebellaire kernen van tottering muizen vonden we inderdaad misvormde PC eindigingen. Omdat PC de cerebellaire kernen sterk inhiberen, is het niet verwonderlijk dat deze neuronen ook een onregelmatig vuurpatroon vertonen. Zoals eerder aangegeven is, genereren neuronen van de cerebellaire kernen het motor output signaal of koppelen ze het signaal terug naar de olijfkern. De onregelmatigheid van het vuurpatroon heeft dus niet alleen invloed op de motor output van het cerebellum, maar door de terugkoppeling, op alle onderdelen van het olivocerebellaire circuit.

In hoofdstuk 5 bediscussiëren we de electrofysiologische en morfologische resultaten voor elk onderdeel van het olivocerebellaire circuit. Naar aanleiding van deze discussie speculeren we over de algemene functie van het olivocerebellaire systeem.

List of publications

M. Sharifzadeh, N. Naghdi, S. Khosrovani, S.N. Ostad, K. Sharifzadeh and A. Roghani (2005) Post-training intrahippocampal infusion of the COX-2 inhibitor celecoxib impaired spatial memory retention in rats. European Journal of Pharmacology 511(2-3):159-166.

S. Khosrovani*, M. Schonewille*, B.H.J. Winkelman*, F.E. Hoebeek*, M.T. G. De Jeu, I.M. Larsen, J. Van Der Burg, M.T. Schmolesky, M.A. Frens & C.I. De Zeeuw (2006) Purkinje cells in awake behaving animals operate at the upstate membrane potential. Nature Neuroscience 9, 459 – 461.

S. Khosrovani*, R.S. Van Der Giessen*, C.I. De Zeeuw and M.T.G. De Jeu (2007) *In vivo* mouse inferior olive neurons exhibit heterogeneous subthreshold oscillations and spiking patterns. Proc Natl Acad Sci U S A. Oct 2; 104(40):15911-6.

S. Khosrovani, C.I. De Zeeuw and F.E. Hoebeek. Purkinje cell input to cerebellar nuclei in *tottering*: ultrastructure and physiology (To be submitted).

S. Khosrovani*, R. S. Van Der Giessen*, S. K. Koekkoek*, S. van Dorp*, J. R. De Gruijl*, A. Cupido*, K. Wellershaus, J. Degen, J. Deuchars, E. C. Fuchs, H. Monyer, K. Willecke, M. T.G. De Jeu, and C. I. De Zeeuw. Role of olivary electrical coupling in cerebellar motor learning (Submitted).

(* Authors contributed equally)

Acknowledgements

I never thought writing a "dankwoord" is so difficult, it feels like saying goodbye to a period of my life that taught me a lot not only about science but also about life.

I would like to start by expressing my deep and sincere gratitude to my supervisor, Professor De Zeeuw. Chris, you changed the path of my life to a great extent by accepting me as an AIO. I will always remember your warm welcome to the department, your great supervision and how you encouraged me throughout my Ph.D. But most of all I am grateful for our friendship which, I am sure, will last for a long time.

I would also like to thank my co-promotor Marcel who made the "de Jeu" Lab a wonderful workplace and home. Marcel you were most helpful to me while writing and preparing this thesis as well as during the challenging research that is the basis of it. I miss our coffee breaks with scientific and non-scientific discussions as well as your wonderful taste in music :)

Besides my two advisors, I would like to thank the rest of my thesis committee for the time they spent reading my thesis and for agreeing to participate in my promotion: Gerard, for always giving insightful comments and whose scientific compliments meant a lot to me; Jerry, for his friendship, discussions and hard questions; Dr. Meijer who kindly agreed to review my work. I warmly thank Christian Hansel for his valuable advice, help and extensive discussions about work and life in general. I wish you a very lovely time in America.

Matthew, thank you for teaching me a lot about the basics of in vivo whole cell recordings in such a short period of time.

I am also very grateful to many teachers in the past: Mrs. Sedghi, my beloved piano teacher; Mrs. Farid, my high school teacher who made me interested in chemistry and pharmacy; and my supervisors in Tehran, Dr. Sharifzadeh and Dr. Naghdi for opening my eyes to Neuroscience.

I am so lucky to have two of my good friends as my paranimfs: dear Corina, even though you were very quiet for the first two years (contradictory to Alexander) in time I discovered that once you started talking you always had something very wise to say. Thank you for being my paranimf! Beste Alexander, my lunch buddy! You can always bring a big smile to my face. I actually miss your loud presence in my daily life. When is the housewarming party?

Dear Ruben, it was a pleasure working with you. We had a wonderful time during the Inferior olive project and I will always remember that Friday afternoon that we patched our very first olivary cell. Thank you for all the help and one big "good luck" with your internship!

Bjorn, thank you for your mental and spiritual support as well as your tea and coffee rituals. You together with Eva are the only people I trust my life with sitting at the back of their bikes. Samantha, thank you for editing my thesis, our Saturday morning yoga sessions and happy cocktail hours. A big thank to Bart, Beerend, Joel, Henk-Jan, Elnaz and Mahban for all the lunches, coffees, chats and gossips. Sweet Aleksandra, thank you for your warm support, I always enjoyed our pleasant chitchats! I wish you strength with cell recordings and give you a big hug. Dear Freek,

thank you for all your help with the bistability and *tottering* projects. Your enthusiasm was very inspiring. Martijn, the trip to Pavia is unforgettable, with all the singing and dancing in Chris' car and especially the fact that we forgot to take our posters. I wish you a very fruitful career. Laurens, good luck with awake whole cell recordings, it is a fantastic yet technically challenging project that has to be done.

Tom, your knowledge of anatomy is overwhelming, thank you for sharing it with the less fortunate of us. The Borst lab; thank you for sharing your electrode puller! Entering your lab always was a joy to me. John, thank you for your friendship, we should go and watch another movie soon. I would like to thank the histology lab and especially Elize, for hours and hours of work behind EM microscope en je Nederlandse lessen. My dear Hans, thank you for all the technical support (from making the brilliant double electrodes to remove all the 50 Hz noise) and also all the Dutch words you taught me :) but mostly thank you for the good atmosphere you brought every time you entered the room. A big "thank you" to Ria, Kenneth, Edith and Loes for always being so friendly and helpful; and to Eddie for all the technical support.

My promotion buddies, Doortje the TV star and Eva the cover girl! Girls, it was a great experience organizing our promotion party. Doortje, thanks for improving my running stamina; Eva, thank you for all the cooking recipes, all the great nights out and gezelligheid. I wish you "good luck" for the big day!

I would also like to thank my new colleagues at CBG for showing interest in my thesis and being so helpful with all the new things I have to learn. Sabine, thank you for giving me the opportunity to pick up (rescue) my pharmacy knowledge.

Dear Sara, I am looking forward to attend more jewelry courses, film festivals and pleasant get-togethers. Fabian, thank you for reassuring me every time I was stressed with my thesis and promotion, but mostly thank you for making me smile. My dear Roya, you are a true friend to me, and that is not something you find every day! I will always be grateful for the interest you show in my life and I am very happy that I am seeing you more often these days. A big kiss for Nahal! Zari joonam, thank you so much for your friendship, for helping me get through the difficult times, for all the support, caring and entertainment you provided. I am looking forward to coming to visit you in Canada.

Ada and Jaap, dank jullie wel voor alle gezellige etentjes en de vele ritjes naar Maastricht. De fiets herinnert me iedere keer aan jullie. Yasi, you know how much I love you! I wish that one day you will come and live so close to me that I can actually walk to your place for a cup of tea. I want to thank my very dear aunt, Dr. Parvin Khosrovani and my lovely grandmother for never stop showing their love and support even from long distance.

My beloved sister Sahar, thank you for always encouraging me in life! It is a pity that you and Leo are not living in Rotterdam anymore so that I could see more of you and my lovely Shayan, Lili and Guiv. Big kiss for all of you!

Lastly, and most importantly, I would like to thank my parents for their support and unconditional love. To them I dedicate this thesis.

Stellingen behorende bij het proefschrift

Electrophysiology of the olivo-cerebellar loop

1. Purkinje cells in an awake behaving mouse do not exhibit long pauses of simple spike activity (this thesis).

2. The inferior olive in intact mammals has four cell types with different, yet relatively stable, frequency settings (this thesis).

3. Subthreshold oscillations and action potentials in the inferior olive influence oneanother (this thesis).

4. Morphological abnormalities in the terminals of Purkinje cells in *tottering* mice do not completely block their functionality (this thesis).

5. The chance of patching a Purkinje cell *in vivo* is higher when you want to patch another cell type from the cerebellar cortex.

6. Due to the compensatory mechanisms in the mutant mice, it is difficult to pinpoint the exact phenotype.

7. The use of anesthetics can easily lead to misjudgment of data.

8. A mouse in the kitchen is different from the one in the lab!

9. When living abroad, one tends to see one's own country from another perspective.

10. If you see the teeth of the gorilla, do not think that he is smiling at you.

11. A lie told often enough becomes the truth. (Lenin)

Sara Khosrovani
23 April 2008, Rotterdam

Sara was born on 12 Feb. 1978 in Tehran, Iran. After graduation from high school in September 1996 she started her Pharmacy study at the Tehran University of Medical Sciences. During this study her attention got focused on Neurosciences. After she obtained her Pharmacy degree, she started the Ph.D. programme at the Neuroscience department of the Erasmus Medical Center which resulted in this thesis. Currently, Sara is working as a pharmaco-vigilance assessor for the Medicines Evaluation Board, The Hague.